Cytoplasmic tails of integrin $\alpha_{IIb}\beta_3$ in the regulation of integrin activation, cell adhesion and spreading

A Thesis

Submitted to the College of

Graduate Studies and Research

In Partial Fulfillment of the Requirements

For the Degree of Doctor of Philosophy

In the Department of Anatomy and Cell Biology

University of Saskatchewan

Canada

By

XINLEI LI

PERMISSION TO USE

In presenting this thesis in partial fulfillment of the requirements for a Postgraduate degree from the University of Saskatchewan, I agree that the Libraries of this University may make it freely available for inspection. I further agree that permission for copying of this thesis in any manner, in whole or in part, for scholarly purposes may be granted by the professor or professors who supervised my thesis work or, in their absence, by the Head of the Department or the Dean of the College in which my thesis work was done. It is understood that any copying or publication or use of this thesis or parts thereof for financial gain shall not be allowed without my written permission. It is also understood that due recognition shall be given to me and to the University of Saskatchewan in any scholarly use which may be made of any material in my thesis.

Requests for permission to copy or to make other use of material in this thesis in whole or part should be addressed to:

Head of the Department of Anatomy and Cell Biology

University of Saskatchewan

Saskatoon, Saskatchewan S7N 5E5

Canada

ABSTRACT

Integrins are major adhesion receptors for the extracellular matrix (ECM). This thesis focuses on the motifs and interactions within integrin cytoplasmic tails during integrin-mediated cell adhesion and spreading. The present study investigated the significance of the skelemin-$\alpha_{IIb}\beta_3$ interaction using Chinese Hamster Ovary (CHO) cells expressing wild-type or mutant $\alpha_{IIb}\beta_3$ receptors defective in skelemin binding. Most mutant cells displayed unimpaired adhesive capacity and spreading on immobilized fibrinogen at the early stages of cell spreading. In addition, they formed normal focal adhesions and stress fibers with no indication of impaired cell spreading. K716A, and H722A mutant cells exhibited the greatest cell spreading, which was associated with enhanced p-Src activation. The K716 residue appeared to be the most important for skelemin binding in previous *in vitro* studies. Here, the protrusions of the leading edge of K716A cells showed strong colocalization of talin with $\alpha_{IIb}\beta_3$ which was associated with a loss in skelemin binding. These data suggest that the binding of skelemin to $\alpha_{IIb}\beta_3$ is not essential for normal cell spreading, but may act to exert contractile forces on cell spreading and coordinate the binding of talin to the membrane proximal region of integrin tails. The functional mode of peptides corresponding to the central motifs of the α_{IIb} and α_V tail, KRNRPPLEED (α_{IIb} peptide) and KRVRPPQEEQ (α_V peptide) was also investigated. Both peptides inhibited Mn^{2+}-activated $\alpha_{IIb}\beta_3$ binding to soluble fibrinogen as well as the binding of $\alpha_{IIb}\beta_3$-expressing CHO cells to immobilized fibrinogen. Breast cancer progression has been linked to tumor cell interaction with ECM. Our α_{IIb} and α_V peptides also inhibited adhesion of two breast cancer cell lines (MDA-MB-435 and MCF7) to α_V integrin ECM ligand vitronectin. Replacement of RPP with AAA significantly attenuated the inhibitory activity of the α_{IIb} peptide. β-tubulin was identified as a potential α_{IIb} peptide-binding partner, suggesting that microtubule cytoskeleton may participate in the regulation of integrin functions. These results provide insights into the mechanisms by which the central motifs of α_{IIb} and α_V tail regulate integrin activation and integrin-mediated cell adhesion.

ACKNOWLEDGEMENTS

I would like to express sincere gratitude to my supervisors, Professors Thomas Haas and David Schreyer. Dr. Haas supported me over the years in my study. I appreciate all his contributions of time, ideas, and funding to make this thesis possible. I especially want to thank him for his continuous support during his medical leave. Dr. Schreyer offered many discussions, comments and corrections of my thesis writing. Their broad knowledge, great encouragement and hard work were of great value for me.

I am very grateful to my advisory committee, Drs. Valerie Verge, Troy Harkness, Ronald Doucette, Lixin Liu and Richard Devon for their insightful comments, critical questions and kind encouragement. Dr. Harkness gave me invaluable feedback on Western blot results and data analysis. Dr. Doucette taught me statistical analysis. My advisory committee earns my deepest gratitude and sincere respect.

I would like to thank our technicians Yongqing Liu and Xingfeng Ma for teaching me technical skills and providing technical assistance whenever needed. Many thanks also to Mark Boyd, Shanna Banmanand and Haixia Zhang for their technical assistance with flow cytometric, confocal microscopic and mass spectrometric measurements, respectively.

I could not finish my PhD thesis without the support of my husband Jianghai Liu. His love and encouragement in these years endowed me with strength during my PhD studies. His enthusiasm for research set an example for me as a good

scientist.

I would like to thank the CIHR, Heart and Stroke Foundation of Canada, College of Medicine at the University of Saskatchewan, and the Arthur-Smyth Memorial scholarship for providing me financial support.

Last but not least, thanks and praise be given to God who has blessed me with the arrival of my sweetheart, Samuel Liu during thesis writing.

DEDICATION

To my dear parents

Hongyuan Li

Guixiu Che

献给我亲爱的父母

For their constant support, encouragement, care, and unfailing love

因为他们不断的支持，鼓励，关怀和无尽的爱

TABLE OF CONTENTS

LIST OF FIGURES

LIST OF ABBREVIATIONS

ACSs	acute coronary syndromes
ADMIDAS	adjacent metal ion dependent adhesion sites
BCA	bicinchoninic acid
BRET	bioluminescence resonance energy transfer
BSA	bovine serum albumin
CHO	chinese hamster ovary
CIB	calcium- and integrin-binding protein
CSK	c-Src kinase
CT	cytoplasmic tail
DCC	N,N'-Dicyclohexylcarbodiimide
DCM	dichloromethane
DIEA	N,N-Diisopropylethylamine
DMEM	dulbecco's Modified Eagle's Medium
DMF	dimethylformamide
Dok1	docking protein 1
ECM	extracellular matrix
ERK	extracellular signal-regulated kinase
EPI	epinephrine
F-actin	Filamentous actin
F_{Ca}/ F_{EDTA}/ F_{Mn}	the mean fluorescence intensity (MFI) of PAC-1 binding in the presence of Ca^{2+}, EDTA, or Mn^{2+}

FAK	focal adhesion kinase
FBS	fetal bovine serum
FL1	cell fluorescence intensity before washing in cell adhesion assay
FL2	cell fluorescence intensity after washing in cell adhesion assay
Fmoc	fluorenylmethyl-carbonyl
G418	geneticin
GAPs	GTPase activating proteins
GEFs	guanine nucleotide exchange factors
GFP	green fluorescence protein
GPCRs	G-protein-coupled receptors
HBTU	O-benzotriazole-N,N,N',N'-tetramethyl-uronium-hexafluoro-phosphate
HOBt	N-hydroxybenzotriazole
HPLC	high-performance liquid chromatography
ILK	integrin linked kinase
IMC	inner membrane clasp
LAD I	leukocytes adhesion deficiency type I
MFI	mean fluorescence intensity
MIDAS	metal ion dependent adhesion site
MMP	matrix metalloproteinase
MRLC	myosin regulatory light chain
NMR	nuclear magnetic resonance

NOE	nuclear overhauser effect
NHS-Biotin	N-Hydroxysuccinidobiotin
OMC	outer membrane clasp
PAC-1	a $\alpha_{IIb}\beta_3$ activation-specific antibody
PBS	phosphate buffered saline
PRP	platelet-rich plasma
PPP	Platelet-poor plasma
PCI	percutaneous coronary intervention
PE	phycoerythryn
PKC	protein kinase C
PMA	phorbol myristate acetate
PMSF	Phenylmethysulfonyl Fuoride
PP2A	protein phosphatase 2A
α/β PS	Drosophila position-specific (PS) genes encode α or β integrin ortholog
PTB	phosphotyrosine-binding
PTP	protein–tyrosine phosphatase
SDS	sodium dodecyl sulphate
SDS-PAGE	SDS-polyacrylamide gel electrophoresis
SkIgC4	skelemin immunoglobulin C2-like repeats 4
SkeC2	skelemin immunoglobulin C2 motifs 4-5 that contain the $\alpha_{IIb}\beta_3$-binding domain

SPR	surface plasmon resonance
Src	a non-receptor tyrosine kinase encoded by the proto-oncogene of *src* which is highly similar to the v-*src* gene of *Rous sarcoma* virus
SyMBS	synergistic metal ion binding site
TBS	tris-buffered saline
TBST	tris-buffered saline and tween 20
TEMED	tetramethylethylenediamine
TIPS	triisopropylsilane
TFA	trifluoroacetic acid
TMD	transmembrane domain
VCAM-1	vascular cell adhesion molecule-1
VEGF	vascular endothelial growth factor
WT	wild-type

CHAPTER 1

INTRODUCTION AND LITERATURE REVIEW

1.1 Integrin functions

Integrins are type I transmembrane proteins consisting of noncovalently linked α and β subunits. In mammals, 18 α subunits pair with 8 β subunits to form a large integrin family with at least 24 distinct integrin heterodimers (*1*) (Figure 1.1).

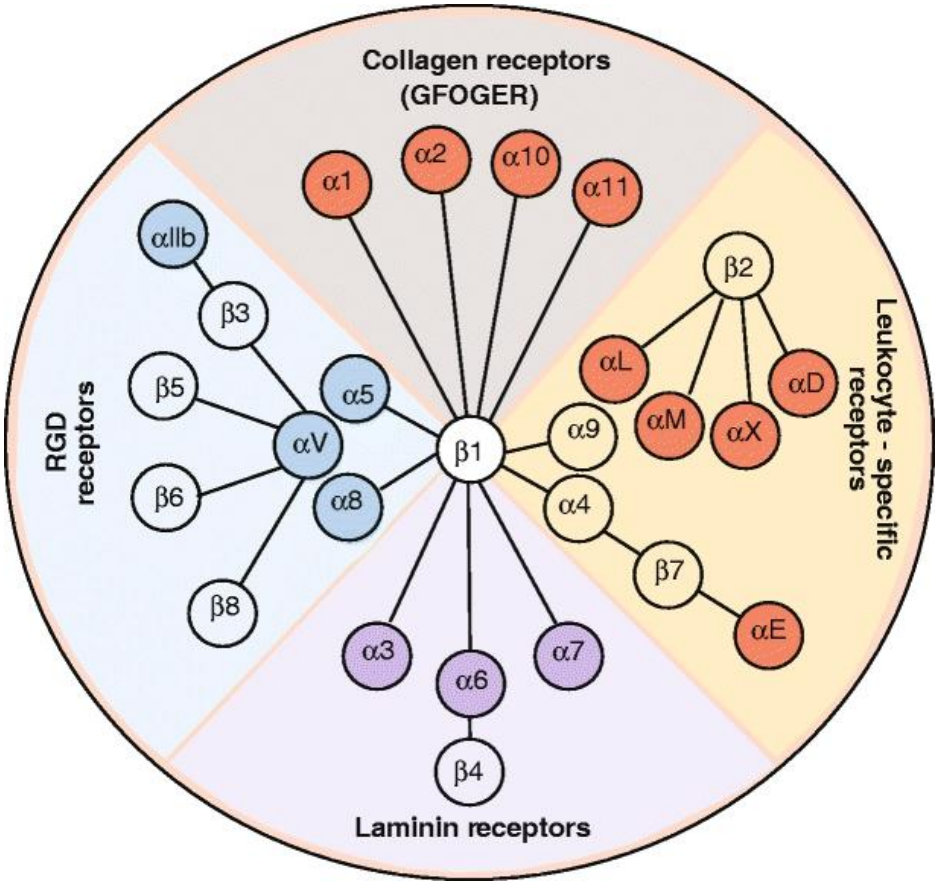

Figure 1.1：The integrin family members. In vertebrates, the integrin family contains 24 heterodimers. They are divided into several subfamilies based on evolutionary relationships (coloring of α subunits), ligand specificity and leukocyte-specific expression in the case of β2 and β7 integrins. Adapted from reference (*1*).

Integrins are essential adhesion receptors that mediate cell-cell and cell-matrix interactions. Their primary function is to mediate cell adhesion, which provides a physical support for a cell and various tissue types. Each integrin family member can bind with multiple ECM proteins, such as bone matrix proteins, vitronectin, collagens, fibronectins, fibrinogen, laminins, thrombospondins, and von Willebrand factor. Integrins also bind with particular motifs or ligands. The preference of integrin binding is determined by the affinity, availability and conformation of ligands in the microenvironment (*2*). Cells expressing particular integrins can adhere or migrate toward a specific region where integrin ligands are available. Integrin attachment of cells to the ECM is important for the developmental processes (*3*). Genetic deletion studies with *Drosophila melanogaster* which have lower integrin redundancy suggested that disruption of αPS or βPS [Drosophila position-specific (PS) genes encode α or β integrin ortholog] resulted in embryonic lethal or defective tissue morphogenesis, such as muscle detachment, dorsal closure defects, delayed gut migration, and blisters in the wing (*3*).

Integrin-mediated cell-cell adhesion is facilitated by the β_2 family. β_2 integrins are leukocyte-specific receptors and bind cellular receptor ligands such as vascular cell adhesion molecule-1 (VCAM-1) and/or intercellular cell adhesion molecule (ICAM) on endothelial cells (*1*, *4*). β_2 integrins are important for many adhesion-dependent processes, including chemotaxis, phagocytosis and homotypic aggregation. The lack of expression of β2 integrins or the expression of dysfunctional β2 integrins lead to leukocyte adhesion deficiency type I (LAD I) disease, a life-threatening condition

associated with recurrent microbial infections with associated neutrophilia (*5*).

Not only can integrins mediate physical attachment of cells to their environment, but they can also be a primary component of sensory machinery for cells (*6*). By binding with their ligands, integrins recognize and sense environmental cues, including chemical or physical stimuli, and transmit these signals into cells. Diverse signalling pathways can be initiated and transmitted by integrin, which influence varieties of cell behaviours, such as cell adhesion, migration, proliferation, differentiation, and apoptosis. These basic biological events determine processes of embryonic development, tissue repair, homeostasis, and immune responses. Abnormal integrin function is linked to the progression of some diseases, such as thrombosis, autoimmune disease, and tumour metastasis.

Our lab is particularly interested in integrin $\alpha_{IIb}\beta_3$, expressed on platelets, megakaryocytes, basophils, mast cells and some tumour cells (*7*). $\alpha_{IIb}\beta_3$ is the most abundant integin expressed on platelets and responsible for platelet aggregation and normal homeostasis. When $\alpha_{IIb}\beta_3$ is activated, it binds to multivalent fibrinogen and von Willebrand factors in plasma, which then bridge to other $\alpha_{IIb}\beta_3$ molecules on adjacent platelets leading to platelet-platelet interaction. Genetic defects in integrin α_{IIb} or β_3 subunit results in Glanzmann thrombasthenia, a bleeding disorder (*8*).

1.2 Integrin activation

Integrins are normally expressed on cells in an inactive state, and are unable to productively bind to their ligands. This is particularly important for immune cells and

platelets circulating in the bloodstream, as integrins must be in a quiescent state under physiological conditions. Stimuli such as cytokines and coagulation factors can quickly cause extracellular changes of integrins, switching integrins from a low ligand binding affinity state to a high affinity state (a process known as inside-out signalling). $\alpha_{IIb}\beta_3$ on platelets represents a typical model to investigate integrin activation. $\alpha_{IIb}\beta_3$ in the low-affinity state does not interact with soluble fibrinogen under physiological conditions. After vascular injury, stimulation by a number of agonists (such as thrombin, ADP, epinephrine) on platelets changes the $\alpha_{IIb}\beta_3$ conformation and increases its affinity to fibrinogen. How these agonists initiate integrin activation (inside-out signalling pathway) is not completely clear, but a recent study suggested that platelet agonists can bind to specific G-protein-coupled receptors (GPCRs) in platelets, and the heterotrimeric G-protein may play a key role in translating the signal from GPCRs to integrin $\alpha_{IIb}\beta_3$ (*9*). Binding of fibrinogen to $\alpha_{IIb}\beta_3$ on platelets results in platelet aggregation. This quick and precisely controlled process is critical in order to prevent blood loss at the site of a wound, while maintaining normal blood flow. Abnormal $\alpha_{IIb}\beta_3$ activation leads to potentially life-threatening thrombosis and is involved in cardiovascular diseases.

Another example of the control of integrin activation is integrin $\alpha_V\beta_3$, which is widely expressed in diverse cell types. $\alpha_V\beta_3$ is used as a marker of angiogenic vascular tissue as quiescent endothelial cells expressed low levels of $\alpha_V\beta_3$ but endothelial cells in angiogenic vessels have increased $\alpha_V\beta_3$ expression (*10*). Activation of $\alpha_V\beta_3$ can be induced by agonists, such as ADP, phorbol myristate

acetate (PMA) and Mn^{2+}. PMA is also a potent activator of protein kinase C (PKC) (*11*). Previous work found that the PKC pathway is important for the inside-out signalling events that activate $\alpha_V\beta_3$ (*11, 12*). In addition, the neutral protease calpain, a secondary signalling molecule in cells, is also required for the modulation of $\alpha_V\beta_3$ activation (*11*). Calpain cleaves a variety of substrates of multiple intracellular signalling pathways, including PKC (*13*). Moreover, $\alpha_V\beta_3$ has been implicated in tumour invasion and metastasis of several tumour types, such as glioma, breast cancer, and melanoma (*14, 15*). In breast cancer, the expression of $\alpha_V\beta_3$ on tumour cells, particularly in its high affinity state, promotes tumour progression and metastasis. Over-expression of the constitutively active mutant $\alpha_V\beta_{3D723R}$, but not wild-type $\alpha_V\beta_3$, in MDA-MB 435 cells resulted in a significant increase in metastatic activity in mouse models (*16, 17*). The drastic increase in metastatic activity of active $\alpha_V\beta_3$ has been attributed to its capability of supporting tumour cell arrest during blood flow through interaction with platelets, up-regulation of the mature form of metalloproteinase-9 (MMP-9) which maximizes tumour cell mobility, and efficient metastasis growth in metastatic tissue through continuous up-regulation of vascular endothelial growth factor (VEGF) (*16, 18, 19*).

1.3 Integrin structure and the conformational change during integrin activation

As a typical integrin, $\alpha_{IIb}\beta_3$ is a heterodimer composed of α_{IIb} and β_3, which are held together by numerous non-covalent protein-protein and protein-metal ion contacts. Each subunit has a large extracellular domain, a single-pass transmembrane

domain, and a short cytoplasmic tail.

1.3.1 Extracellular domain

The extracellular domain of integrin is a ligand binding region. The first X-ray crystal structure of the full-length extracellular domain of integrin was obtained from $\alpha_v\beta_3$ and its complex with the RGD peptide ligand (*20, 21*). The structure of $\alpha_v\beta_3$ revealed the inter-subunit interface, ligand binding sites, some previously unpredicted modules, and novel calcium-binding sites. Ligand binding sites form a globular headpiece which is followed in each subunit by two long legs. The two subunit interface also lies within the head between the seven-bladed β–propeller in α_v subunits and the βA-domain in β_3 subunits (Figure 1.2). The β-propeller domain of the α subunit contains Ca^{2+}-binding motifs that are important for formation of the inter-subunit interface. In the absence of a ligand, the structure folds into an extremely bent conformation and ligand binding induces an extended conformation as shown in Figure 1.2. Electron microscopy studies of $\alpha_v\beta_3$ reconstituted in lipid bilayers showed an extended conformation, especially when integrin was activated by Mn^{2+} and small-molecule ligands (*22, 23*). Therefore, there is a general acceptance that a bent structure represents an inactive state and that the extended structure exposes ligand binding sites and defines the active state.

The crystal structures of $\alpha_{IIb}\beta_3$ with or without a bound ligand have also been resolved (*24, 25*). The $\alpha_{IIb}\beta_3$ structure is very similar to that of $\alpha_v\beta_3$ as shown in Figure

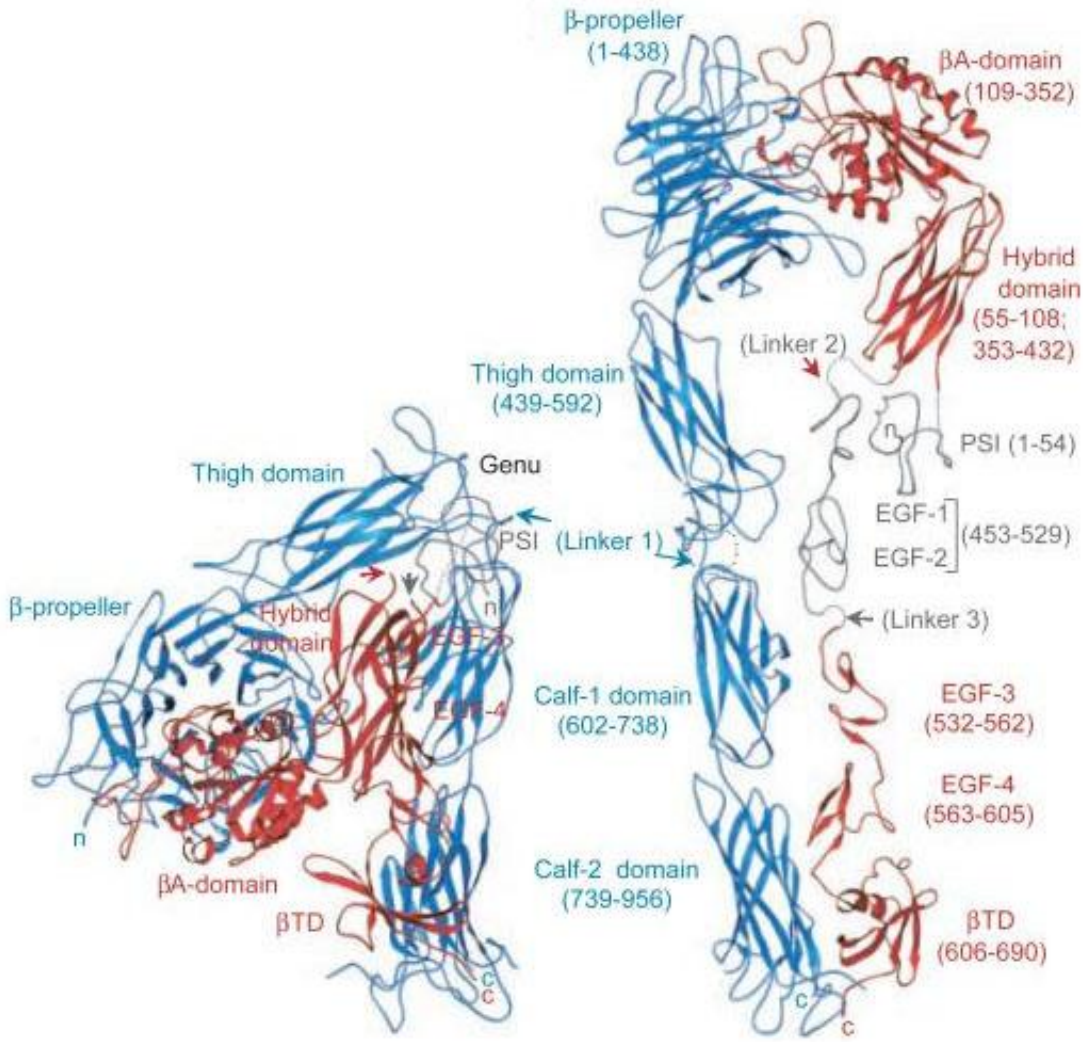

Figure 1.2: Ribbon schematic of crystallized $\alpha_v\beta_3$ in a bent (left) and extended conformation (right). α_v is shown in blue and β_3 in red. Its 12 known and novel domains assemble into a globular "head" and two "tails''. Adapted from reference (*21*).

1.2. However, an intermediate form of $\alpha_{IIb}\beta_3$ between the bent and extended form was reported in a cryo-electron microscopy (cryo-electron microscopy: imaging specimens in a transmission electron microscope under cryogenic conditions) study (*26*). The bent conformation of $\alpha_{IIb}\beta_3$ incorporated into liposomes was also observed in the presence of Mn^{2+} (*27*). Quantitative analysis of electron microscopic images of

lipid-embedded $\alpha_{IIb}\beta_3$ revealed that activation of integrin shifted the conformational equilibrium in favour of the extended form that leads to an increase in ligand binding affinity (*28*).

Three metal binding sites in the βA domain of the β_3 subunit support the ligand binding site (*24*). They are occupied by the divalent cations Ca^{2+} and Mg^{2+}. A metal ion dependent adhesion site (MIDAS) in the βA-domain binds with Mg^{2+} and participates in ligand binding. MIDAS is flanked by two Ca^{2+} binding sites, named the adjacent metal ion dependent adhesion site (ADMIDAS) and the synergistic metal ion binding site (SyMBS) (*24*). ADMIDAS binds an inhibitory Ca^{2+} ion and replacement of Mn^{2+} at this site results in a structural change that produces an active integrin (*29*).

1.3.2 Transmembrane domain

The transmembrane domains (TMDs) of integrins are single membrane-spanning structures, comprised of about 20 amino acid residues, and are highly conserved across integrins. The TMD of integrin $\alpha_{IIb}\beta_3$ is rich in hydrophobic sequences and closely resembles that of many of the other 18 α and 8 β human subunits. Its C-termini are located close to lysine residues K989 in α_{IIb} and K716 in β_3, which begin the cytoplasmic regions. The TMD domain is critical for integrin activation and for transmitting signals across the plasma membrane. Studies of nuclear magnetic resonance (NMR) structure (*26, 30, 31*), disulfide bond scanning (*32*), and Leu substitution (*33*) found that there is an α-β heterodimeric TMD interaction in integrin

in its resting state. Dissociation of the α-β interaction at the TMD triggers receptor activation and signalling (*33-35*).

NMR is a useful tool to study a weak and dynamic complex. By using NMR, most of the integrin TMD and cytoplasmic tail structural data were obtained in a variety of membrane mimetic solvents. NMR structures of the $\alpha_{IIb}\beta_3$ TMD show that the α_{IIb} TMD adopts a short and straight helix structure, whereas the β_3 TMD forms a long and tilted helix, which extends to the intracellular side and forms a continuous helix with the membrane-proximal region of β_3 cytoplasmic tails (*32, 36*). At the N-terminus of the β_3 TMD, Gly residues at 708, 976 and 972 allow close interhelical packing, which explains the observation that mutational substitution of either Gly residue with a bulky amino acid results in constitutively active integrin (*33*). This helical TMD packing is referred to as the outer membrane clasp (OMC) that stabilizes the low-affinity state of the integrin (*31*).

1.3.3 Cytoplasmic tails: structures and interactions

Integrin cytoplasmic domains are generally short, but vital in regulating integrin ligand-binding competency and signalling functions. The cytoplasmic tails are highly similar between α_{IIb} and other integrin α-subunits, which are composed of a highly conserved N-terminus followed by a variable C-terminus (Figure 1.3).

Early mutational studies show that deletion of almost the entire α_{IIb}-cytoplasmic tail (G991–E1008) or deletion of α or β membrane-proximal regions constitutively activates $\alpha_{IIb}\beta_3$ (*37, 38*). Therefore, the membrane-proximal regions of $\alpha_{IIb}\beta_3$ tails were

Figure 1.3: Sequence alignment of various human integrin α-cytoplasmic domains. The sequence identity and similarity are highlighted in red and purple. Adapted from reference (*4*).

suggested to negatively regulate integrin activation (*38*). The opposing charged Arg995 in α_{IIb} and Asp723 in β_3 were proposed to form a salt bridge (*39*). Charge reversal of either one of these residues (R995D or D723R) or substitution of either one with non-charged residues (for example, R995A) resulted in the expression of a constitutively active $\alpha_{IIb}\beta_3$. However, when both charges were reversed, the integrin stayed inactive (*39*). These studies indicate that the electronic interaction between membrane-proximal regions of α_{IIb} or β_3 maintains integrins in an inactive state, while breaking this interaction makes the integrin active (*39*). The interaction between α_{IIb} and β_3 cytoplasmic peptide can be detected by surface plasmon resonance (SPR).

Their heterodimerization occurred in a 1:1 stoichiometry with a weak affinity in the micromolar range, which was impaired by the R995A substitution or deletion of KVGFFKR in α_{IIb} (*40*).

The structures of $\alpha_{IIb}\beta_3$ cytoplasmic tails have been characterized under heterodimeric conditions (*41-44*). Most structural studies of $\alpha_{IIb}\beta_3$ identified electrostatic and hydrophobic interactions in the membrane proximal regions, which support the previous mutational studies. The interaction occurred between the conserved ^{990}GFFKR^{995} in α_{IIb} subunits and the conserved ^{722}HDRKE^{726} in β_3 tails. The current view is that both the interactions through the membrane-proximal regions and packing of TMDs are required to keep the resting integrin receptor in an inactive state and disrupting either interaction activates integrins (*35, 45*). Evidence for this view comes from the mutational study showing that the individual effects on integrin activation produced by mutations in the TMD or tail interface were weak, whereas the combination of the two mutations had a strong synergistic effect (*36*).

The membrane distal region of the α_{IIb} cytoplasmic tail has a significant structural feature, described as a turn formed at RPP^{999}. The NMR structure of a synthetic peptide encompassing the α_{IIb} cytoplasmic tail reveals a “closed” conformation (Figure 1.4A) (*4*). The highly conserved N-terminal membrane-proximal region forms an α-helix followed by a turn at PP which allows the acidic C-terminal loop to fold back and interact with the positively charged N-terminal helix. Replacing the double prolines with alanines (P998A/P999A) resulted in misfolding of α_{IIb} (Figure 1.4B). Although the N-terminal α-helix is retained in the mutant peptide, the double mutation

disrupts the turn, thereby preventing interactions between the N-terminal helix and C-terminal region and resulting in an "open" conformation. The structure of the mutant is apparently less rigid, with a significantly reduced number of Nuclear Overhauser Effect (NOE) constraints in its NMR signals as a result of disruption of N- and C-terminal contacts. Furthermore, mutation of $\alpha_{IIb}\beta_3$ (P998A/P999A) expressed in CHO cells rendered $\alpha_{IIb}\beta_3$ constitutively active to bind extracellular ligands, resulting in fibrinogen-dependent cell-cell aggregation (*46*).

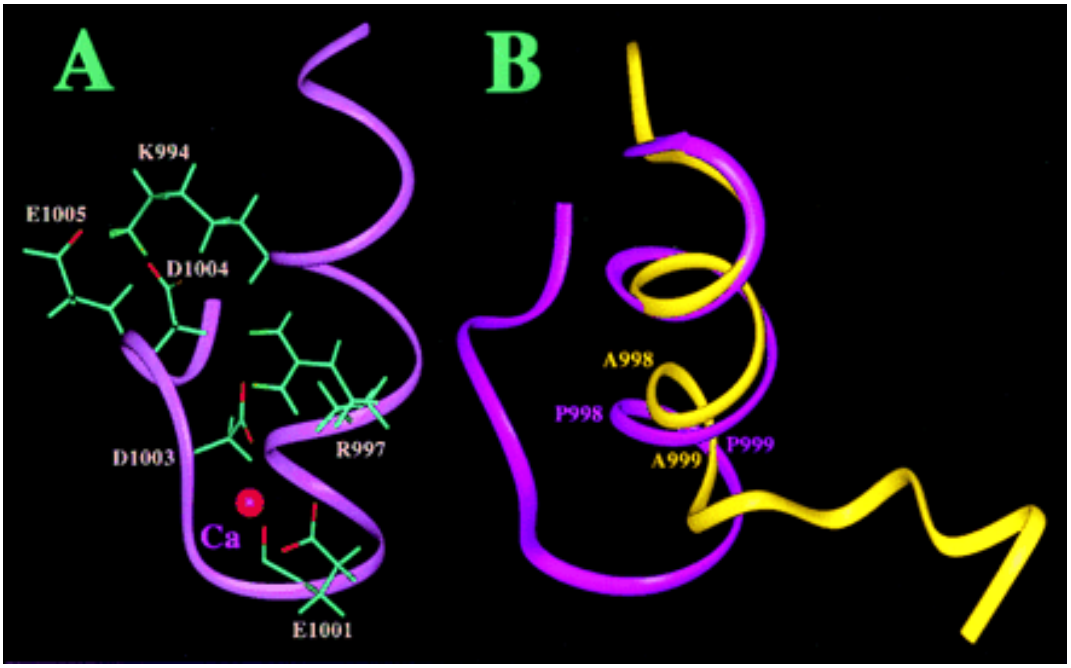

Figure 1.4: Structural highlights of the cytoplasmic domain of α_{IIb}. (*A*) Backbone of wild type α_{IIb} showing the residues participating in the loop structure formation between the N-terminal helix and C-terminal region. The interactions between the N and C termini are primarily through an electrostatic network between the side chains of K994, R997, E1001, D1003, D1004, and E1005. (B) Backbone overlay of wild-type α_{IIb} (purple) and mutant α_{IIb} (yellow) showing the structural difference. Adapted from reference (*4*).

One possible reason for the activation of the mutated $\alpha_{IIb}\beta_3$ (P998A/P999A) is because the downstream activators can bind to the integrin tails when they are "open" (Figure 1.4) (*4*). Multiple proteins have been identified that bind to α_{IIb} tails. For example, the α_{IIb} cytoplasmic tail interacts with the chloride channel ICln, the calcium- and integrin-binding protein (CIB), and the catalytic subunit of protein phosphatase 1 (*47-50*). The binding of these cytoplasmic proteins may serve to regulate integrin activation and function. However, almost all of the proteins were reported to bind to the membrane proximal region of α_{IIb} tails. Therefore, searching for proteins that interact with the central turn motif of α_{IIb} tails may provide useful insights for understanding the significance of the turn structural feature which still remains uncertain.

Compared with α_{IIb} tails, the structure and function of β_3 integrin tails have been more extensively studied. There are two well-defined motifs within β integrin tails: the $NPxY^{747}$ motif (x stands for any amino acid and is a leucine in the β_3 tail) and the $NxxY^{759}$ motif (xx is isoleucine and threonine in the β_3 tail). These motifs represent recognition sequences for phosphotyrosine-binding (PTB) domains (*51*). $NPxY^{747}$ serves as the binding site for talin, a well-established integrin activator. Talin binding has previously been assumed to be the final and common step of integrin activation (*52, 53*). The PTB domain within the head domain of talin binds to integrin β_3 tails with much higher affinity (Kd～100nM). Y^{747} of $NPLY^{747}$ within β3 tails is necessary for this interaction (*54, 55*). An NMR study showed that the talin-binding site on the β_3 tail extended to the membrane proximal region, completely overlapping the region

of β_3 interaction with α_{IIb}. Adding a talin head destroyed the NMR signals of a α_{IIb}-β_3 tail interface (*43*). Reconstitution of physiological integrin activation with nanodiscs and a single lipid-embedded integrin showed that talin binding alone was sufficient to activate integrin $\alpha_{IIb}\beta_3$ (*28*). These studies are consistent with the model that the membrane-proximal regions form the inner membrane clasp (IMC) that maintains the low-affinity state, and breaking this clasp induces integrin activation (*31*)..

However, it is interesting that although many PTB-domain-containing proteins bind integrins, only talin exhibits the capacity to activate integrins. A further study found that a second interaction happens between talin and the membrane proximal helix of β3 tails, which causes α and β tail separation and in turn the extended and active conformation of the integrin extracellular domain (*56*). Several integrin activation inhibitors with PTB domains have been identified. These inhibitors, such as docking protein 1 (Dok1) and filamin, can bind to the β_3 NPLY^{747} motif through its PTB domain but do not activate integrin, and thereby can function as competitive inhibitors of talin binding (*51, 57*).

Recently, another protein, kindlin, has been identified as a direct integrin activator. Platelets lacking kindlin-3, which is specific to hematopoietic cells, were unable to activate integrins despite normal talin expression (*58*). Kindlin-1 and kindlin-2 can function as co-activators of talin and enhance the ability of overexpressed talin head domain to activate integrin $\alpha_{IIb}\beta_3$ in endothelial cells and CHO cells (*59, 60*). Their binding to β_3 tails requires the β_3 C-terminal region (NITY^{759}) (*59, 60*).

1.3.4 Integrin clustering

In addition to conformational changes of individual integrins, integrin activation promotes the lateral assembly of integrins (integrin clustering) within the plane of the plasma membrane. Integrin conformational changes and clustering are complementary for a cell to bind strongly to the ECM and for integrin signalling (*61*). Ligand affinity of individual integrins is increased by integrin activation, but for a cell to bind strongly to the ECM, it is not enough. Integrin clustering increases the avidity of binding so that the sum of hundreds or thousands of weak interactions constitute a tightly bound adhesive unit (*3*). In addition, integrin clustering is important for integrin outside-in signalling, increasing the local concentration of integrin-associated signalling molecules and triggering the activation of Src (a non-receptor tyrosine kinase encoded by the proto-oncogene of *src* which is highly similar to the v-*src* gene of *Rous sarcoma virus*) and FAK (focal adhesion kinase), as discussed in section 1.5.3.2 of this chapter.

$\alpha_{IIb}\beta_3$ clustering is promoted by extracellular and intracellular factors, including the binding of multivalent ligands, ligand self-association, relief from cytoskeletal constraints, and homomeric interactions of the transmembrane domains (*62-65*). Optimum oligomerization requires the participation of the integrin's transmembrane and cytoplasmic regions (*66*). However, whether the activated integrins can cluster spontaneously remains controversial. Protein fragments encompassing the transmembrane helix plus cytoplasmic tails of the α and β subunits of $\alpha_{IIb}\beta_3$ were able to form homodimers or homooligomers in phospholipid micelles (*67, 68*). It is possible that integrin TMDs interact heteromerically in the inactive state, but when

integrins are activated, the transmembrane domains separate and homooligomerize, which drives lateral clustering (*62*). However, cysteine scanning mutagenesis of integrin $\alpha_{IIb}\beta_3$ transmembrane domains did not reveal a specific interaction of these domains after integrin activation in living cells (*69*). Electron microscopic images of purified and activated $\alpha_{IIb}\beta_3$ integrins that were reconstituted into lipid bilayers did not show spontaneous clustering, but integrins clustered after fibrinogen binding (*22*). In a study using β-gal complementation and bioluminescence resonance energy transfer (BRET) assays to detect integrin clustering, direct activation of $\alpha_{IIb}\beta_3$ by $MnCl_2$ or an activating antibody did not cause clustering in the absence of fibrinogen (*64*).

1.4 Integrin outside-in signalling

Once integrins are active and clustering, they can transmit information into cells, a process known as outside-in signalling. These intracellular changes can be divided into three temporal stages: immediate, short-term and long-term (*3*). Immediate intracellular changes include rapid phosphorylation events, particularly tyrosine phosphorylation of specific substrates, and an up-regulation of lipid second messengers such as phosphatidylinositol-4,5-bisphosphate (PtdIns-4,5-P_2) and phosphatidylinositol-3,4,5-triphosphate (PtdIns-3,4,5-P_3). Short-term changes consist of cytoskeletal rearrangements, which are required for cell spreading, migration and polarity establishment. This step usually occurs within one hour of cell adhesion, and involves dynamic connections of integrins to the cell cytoskeleton, and activation of kinases and signal transduction pathways to regulate cytoskeletal rearrangements.

Long-term attachment to the ECM ultimately results in changes in signalling pathways and gene expression that influence the survival, growth, and differentiation of cells. Figure 1.5 shows the major signalling pathways and key players located downstream of integrin activation.

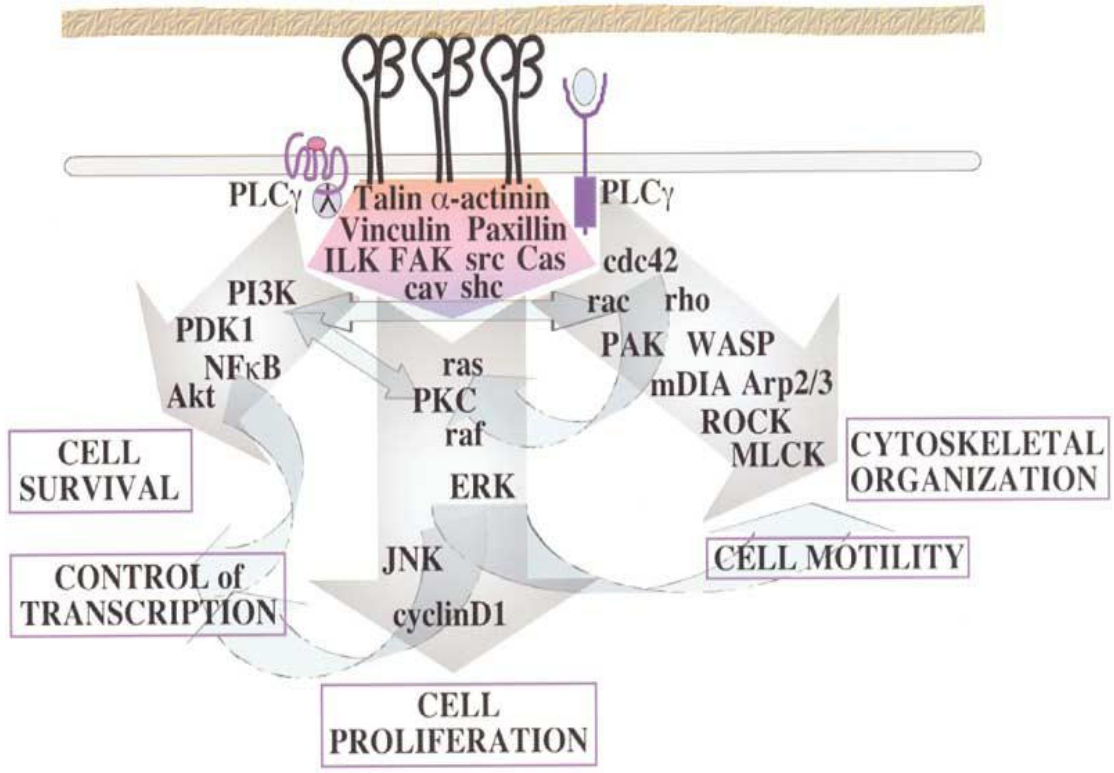

Figure 1.5: Integrin outside-in signalling. Major signalling pathways and key players downstream of integrin activation are illustrated. Integrin regulates downstream signalling pathways in cooperation with growth factor receptors to influence cell proliferation, differentiation, cell shape and migration. Integrin-associated proteins linking integrins and these signal transduction pathways are shown within the pink-purple pentagon beneath the clustered integrins. Integrins activate ERK and JNK to regulate cell proliferation. Integrins regulate Rho GTPase activity through the Src/FAK complex, resulting in cytoskeletal organization and regulation of cell motility. Integrins also activate PI3K and regulate cell survival through Akt. Adapted from reference (*1*).

The inside-out and outside-in signalling pathways constitute the bidirectional signalling across integrin receptors. Cytoplasmic tails of integrins serve as receivers

and transmitters of the bidirectional signal. Integrin cytoplasmic tails possess no enzymatic or kinase activity. One of the primary mechanisms of signal transduction is via recruiting cytoplasmic binding proteins following integrin activation and clustering. An overwhelming collection of cytoplasmic molecules that directly or indirectly interact with $\alpha_{IIb}\beta_3$ has been identified (*70, 71*).

1.5 Integrin mediated cell adhesion and spreading

1.5.1 Integrin adhesome

Integrins mediate cell-matrix adhesion by linking the ECM to the actin cytoskeleton (*1*). First, ligand-bound integrins cluster together and engage other proteins to organize into small and transient cell-ECM contacts called nascent adhesions (*72, 73*). As cells spread and migrate, nascent adhesions either disassemble or progress to larger dot-like adhesions called focal complexes, which locate slightly back from the leading edge and persist for several minutes (*74*). In more fully spreading cells, focal complexes can mature into larger and elongated focal adhesions. Focal adhesions reside at the ends of actin stress fibers (bundles of actin filaments) (*74*). Focal adhesions and stress fibers are cellular structures that are important for exerting contractile forces during cell migration.

Adhesion sites (nascent adhesions, focal complexes and focal adhesions) are large multiprotein complexes consisting of at least 180 signalling, structural, and adaptor molecules (*75*). These molecules and their interactions (at least 742) form a complex network termed the ‘integrin adhesome’ (*75*). In general, the integrin adhesome is

divided into structural and regulatory/signalling sub-networks (*75, 76*). The structural sub-network serves as a mechanical linkage between the ECM and cell cytoskeleton and generates traction force required for cell spreading and migration (*1*). Integrins anchor the intracellular cytoskeleton to the ECM by recruiting cytoskeletal proteins, such as talin, filament, α-actinin and tensin (*76*). These proteins can bind to F-actin and therefore couple integrins to the cytoskeleton directly (*70*). The regulatory/signalling sub-network includes multiple biochemical signalling hubs for many cellular processes, including actin polymerization and actomyosin contraction, cell proliferation and survival, and gene expression (*77, 78*). Integrins recruit and activate various catalytic proteins, such as FAK, integrin linked kinase (ILK), Src family kinase (SFK) and protein phosphatase 2A (PP2A). They facilitate the propagation of signal-transduction pathways from adhesion sites, and translate environmental cues into biochemical signals within cells (*70*).

1.5.2 Cell spreading: integrin-mediated control of cell protrusion and contraction

Cell spreading on the ECM requires two fundamental cellular processes, actin polymerization and actin-myosin contraction, the balance of which are tightly controlled and organized by integrin outside-in signalling (*79, 80*). After spherical cells in suspension adhere to the ECM, they quickly spread to a more flattened shape. They form protrusions at the cell leading edge, broad lamellipodia and spike-like filopodia. Formation of cell membrane protrusions is driven by actin polymerization (*81*). Actin polymerization is catalyzed by the ARP2/3 complex, which makes a

branched actin filament network through its actin nucleation function (*82*). After spreading, the cells form specialized structures such as stress fibers and focal adhesions. Contraction of actin stress fibers is mediated by myosin. During contraction, actin filaments do not shorten, but myosin mediates actin filaments to slide past each other (*83*).

The balance between actin-mediated protrusions and myosin-mediated contractions is controlled by members of the Rho GTPase family, particularly Rac, RhoA, and CDC42 (*77, 84*). The activity of ARP2/3 is regulated by Rac and CDC42 (*72, 85*). Myosin activity is regulated by phosphorylation of its myosin regulatory light chain (MRLC) at Thr18/Ser19 (*86*). Phosphorylation of MRLC is dependent on several protein kinases and phosphatases, most of which are downstream effectors of Rho GTPases (*72*).

As initial cell adhesion and spreading occurs, Rac and CDC42 are activated at the cell leading edge to mediate the formation of actin-rich membrane protrusions (*80*). Rac and CDC42 probably have overlapping functions to enhance protrusion formation. Whereas the expression of activated CDC42 alone produces filopodia, and expression of Rac stimulates formation of broad lamellipodia (*3*), RhoA promotes cell contractility by increasing phosphorylation of MRLC (*87*). At later stages of cell spreading, RhoA activation is necessary for maturation of focal adhesions and retraction of the cell rear edge (*13, 80*).

Two groups of molecules acting downstream of integrin outside-in signalling, guanine nucleotide exchange factors (GEFs) and GTPase activating proteins (GAPs),

directly control Rho GTPase activity (*80*). Rho family GTPases are active when they are GTP-bound and inactive when bound to GDP. Activation is catalyzed by GEFs and inactivation is promoted by GAPs that stimulate the intrinsic GTPase activity of the Rho proteins. In one example of this pathway, integrin ligation and clustering lead to activation of tyrosine kinases FAK and Src, which phosphorylate and recruit the scaffolding protein p130Cas (*88*). Tyr phosphorylation of p130Cas recruits SH2-containing adaptor protein Crk, which in turn recruits or activates Dock180. Dock180 is a GEF for Rac and mediates GTP loading and membrane targeting of Rac (*89, 90*). Active Rac promotes protrusion at the leading edge of the cell via WASP/WAVE-dependent activation of the Arp2/3 complex (*91*).

1.5.3 Integrin cytoplasmic tail-binding proteins

Integrin cytoplasmic tails play a critical role in regulating cell adhesion and spreading. Integrin cytoplasmic tails serve as a scaffold for adhesion components which in turn recruit other additional components leading to adhesome assembly (*92, 93*). Many binding proteins have been identified, but there are relatively few binding sites within α_{IIb} and β_3 cytoplasmic tails (*47, 70, 71*). For example, Src-family kinase Fyn (*94*), paxillin (*95*) and skelemin (*96*) can each bind to the membrane-proximal region of β_3 cytoplasmic tails. The membrane-proximal region of β_3 tails is also involved in the formation of the interface with α_{IIb} tails in inactive integrins. Once integrins bind to their ECM ligands, unclasping the interface may unmask binding sites for these proteins and enable their recruitment (*70*).

1.5.3.1 Proteins linking integrins to the cytoskeleton

Talin is the best-studied protein that is recruited by integrin cytoplasmic tails into adhesions. Talin contains a globular head and a long rod domain. The head domain is sufficient for integrin activation by binding to integrin cytoplasmic tails (*28*). The talin rod contains many functional domains, including domains responsible for dimer formation, a direct actin-binding site at the carboxy-terminus, a second integrin-binding site and several binding sites for vinculin (*97*). Talin accumulates at nascent adhesions which form within 15 minutes after cells are plated on the ECM (*98*). Microinjection of antibodies to talin or talin antisense RNA disrupts stress fibers and inhibits cell adhesion, spreading and migration (*99*). The ECM–integrin–cytoskeletal linkage provides a migration force at the leading edge of a migratory cell. A previous study showed that the binding of talin to minimal complexes of ligated integrins is an early step in the formation of integrin-mediated ECM–cytoskeleton connections (*100*). After $\alpha_V\beta_3$ binding to fibronectin, a weak bond connecting fibronectin and cytoskeleton was established to provide the initial mechanical force (*100*). However, this bond was disrupted in fibroblasts deficient in talin expression (*100*). Reexpression of wild-type talin1, but not talin1 lacking the actin-binding site, restored the weak force (*100*).

Other cytoskeletal proteins including filamin, α-actinin, myosin, and skelemin are reported to directly bind with β_3 tails (*70, 101*). Filamin and α-actinin are also actin-binding proteins. Filamin has important roles for actin crosslinking and is

involved in cell spreading and motility by connecting integrins to the cytoskeleton (*57, 102*). α-actinin is also an effective actin cross-linker (*103, 104*), and has essential roles in the assembly and maturation of nascent adhesions (*105*).

Skelemin is another cytoskeletal protein that can interact with integrin cytoplasmic tails (33). Skelemin is a myosin-binding protein and was originally found to concentrate at the periphery of M-disc (the region in the middle of myosin bundles) in muscle cells (*106, 107*). *In vitro* studies mapped the skelemin binding site at the membrane proximal regions of α_{IIb} and β_3 tails (*96*). It is of interest that skelemin co-localizes with $\alpha_{IIb}\beta_3$ in newly formed adhesions, but does not appear to be present in focal adhesions (*108*). However, the significance of skelemin binding is not yet clear.

1.5.3.2 FAK and Src: switching on integrin signalling

FAK and Src are crucial mediators of integrin signalling pathways that regulate the activation of Rho-GTPases. Both of them are non-receptor tyrosine kinases and their recruitment to the integrin cytoplasmic tail is an early event in adhesion assembly and acts to initiate integrin outside-in signalling.

The N-terminal domain of FAK binds to integrin-tail peptides *in vitro* (*95*). Ligand engagement and clustering of integrins results in rapid autophosphorylation of FAK at Tyr397, as well as several additional sites within the kinase and C-terminal domains (*109*). Phosphorylation at Tyr397 leads only to a limited activation of FAK, but it generates an SH2-mediated interaction with Src. This interaction enzymatically

activates Src by releasing autoinhibition imposed by the interaction between its SH2 domain and the inhibitory phosphorylated tyrosine (Tyr529). Src in turn phosphorylates other tyrosine sites of FAK, leading to maximal activation of FAK (*109, 110*).

FAK activation is closely associated with focal adhesion formation and cell migration (*111*). FAK-null fibroblasts exhibit enhanced paxillin phosphorylation and adhesion formation, suggesting FAK activity is essential for efficient focal adhesion turnover in cell migration (*112*). FAK inhibition could result in compromised cell mobility whereas enhanced FAK activity promotes cell migration (*111*).

The Src family of kinases contains nine members; Src, Fyn, Yes, Lck, Hck, Blk, Fgr, Lyn and Yrk, where Src is considered to be a principle player in $\alpha_{IIb}\beta_3$-mediated signalling (*3*). Src constitutively associates with $\alpha_{IIb}\beta_3$ in platelets (*113-115*). The association is mediated by interaction of the SH3 domain of Src with the four terminal residues of the β_3 tail, ^{759}YRGT (*115*). This association is important for integrin functions. For example, disrupting the interaction of integrin $\alpha_{IIb}\beta_3$ with Src kinase, either by substitution of β_3 Thr762 with Ala or by treatment with an RGT synthetic peptide into human platelets leads to decreased platelet spreading on fibrinogen (*116, 117*). A "β3 (Δ760-762)" knock-in mouse strain was generated, which lacked RGT residues of β3 tails necessary for the interaction with Src, but retained residues necessary for talin-dependent fibrinogen binding. The mice had variably prolonged tail bleeding times. Their platelets showed reduced spreading after plating on fibrinogen (*118*).

Activity of Src is negatively regulated by a phosphorylated tyrosine residue (Tyr529), which binds to the SH2 domain of Src leading to a closed conformation and inactivation of Src. Csk (c-Src terminal kinase) is a negative regulator of Src kinases, acting by phosphorylating Tyr529 to maintain Src autoinhibition. Dephosphorylation by protein–tyrosine phosphatase (PTP) at Tyr529 and phosphorylation at Tyr418 leads to Src activation. In resting platelets, Src forms a complex with $\alpha_{IIb}\beta_3$ and Csk (*113*). Fibrinogen binding to $\alpha_{IIb}\beta_3$ leads to Csk dissociation from $\alpha_{IIb}\beta_3$, PTP-1B recruitment to this inhibitory complex to dephosphorylate Tyr529, and autophosphorylation at Tyr418 (*113-115*). The clustering of integrins brings Src molecules into close proximity, potentially promoting Src transactivation. Another possible mechanism of Src activation is via FAK. Upon autophosphorylation, FAK Tyr 397 constitutes a docking site for the Src SH2 domain and relieves the intramolecular, inhibitory interactions on Src to activate the protein (*119*).

Src is required for integrin-mediated adhesion and spreading. Pharmacological and genetic inhibition of Src in a variety of cell types impaired adhesion, while exogenous expression of activated Src promoted cell adhesion and spreading (*91*). For example, in Src-deficient fibroblasts, cell spreading is inhibited on fibronectin or vitronectin. The defective spreading is rescued by re-expression of Src (*120, 121*). In a study using epithelial cancer cell lines as a model, elevation of Src expression and activation has been implicated in progression of cancer cells to metastatic cells, which is not linked to enhanced cell growth, but rather to enhanced cell attachment to ECM and assembly of adhesion complexes (*122*).

Src mediates Tyr phosphorylation of FAK, $p130^{CAS}$, paxillin and other adhesion molecules (*123, 124*). Characterization of these proteins revealed that they are major components of integrin-dependent signalling pathways. As previously described, Src phosphorylates FAK leading to full activation of FAK, and Src and FAK function as a complex to initiate integrin downstream signalling (*91*). $p130^{CAS}$ and paxillin are scaffold proteins, in which the phosphorylation of their Tyr residues recruits and organizes signalling molecules.

1.5.4 Physiological and pathological implications

Platelets and $\alpha_{IIb}\beta_3$-expressing CHO cells adherent to fibrinogen are broadly used model systems to study cell adhesion and spreading. Upon activation by inside-out signalling, $\alpha_{IIb}\beta_3$ integrins on platelets are capable of binding to soluble fibrinogen to form a thrombotic clot. During this process, $\alpha_{IIb}\beta_3$ integrins not only mediate platelet-platelet interactions, but also transmit an array of signals into the platelets, inducing a series of coordinated events including platelet adhesion, shape change, spreading on fibrinogen or fibrin matrix and clot retraction (*125*). First, $\alpha_{IIb}\beta_3$ adhesion to fibrin stimulates dramatic cell shape changes. Discoid platelets develop spike-like filopodia and lamellipodial extension to mediate full spreading over the damaged area and thus seal the vessel wall (*88*). The morphologic changes are associated with dynamic actin polymerization and reorganization. After platelets adhere and aggregate at the wound site, the next step is the retraction of clots through contractile forces generated by the platelet actomyosin network and to ‘shrink’ the

thrombus' size (*125*). Retraction of clots stabilizes platelet aggregates, restores blood flow and also draws the wound edges together during wound repair. $\alpha_{IIb}\beta_3$ outside-in signalling leading to cytoskeletal reorganization and development of contractile force is crucial for these processes (*126*).

Tumor progression has been associated with altered integrin-mediated adhesion. To undergo metastasis, circulating tumour cells must attach to vascular endothelial cells or components of the vessel wall. They enter the blood flow to reach the target organs, and then colonize and grow in distant organs. Specific interactions of tumour cells with the favourable environments of distant organs help initiate and promote tumour metastasis and growth (*127*). Highly tumorigenic breast cancer cells expressing β_1 and β_3 integrin family members adhere rapidly to bone ECM, suggesting an important contribution of integrin-matrix interaction to the establishment of breast cancer cells in bone (*128*). Furthermore, integrin adhesion to the ECM provides the traction force necessary for tumour cell motility and invasion of distant organs (*129*). Intravenous inoculation of MDA-MB-231 transfectants overexpressing $\alpha_v\beta_3$ in animals increased bone metastasis when compared with the inoculation of mock-transfected cancer cells (*130*). Treatment of animals with antagonists of $\alpha_v\beta_3$ reduces bone metastasis (*130, 131*). Integrins also regulate ECM remodelling and protease activity such as matrix metalloproteinase (MMP), and support tumor cell proliferation in either adhesion-dependent or −independent mechanisms (*129*).

1.6 $\alpha_{IIb}\beta_3$ antagonism

Excessive platelet aggregation is a key event in myocardial infarction and other thrombotic diseases. $\alpha_{IIb}\beta_3$ has become an attractive pharmacological target for antithrombotic therapy because of its importance in platelet aggregation. A number of $\alpha_{IIb}\beta_3$ antagonists have undergone clinical testing for their potential use as short-term and long-term cardiovascular therapeutics. In the 1990s, three intravenous $\alpha_{IIb}\beta_3$ antagonists approved by the FDA were: abciximab, a mouse/human chimeric antibody fragment c7E3 Fab; eptifibitide, a snake venom disintegrin-derived cyclic peptide; and tirofiban, a RGD peptidomemetic. These inhibitors have been approved for and are widely used for treatment of patients with acute coronary syndromes (ACSs), and have especially benefited patients undergoing percutaneous coronary intervention (PCI). The major side effect of these agents is bleeding complications. Choosing an optimal dosing was a challenge, as the window between the therapeutically efficacious doses to prevent platelet aggregation and higher doses that can lead to bleeding is narrow (*132*).

To achieve long-term suppression of platelet aggregation and to prevent cardiovascular diseases, orally active $\alpha_{IIb}\beta_3$ antagonists were developed. However, the clinical trials were disappointing, with lack of efficacy and increased mortality of patients with ACS (*133*). One potential contributing factor is the activating property of the $\alpha_{IIb}\beta_3$ antagonists. An early study in 1991 showed that RGD peptide binding could induce a high affinity fibrinogen-binding conformation of $\alpha_{IIb}\beta_3$ (integrin activation) and subsequent platelet aggregation (*134*). Several $\alpha_{IIb}\beta_3$ antagonists are

ligand-mimetics, suggesting they may possess partial agonist effects. The monoclonal antibody abciximab, when used at low concentrations, also demonstrated an intrinsic activating property, resulting in fibrinogen binding to $\alpha_{IIb}\beta_3$ and activation of platelets (*135*). Specific types of $\alpha_{IIb}\beta_3$ antagonists can augment agonist-induced release of α-granules, a marker of platelet activation (*136*). In fact, platelet activation has been reported in patients with ACS receiving oral $\alpha_{IIb}\beta_3$ antagonist at low concentrations (*137*).

An alternative strategy is to target the intracellular events of integrin signalling. Mice harbouring the point mutation (L746A) in the β_3 tail that selectively disrupted interactions only with talin were resistant to both pulmonary thromboembolism and thrombosis of the carotid artery, but exhibited limited bleeding (*138*). This study suggested that targeting of β_3 integrin–talin interactions may have advantages over current $\alpha_{IIb}\beta_3$ antagonists due to a reduced risk of pathological bleeding. In addition, membrane permeable peptides corresponding to specific segments of the cytoplasmic tails of α_{IIb} and β_3 were shown to inhibit activation of $\alpha_{IIb}\beta_3$ (*139-141*). However, these intracellular approaches to inhibit $\alpha_{IIb}\beta_3$ are only in the early stage of development.

1.7 Rational and hypothesis

Integrin inside-out signalling increases the affinity of integrins for ECM ligands. Ligated integrins generate outside-in signalling that controls many critical intracellular changes. Both inside-out and outside-in signalling of $\alpha_{IIb}\beta_3$, the

predominant integrin expressed in platelets, is important to form a stable thrombus *in vivo*. Binding of fibrinogen by the extracellular domain of $\alpha_{IIb}\beta_3$ directly supports platelet-platelet interactions. Occupied $\alpha_{IIb}\beta_3$ integrins cluster and trigger outside-in signalling that stabilizes the aggregate and supports wound healing responses.

The interaction of intracellular molecules with the integrin's cytoplasmic domain regulates the integrin activation state and/or integrin outside-in signalling. There are particular amino acids or motifs in both α and β cytoplasmic tails of $\alpha_{IIb}\beta_3$ that serve as binding sites for intracellular binding partners. Their interactions could generate an activation signal that leads to conformational changes within the ligand binding site, resulting in the expression of a competent receptor. In addition, some interactions occur after ligand binding, and could influence outside-in signalling and regulate intracellular events, such as cytoskeleton reorganization, cell spreading and motility.

Among the cellular proteins that can directly interact with integrin cytoplasmic domains, skelemin is of particular interest as it can bind with the membrane proximal regions of both α_{IIb} and β_3 tails and shows dynamic co-localization with $\alpha_{IIb}\beta_3$ in newly formed adhesions (*96*) (*108*). We hypothesize that skelemin is not involved in the regulation of integrin activation, but is an important modulator for integrin outside-in signalling and acts to fine-tune the cell spreading process together with other cytoskeletal proteins.

In addition, both α_{IIb} and α_v integrin subunits can pair with β_3 subunits to form functional receptors, and they also share the central-turn motif within their cytoplasmic tails. These characteristics reveal a possible convergence in the

regulatory control of $\alpha_{IIb}\beta_3$ and $\alpha_V\beta_3$. Previous studies showed the antagonistic effects of the turn motif peptide derived from α_V tails. Here, it is hypothesized that the turn motif of α_{IIb} tails is important for the regulation of integrin functions. The turn motif-derived peptide (α_{IIb} peptide) may not only inhibit $\alpha_{IIb}\beta_3$-ligand engagement, but also target α_v integrins. To explore this hypothesis, the modes of function of the α_{IIb} peptide have been investigated.

1.8 Specific aims

1.8.1 Aim 1: Evaluate the contribution of skelemin-$\alpha_{IIb}\beta_3$ interaction to integrin bi-directional signalling

To determine the functional consequences of these interactions on $\alpha_{IIb}\beta_3$ bi-directional signalling, expression of $\alpha_{IIb}\beta_3$ on CHO cells was used to examine integrin inside-out and outside-in signalling. A series of stable CHO cell lines were established, which expressed mutant $\alpha_{IIb}\beta_3$ receptors where skelemin binding residues at the membrane proximal region of integrin tails were mutated by alanine substitution. Cell surface expression of receptors and integrin activation states of mutant cells were first examined by flow cytometry. Transfection of skelemin immunoglobulin C2 motifs 4-5 that contain the $\alpha_{IIb}\beta_3$-binding domain (skeC2) into wild-type and mutant cells was used to characterize whether skelemin is involved in the regulation of integrin activation. To study the effects of the skelemin-integrin interaction on integrin outside-in signalling, three major experimental techniques were used, cell adhesion, cell spreading, and activation of downstream signalling molecules.

Confocal microscopy experiments were employed to determine whether skelemin colocalizes with $\alpha_{IIb}\beta_3$ in wild-type and mutant cells. As talin contact sites on $\alpha_{IIb}\beta_3$ overlap those of skelemin, the study of skelemin and talin colocalization with $\alpha_{IIb}\beta_3$ also gives insights into whether the binding of the two proteins with integrin is mutually exclusive.

1.8.2 Aim 2: Determine the mode of action of bioactive cell permeable cytoplasmic peptides

There are activating and inhibitory functional motifs within the cytoplasmic tails of $\alpha_{IIb}\beta_3$. To test the capacity of cytoplasmic peptides to influence integrin activation on live cells, myristoylation of peptides was used as a means of efficient and non-invasive intracellular delivery. Our previous data indicate that the inhibitory capacity of the α_V cytoplasmic tail peptide resides near the PP-turn motif. A peptide that derived from the turn motif of α_{IIb} tails, its homologous α_V peptide, and mutant peptide RPP/AAA and its scrambled form were synthesized. The functional properties of these peptides were examined in $\alpha_{IIb}\beta_3$-expressing CHO cells and the breast cancer cell lines, MDA-MB-435 and MDF-7. Cell adhesion assays and soluble ligand binding were performed to examine the inhibitory capacity and specificity of the peptides. To identify proteins that interact with the α_{IIb} peptide, CHO cell lysates were immunoprecipitated with biotinylated peptides. Bound proteins were separated by sodium dodecyl sulfate polyacrylamide gel electrophoresis (SDS-PAGE), excised and subjected to mass spectrometry analysis. Furthermore, integrin downstream signalling

molecules in peptide-treated cells were examined with Western-blot. Whether the peptides still possess inhibitory capacity after ligand engagement was also investigated.

CHAPTER 2 MATERIALS AND METHODS

2.1 Cell culture

CHO, MDA-MB-435 and MCF-7 cells were cultured in Dulbecco's Modified Eagle's Medium (DMEM) containing 10% fetal bovine serum (FBS), 100 units/ml penicillin, and 100 μg/ml streptomycin at 37℃ in a humidified atmosphere of 5% CO_2 and 95% air. Stable $\alpha_{IIb}\beta_3$-expressing CHO cells were maintained in the presence of 400 μg/ml G418 (Geneticin) and 300 μg/ml hygromycin B and cultured in DMEM containing 10% FBS, 100 units/ml penicillin, and 100 μg/ml streptomycin. Hek293 cells were cultured in RPMI-1640 medium containing 10% FBS, 100 units/ml penicillin, and 100 μg/ml streptomycin at 37℃ in a humidified atmosphere of 5% CO_2 and 95% air.

2.2 Generation of stable $\alpha_{IIb}\beta_3$-expressing CHO cell lines

The cDNAs for α_{IIb} and β_3 integrin subunits were cloned into pcDNA3.1 vectors harbouring neomycin and hygromycin resistance genes respectively. Mutations were carried out with the use of a site-directed mutagenesis strategy. All sequences were verified by DNA sequencing. CHO cells were transfected using Lipofectamine (Invitrogen Corp.) with the respective plasmids for both α_{IIb} and β_3 subunits according to the manufacturer's instructions. At 48 hours after transfection, cells were harvested, diluted, and grown in fresh medium containing the selection reagent, G418 (600 μg/ml) and hygromycin B (500 μg/ml). Selection media was changed every 2-3 days

until cell colonies formed. To obtain single cell clones, cells were treated with Trypsin-EDTA for 3 minutes before cells completely detached. Each colony was gently sucked up with a 200 μl pipette and immediately transferred to a 96-well plate containing the appropriate selection agent. After the cells grew to full confluence, they were harvested and their integrin expression levels were evaluated with flow cytometry. Briefly, 1×10^6 cells from each clone were trypsinized, suspended in PBS and incubated with 5 μg/mL anti-β_3 antibody (CD61, Invitrogen) for one hour on ice, followed by labelling with goat anti-mouse Alexafluor 488-labelled antibody (Invitrogen), and then analyzed using flow cytometry The clones with the highest fluorescence intensity were chosen and grown in culture medium containing 400 μg/ml G418 and 300 μg/ml hygromycin B. After 1-2 months growth, a stable cell line was generated with more than 95% β_3 positive.

2.3 Flow cytometry

CHO cells were grown to 70–80% confluence and trypsinized. After quenching with complete medium, the cells were suspended in Tyrodes buffer containing 1 mM $CaCl_2$, 1 mM $MgCl_2$, 0.1% glucose and 0.1% BSA. To measure cell surface levels of integrin, CHO cells were incubated with 5 μg/mL anti-β_3 mAb (Invitrogen) for one hour on ice. Cells were then washed, incubated with a secondary goat anti-mouse phycoerythryn (PE)-labelled antibody, and analyzed by flow cytomety.

For PAC-1 binding, 5×10^5 cells were harvested and pre-treated with Tyrodes buffer containing 2 mM Ca^{2+}, 200 μM Mn^{2+} or 2 mM EDTA at 37℃ for 15 minutes.

Cells were then incubated with PAC-1 (10 μg/ml, Becton Dickinson) at room temperature for one hour, washed and then incubated with PE-labelled goat anti-mouse Ig (BD Biosciences) for one hour on ice. Cells were analyzed by flow cytometry. The mean fluorescence intensity was used to provide a measure of ligand binding affinity of integrins.

To assess the effect of skelemin fragment expression on the integrin affinity state, cells were transiently transfected with green fluorescence protein (GFP) or GFP-skeC2 using Lipofectamine (as above). After 48 hours, cells were harvested and pre-treated with Tyrodes buffer containing 2 mM Ca^{2+}, 200 μM Mn^{2+} or 2 mM EDTA at 37℃ for 15 minutes. PAC-1 binding assays were carried out following the above method. An integrin activation index was used to compare integrin activation levels in GFP and GFP-skeC2 transfected cells for each mutant. The activation index was calculated using the following formula: $100 \times (F_{Ca} - F_{EDTA})/F_{Mn}$, where F_{Ca} is the mean fluorescence intensity (MFI) of PAC-1 binding in the presence of Ca^{2+}, F_{EDTA} is the PAC-1 binding in the presence of EDTA, and F_{Mn} is the maximal PAC-1 binding in the cells treated with Mn^{2+}.

2.4 Cell adhesion assay

The day before performing the cell adhesion assay, 96-well tissue culture plates were coated overnight at 4℃ with 50 μl of 20 μg/ml fibrinogen, 5μg/mL vitronectin or heat-denatured 1% bovine serum albumin (BSA). Cells were grown to 70–80% confluence and detached with Trypsin-EDTA. After quenching the trypsin with

complete medium, cells were suspended in PBS. Cell number was counted on a coulter counter (Beckman Coulter) to obtain 5×10^4/well. Cells were incubated with cell permeable, non-fluorescent dye Calcein AM (10 μM Invitrogen) at 37℃ for 30 minutes in the dark. Calcein-AM is hydrolyzed by intracellular esterases to the cell membrane-impermeable green-fluorescent Calcein. Because the esterase activity is proportion to the number of viable cells, the fluorescence produced is used as a measure of the cell number. Labelled cells were washed twice and resuspended at 5×10^5 cells/mL in Tyrode's buffer containing 1 mM $CaCl_2$, 1 mM $MgCl_2$, 0.1% glucose and 0.1% BSA. The cells were then added to each well (4×10^5 cells in 100 μl) and incubated at 37℃ for 30 minutes. Once cells were added, the cell fluorescence intensity for each well (FL1) was measured on the SpectraMax M2e microplate reader at 494 nm excitation and 517 nm emission wavelengths. After adhesion on ligand at 37℃ for 30 min, unbound or weakly attached cells were removed by washing twice with PBS. The cell fluorescence intensity after washing (FL2) was measured. Cell adhesion was quantified with the percentage of fluorescence intensity of attached cells relative to that of total cells (100 ×FL2/FL1).

For peptide treatment, the peptide stock solution (2.5 mM) was added into cell suspensions after cells were labelled by Calcein AM. Cells were treated with peptides for 20 minutes at 37℃. Then 100 μL of cell suspension (5×10^4/well), in the presence of peptides, was added to a ligand-coated 96-well plate. The cell fluorescence intensity before and after washing was measured and cell adhesion was quantified as described above.

For function-blocking cell adhesion experiments, labelled breast cancer cells were incubated with 10 μg/mL of each antibody for 20 minutes at room temperature. Then 100 μL of cell suspension (5×10^4/well) in the presence of antibodies was added to a ligand-coated 96-well plate. Three antibodies were used as function-blocking antibodies; $\alpha_v\beta_3$ (MAB1976, Millipore), $\alpha_v\beta_5$ (MAB1961, Millipore) and $\alpha_v\beta_6$ (MAB2077Z, Millipore). The cell fluorescence intensity before and after washing was measured and cell adhesion was quantified as described above.

2.5 Platelet aggregation assay

Blood was drawn by venepuncture using 3.2% buffered sodium citrate as the anticoagulant. Platelet-rich plasma (PRP) was prepared by centrifugation at 150 g for 15 minutes and used within 4 hours. The PRP was carefully removed and platelet poor plasma (PPP) was obtained by centrifuging the remaining blood at 1200 g for 15 minutes. The platelet count of PRP was measured on a coulter counter (Beckman Coulter) and adjusted to 2 x 10^8 platelets/ml using PPP. PRP (450 μl) was transferred to siliconized glass aggregometer tubes. The aggregometer tubes were transferred to a 560CA whole blood lumi-aggregometer (Chronolog Corp.) which measures the changes in light optical density for each sample. The PRP was warmed to 37℃ for five minutes. In peptide post-treatment assay, platelet aggregation was initiated by the addition of ADP (10 μM) and epinephrine (EPI) (20 μM). Five minutes later, 50 μl of the test peptide or control peptide were added and the samples were monitored for an additional five minutes. In peptide pre-treatment assay, the PRP was treated with 50

μM peptides. Then ADP (10 μM) and EPI (20 μM) were added and platelet aggregation was monitored.

2.6 Immunohistochemistry

Falcon 4-well culture slides were treated with 1% SDS, rinsed with PBS and then coated with 20 g/ml of fibrinogen or 5 μg/ml vitronectin overnight at 4℃. Cells were seeded and adhered to culture slides for different times. Cells were fixed in 4% paraformaldehyde for 10 minutes, permeabilized by 0.2% (V/V) Triton X-100 for 10 minutes, washed three times and blocked with 1% BSA in PBS. Filamentous actin (F-actin) was stained using Alexa Fluor 594 phalloidin (Invitrogen) for 30 minutes at a 1:40 dilution, and visualized using fluorescence microscope.

Focal adhesions were stained using an antibody to vinculin (hVin-1, Sigma) and then a fluorescein-conjugated secondary antibody. For visualization of integrin distribution, cells were fixed in 4% paraformaldehyde, incubated with β_3-specific mAb (AP3, GTI Diagnostics) overnight at 4℃ and then a fluorescein-conjugated secondary antibody for two hours. Permeabilization is not required for staining integrin receptors. For visualization of integrin and skelemin/talin colocalization, β_3 integrins were first stained as described above, and then talin (C-20, Santa Cruz) or skelemin (rabbit IgG from Dr. T. Ugarova) was stained with BD Cytofix/Cytoperm solution (BD Biosciences) following the manufacturer's instructions. This sequential approach preserved the cell surface antigens during the intracellular staining.

2.7 Co-immunoprecipitation

Wild-type and mutant CHO cells were transfected with GFP-skeC2 plasmids for 48 hour, then harvested and allowed to adhere to fibrinogen-coated dishes for one hour at 37 ℃. Cells were solubilized with lysis buffer [20 mM Tris-HCl (pH 7.4), 150 mM NaCl, 1% Triton X-100, 1 mM $CaCl_2$, 1 mM Phenylmethylsulfonyl Fluoride (PMSF), 100 μg/mL leupeptin, and 10 mM benzamidine] for one hour at 4 ℃. After centrifugation at 12,000 rpm (15 minutes, 4 ℃), the supernatant was collected as total cell proteins. Protein concentrations of lysates were determined via the bicinchoninic acid (BCA) assay (Sigma). Lysis buffer was added to make each sample up to a final volume of 600 μl, and contain equal amount of protein for each co-immunoprecipitation (600 μg to 1000 μg total proteins). The lysates were incubated with 2 μl anti-GFP serum (Invitrogen) for two hours at 4 ℃. The immunocomplexes were captured by incubation with 40 μl of Protein G-agarose overnight at 4 ℃ and washed three times. The immunocomplex samples were boiled in 20 μl 3× sample loading buffer [New England Biolabs; 187.5 mM Tris-HCl, 6% sodium dodecyl sulphate (SDS), 30% glycerol and 0.03% phenol red] for 5 minutes. Samples were then frozen or prepared for Western blot analysis.

2.8 Western-blot

CHO cells were harvested, washed and suspended in Tyrodes buffer containing 1 mM $CaCl_2$, 1 mM $MgCl_2$, 0.1% glucose and 0.1% BSA. Cells were allowed to adhere on fibrinogen-coated culture dishes for one hour at 37 ℃. The buffer was removed,

and cells were scraped from the tissue culture dish in cold PBS. Cell suspension was pooled, centrifuged, and the cell pellet was lysed for one hour at 4 ℃ in 120 μl of lysis buffer (CelLytic^{TM} M, Sigma) with protease inhibitor cocktail (Sigma) and protein phosphatase inhibitor (Millipore).

After starving with FBS-free media for 12 hours, MDA-MB-435 cells were detached with Trypsin-EDTA. Trypsin was quenched with complete medium and cells were then resuspended in Tyrode's buffer. Cells were incubated with 100 μM peptides at 37 ℃ for 20 minutes, and plated on vitronectin-coated dish. After 1 hour to allow for adhesion at 37 ℃, floating cells as well as adherent cells were collected and lysed in lysis buffer (CelLytic^{TM} M, Sigma) that contained protease inhibitors (Sigma) and protein phosphatase inhibitors (Millipore).

Cell lysate was kept on ice for 1 hour, followed by centrifugation at 12,000 rpm (15 minutes, 4 ℃). Protein concentrations of supernatant were determined via BCA assay (Sigma) to make sure of equal protein loading. Total proteins (50-100 ug) were boiled for 5 minutes in 3× sample loading buffer (New England Biolabs, 187.5 mM Tris-HCl, 6% SDS, 30% glycerol and 0.03% phenol red) and resolved by 7.5% SDS-PAGE. Proteins were then transferred to nitrocellulose membrane (Whatman) with a semi-dry protein transfer apparatus (40 minutes at 240 mA). The membrane was blocked with 5% TBST (Tris-Buffered Saline and Tween 20) blocking milk [TBS (100 mM Tris-Cl pH 8, 150 mM NaCl), 0.01% Tween (v/v), 5% non-fat milk] for 30 minutes at room temperature. 5% BSA in TBST was used to block membranes for detecting phosphorylated proteins. After blocking, membranes were incubated

overnight at 4℃ with primary antibodies as follows: anti-pY416-Src (100F9, Cell Signalling), anti-Src (mAb327, Calbiochem), anti-β_3 antibody (N20, Santa Cruz), anti-pY397 FAK (Santa Cruz), FAK (A-17, Santa Cruz), β-actin (Santa Cruz), phospho-Erk1/2 (197G2, Cell Signalling), and Erk1 (K-23, Santa Cruz).

Primary antibody was removed and membranes were washed 4-5 times with TBST. Membranes were then incubated with secondary antibodies conjugated with horseradish peroxidase in 5% TBST blocking milk for two hours at room temperature. Membranes were then washed with TBST three times. Proteins were detected by rinsing membranes with a 1:1 dilution of Chemiluminescence Substrate (PerkinElmer) and exposing them to X-ray film (Santa Cruz).

2.9 Peptide synthesis

Peptides were synthesized on an Applied Biosystems 433A peptide synthesizer at 0.25 mM scale using fourfold excess of 9-Fluorenylmethyl-carbonyl (Fmoc)-amino acids relative to the p-alcoxybenzyl-alcohol resin (Wang resin). Coupling was performed with 0.5 M N-Hydroxybenzotriazole/O-Benzotriazole-N,N,N',N'-tetramethyl-uronium-hexafluoro-phosphate (HOBt/HBTU).

The myristoylated peptides were synthesized by a covalent linkage of myristic acid to the N-terminal amino group of the lysine residue. Briefly, 1 ml N,N-Diisopropylethylamine (DIEA) in dimethylformamide (DMF) was added to the peptide-resin vessel and mixed for 5 minutes. The resin was drained and washed with DMF two times. 520 mg myristic acid was dissolved in dichloromethane (DCM) with

heating (at about 40 ℃, 10-15 seconds) and vortexing. Repeat heating and vortexing process until fully dissolved. Then 460 mg N,N'-Dicyclohexylcarbodiimide (DCC) dissolved in DMF were added to the myristic acid solution. After 5 minutes, the mixture of myristic acid and DCC was added to the peptide-resin vessel, with myristoylation was carried out under constant shaking. Myristoylation was monitored by the use of ninhydrin test (Applied Biosystems), which yields deep-blue or purple color by reacting with primary amines when the N-termini of peptides are not myristoylated. Completion of myristoylation was shown by a colorless negative result.

The myristoylated peptides on resin were washed and dried under high vacuum over night. The side-chain protecting groups on peptides were removed and peptides were cleaved from the resin by treatment with 10 ml trifluoroacetic acid (TFA):phenol:water:triisopropylsilane (TIPS) (88:5:5:2) for 4 hours.

Crude peptides were purified by semi-preparative reversed phase high-performance liquid chromatography (HPLC) on a C18 column (C18 is a silica-based column with octadecyl carbon chains bonded on silica). Purified peptides were analyzed on a Varian ProStar HPLC using a C18 column, 250 × 4.6 mm.

The biotin group was labelled on the amino group of Lys side chain. Briefly, 20 mg myristoylated peptide was dissolved in 4 ml DMF. 175 µl DIEA was added to the peptide solution. Immediately before use, a solution of N-Hydroxysuccinidobiotin (NHS-Biotin) was prepared by dissolving 19 mg NHS-Biotin in 500 µl DMF. The NHS-Biotin solution was then added to the peptide solution. The reaction mixture was

protected from light and stired with a magnetic stirring bar. After 4 hours of reaction, biotinylated peptides were purified by semi-preparative reversed phase HPLC on a C18 column.

The molecular weight of each peptide was confirmed by mass spectrometry and the purity was over 98%, as assessed by analytical HPLC (Figure 2.1A and B). The peptides were dissolved in 10% ethanol with pH 7-9 adjusted with 1M KOH. Cellular uptake and intracellular distribution of bio-peptides was studied by immunocytochemistry. The immunofluorescence microscopic image of the bio-α_v peptide distribution is representatively shown in Figure 2.1C.

2.10 Peptide electrophoresis on 20% SDS-PAGE gel

The electrophoretic mobility of peptides was assessed by using a 20% SDS-PAGE gel. Gels were cast and run using the BioRad Mini-PROTEAN® Electrophoresis system (BioRad). To prepare 6 ml separating gel solution, 3 ml 40% acrylamide, 2 ml 3 M Tris-Cl (pH 8.45), 60 μL 10% SDS(w/v), 200 μL H_2O and 634 μL glycerol were mixed. 50 μL ammonium persulfate (APS) and 5 μL tetramethylethylenediamine (TEMED) were added, mixed gently and then immediately poured between two glass plates immobilized in a casting apparatus. The gel solution was topped with a thin layer of ethanol to ensure a level surface. To prepare the stacking gel, 0.26 ml 40% acrylamide, 0.62 mL 3 M Tris-Cl (pH 8.45), 20 μL 10% (w/v) SDS and 1.62 mL H_2O were mixed. Once the separating gel is solidified, the ethanol was poured off and a stacking gel solution was poured on top of the separating gel and a gel comb was

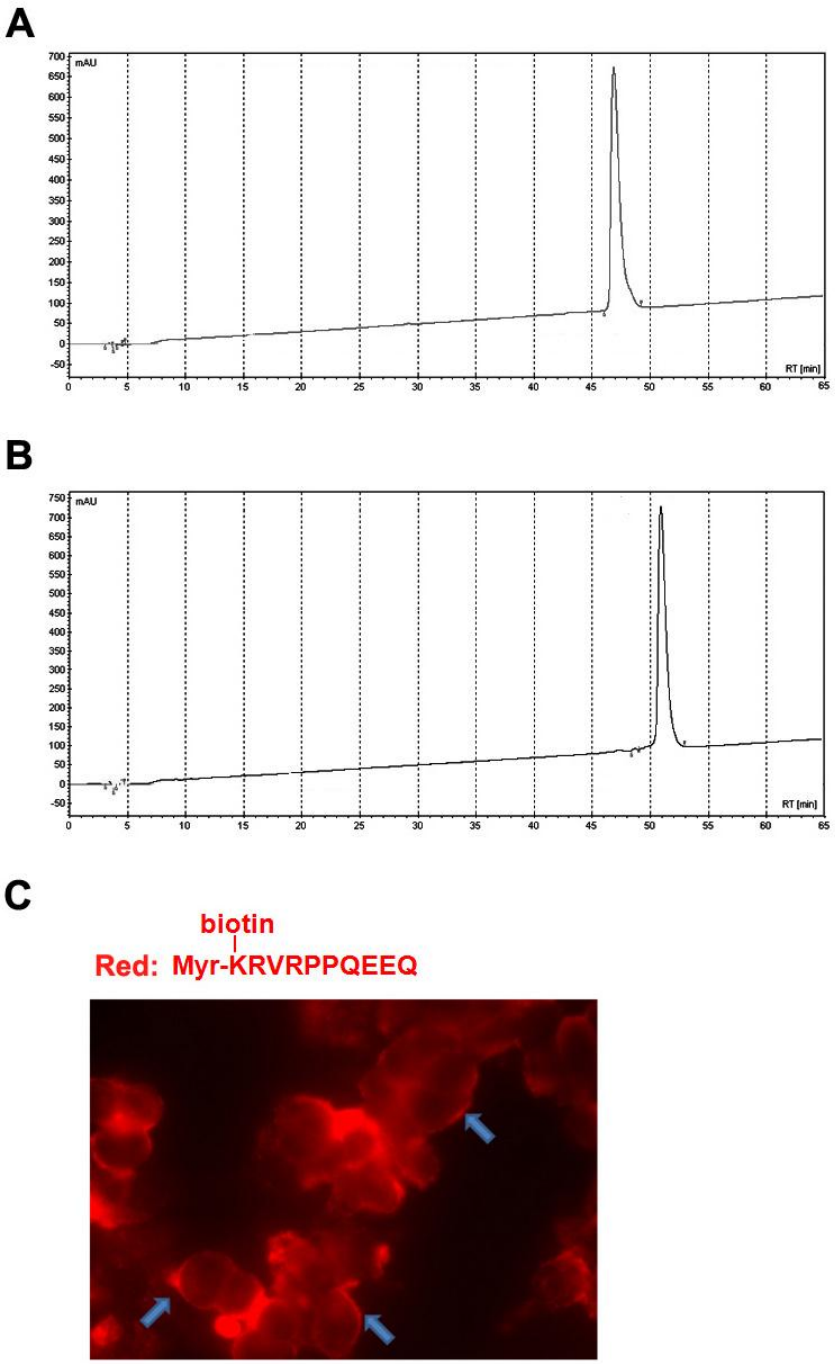

Figure 2.1 Purity and cellular distribution of the α_v peptide. (A, B) Histograms show HPLC tracings of the α_v (A) and bio-α_v (B) peptides. The solvent was aqueous acetonitrile with 0.1% TFA run at a flow rate of 1 ml/min. The gradients were 1–60% acetonitrile over 60 min. Detection was light absorption at 215 nm, where the peptide bond absorbs. (C) Cellular distrubution of the bio-α_v peptide. The α_V peptide was biotin labelled. After treated with bio-α_v for 30 minutes, MCF-7 cells were fixed in 4% paraformaldehyde for 10 min, and permeabilized by 0.2% (V/V) Triton X-100 for 5 min. Peptide was then stained by PE-labelled avidin and visualized by immunofluorescence microscope. The picture showed that most peptides were accumaulated on the plasma membrane, as indicated by the blue arrow.

inserted in the stacking gel. Before electrophoresis, 1 μg peptide sample was incubated with 3X SDS sample buffer (New England Biolabs; 187.5 mM Tris-HCl, 6% SDS, 30% glycerol and 0.03% phenol red, 0.125 mM DTT) at 70 ℃ for 10 min. The gel was run in tricine-SDS running buffer (100 mM Tris, 100 mM Tricine, 0.1% SDS) at a constant 150 Volts until desired peptides or proteins were sufficiently separated. Peptide bands were visualized by staining with 0.025% (w/v) Coomassie Blue R250. Briefly, the gel was placed in fixative solution (40% methanol, 10% acetic acid) and equilibrated for 30 minutes. Gels were stained in stain solution (0.025% (w/v) Coomassie Blue R250, 10% acetic acid) for one hour and distained in 10% acetic acid three times for 15 minutes or until the desired background was achieved.

2.11 Mn^{2+} stimulated fibrinogen binding assay

$\alpha_{IIb}\beta_3$-transfected CHO cells were harvested, and suspended at 1×10^7/ml in Tyrodes buffer containing 1 mM $CaCl_2$, 1 mM $MgCl_2$, 0.1% glucose and 0.1% BSA. 100 μl cell suspension was treated with different concentrations of each peptide for 15 minutes at 37 ℃, and stimulated with 400 μM Mn^{2+} for another 15 minutes. 5 μl 1.5 mg/ml Alexafluor 488-labelled fibrinogen (Molecular Probes) was then added to the cell suspension and incubated for 45 minutes at room temperature. Cells were washed twice with fibrinogen binding analyzed by flow cytometry.

In addition to flow cytometry, CHO cells prepared as above were analyzed by immunocytochemistry. Cell cultures were fixed with 4% paraformaldehyde for 10 minutes and stained with anti-β_3 antibody (AP3, GTI. Diagnostics), followed by the

addition of PE-labelled goat anti-mouse antibody. Cells in mounting media were plated on coverslips and visualized by confocal microscopy.

2.12 Co-immunoprecipitation with streptavidin-coated Dynabeads

25 μl Streptavidin-coated Dynabeads (M-280, Invitrogen) were washed in PBS three times, re-suspended and incubated for 2 hours at room temperature with constant rotation with or without 20 μg biotinylated peptides. Beads were washed four times in PBS. $\alpha_{IIb}\beta_3$-transfected CHO cells were harvested and lysed in lysis buffer (CelLytic™ , sigma) with protease inhibitor (Sigma). 120 μl cell lysate was diluted with 450 μl PBS, and incubated with activated beads at 4℃ overnight. Unbound proteins were removed by extensive washing in a buffer (20 mM tris pH 7.4, 1% triton-100, 50 mM NaCl, 1 mM Ca^{2+}, 1 mM Mg^{2+}). Associated proteins were eluted by boiling for 8 minutes in SDS sample buffer with DTT. Proteins were separated by 7.5% SDS-PAGE and visualized within the gel using silver staining (ProteoSilver™ Silver Stain Kit, Sigma). The gel bands of interest were cut out, trypsinized and the proteins within them were identified by mass spectrometry.

CHAPTER 3

SKELEMIN IN $\alpha_{IIb}\beta_3$ –MEDIATED CELL SPREADING

This chapter has been published as a paper in

Biochemistry (2013) 52: 681–689

*Contents of this chapter have been adapted / reproduced from the published article with permission from the journal "*Biochemistry*"*

3.1 Introduction

The role of integrin in cell adhesion, spreading and migration relies on its connection to the cell cytoskeleton. A numbers of proteins are recruited directly or indirectly via adaptors to the cytoplasmic tails of integrin, for example, talin, filamin, α-actinin and myosin (*71*). These proteins promote integrin-actin cytoskeleton linkage which influences reorganization of the actin cytoskeleton and generates traction forces necessary for cell spreading and migration. Skelemin was reported to bind to the β_1 and β_3 cytoplasmic tails via yeast two-hybrid assays (*142*). Skelemin is a cytoskeletal protein first identified in the periphery of the sarcomeric M-line of myosin thick filaments in striated muscles (*143*). In muscle cells, skelemin cross-linked myosin filaments to maintain the thick filament lattice (*144*), and to serve as a linker between M-band and intermediate filaments through a desmin binding domain (*107*). Skelemin is a myomesin isoform and belongs to a member of a family of myosin associated proteins. Skelemin and myomesin are encoded by the same gene but alternative

splicing gives rise to the insertion of a serine/proline-rich domain in the center of skelemin (*145*). Recent studies have confirmed the presence of skelemin in non-muscle cells, such as platelets and CHO cells (*108, 142, 146*). In addition, after adhering to immobilized ligand fibrinogen, skelemin can interact and co-localize with integrin $\alpha_{IIb}\beta_3$ at the initial stage of cell spreading, suggesting that skelemin serves as a cross-linker between integrin and the myosin cytoskeleton in non-muscle cells (*108, 142, 146*).

Skelemin is one of very few proteins reported to bind to both the α_{IIb} and β_3 cytoplasmic tails of an integrin (*96, 146*). It contains five repeats of fibronectin type III motifs and seven repeats of immunoglobulin superfamily C2-like motifs (*107*). The primary interaction of skelemin with $\alpha_{IIb}\beta_3$ involves the skelemin immunoglobulin C2 motif 5 and the membrane proximal regions of the $\alpha_{IIb}\beta_3$ cytoplasmic tails, while there is an additional low affinity contact between the skelemin immunoglobulin C2 motif 4 and the C-terminus of β_3 tails (*96, 142*). However, the functional significance of skelemin-integrin interactions has not been fully explored. In this chapter, integrin affinity state, outside-in signalling and related functions in CHO cells overexpressing mutant integrins lacking the capacity of bind skelemin were investigated. Dr. Haas and his collaborators previously identified the critical residues in the α_{IIb} and β_3 tails involved in skelemin binding (*146*). Here, alanine substitutions were introduced at Arg995, Arg997 and Leu1000 in the α_{IIb} tail region, and Lys716 and His722 in the β_3 tail region (Figure 3.1). Stably expressed single, double or triple mutations in CHO cells were established, namely R995A,

R997A, R995A/R997A, L1000A, R995A/R997A/L1000A, K716A, H722A, and R995A/R997A/K716A. Integrin-mediated cell adhesion, cell spreading, activation of FAK and Src were investigated, and the distribution of $\alpha_{IIb}\beta_3$, skelemin and talin were measured in the protrusions of the cell leading edge.

3.2 Results

3.2.1 Integrin expression

The expression of wild-type and mutant integrin was assessed by flow cytometry using a β_3-specific antibody (Figure 3.1). The percentage of cells expressing $\alpha_{IIb}\beta_3$ receptors in the mutant cell lines were comparable to those of wild-type cells, except for K716A which had only 70% of cells expressing comparable amount of integrins.

3.2.2 Association of skelemin with mutant integrins

Experiments were then performed to confirm that our mutations resulted in a decreased association of skelemin with the expressed integrins. In cells, skelemin is present as either a soluble cytoplasmic protein or as an insoluble cytoskeletal-bound protein. The relative abundance of soluble endogenous skelemin in our cell lines was very low and therefore the interaction between endogenous skelemin and $\alpha_{IIb}\beta_3$ was difficult to evaluate by co-immunoprecipitation and western blot. Therefore, to overcome this problem, co-immunoprecipitation experiments were performed using recombinant GFP-skeC2 fusion protein (skeC2: skelemin immunoglobulin C2 motifs

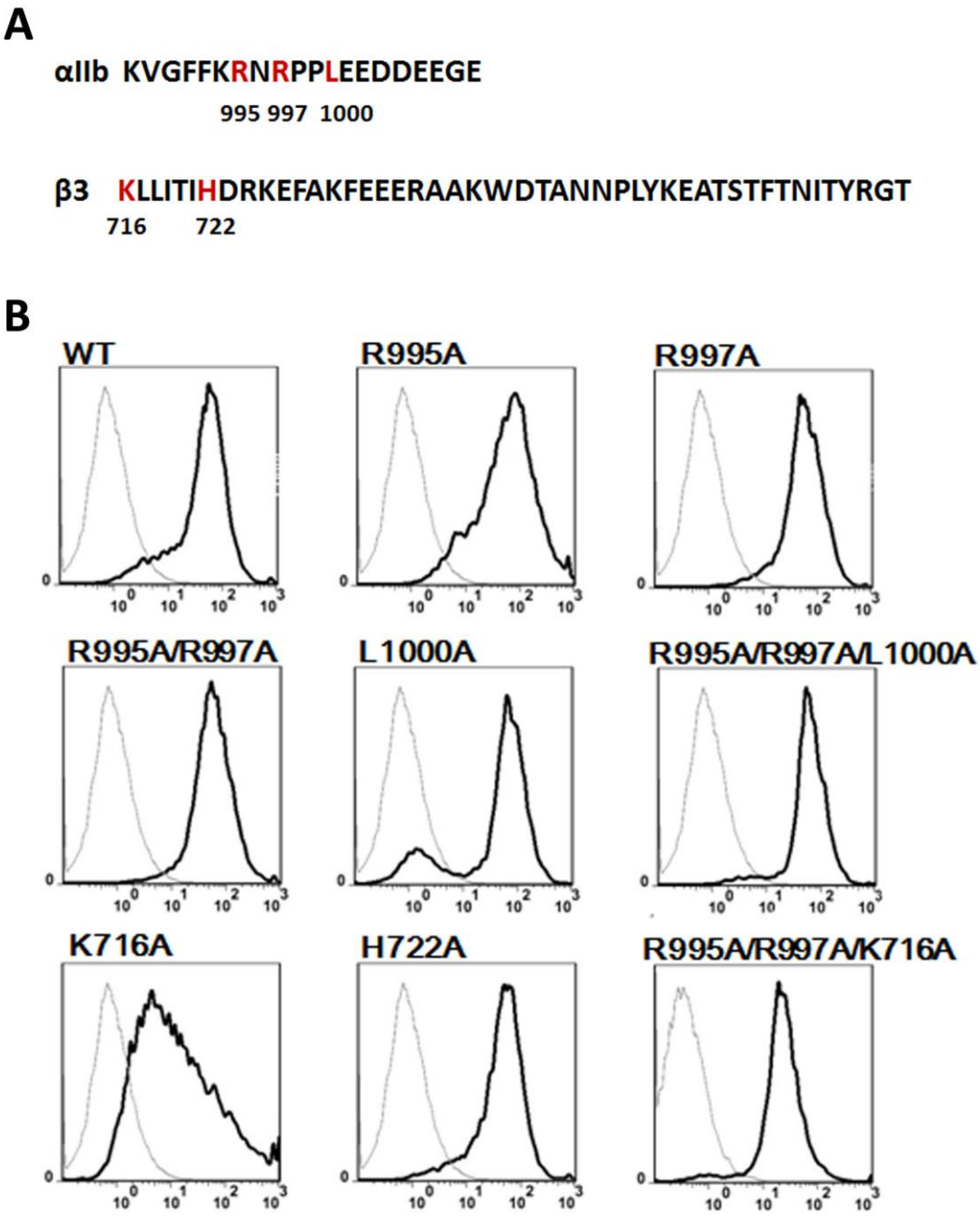

Figure 3.1 Amino acid sequences of α_{IIb} and β_3 cytoplasmic tails and cell-surface expression levels of wild-type and mutant $\alpha_{IIb}\beta_3$ CHO cells. (A). Amino acid sequences of α_{IIb} and β_3 cytoplasmic tails. Residues targeted for alanine substitutions are underlined and sequence numbers displayed. (B). Cell-surface expression levels of CHO cells transfected with wild-type and mutant $\alpha_{IIb}\beta_3$. Cells were harvested, and incubated with Tyrode-Hepes Buffer alone (grey line) or with an anti- β_3 antibody (black line). A PE-labelled secondary antibody was used to detect bound anti-β_3 antibody and flow cytometry analysis was performed in Tyrode-Hepes buffer. Cells incubated only with the secondary antibody (grey line) were used as controls. Histograms were generated using FlowJo. The data are representative of three separate experiments.

4-5 that contain the $\alpha_{IIb}\beta_3$-binding domain). Wild-type, R995A/R997A/L1000A, H722A and K716A cells were transiently transfected with plasmids of GFP-skeC2 or GFP alone (control). After 48 hours of transfection, cells were harvested and allowed to adhere to immobilized fibrinogen for 1 hour. Cell lysates were subjected to immunoprecipitation with antibodies against GFP, then western blot analysis (Figure 3.2). Two GFP-immunoreactive proteins were detected, GFP (～27 kD) and the GFP-skeC2 fusion protein (～90 kD). An apparent MW of 90 kD is consistent with the predicted size of the fusion protein. A long transfer time (40 min) was used to ensure sufficent transfer of proteins from the gel to the nitrocellulose membrane under semi-dry transfer conditions. Low MW proteins in a pre-stained protein ladder passed through the membrane, which indicated that some GFP proteins (～27 kD) might be also over-transferred, leading to decreased band intensity (Figure 3.2). Immunoblotting with an anti-β_3 antibody revealed that β_3 proteins were co-immunoprecipitated with GFP-skeC2, but not with GFP (Figure 3.2). In comparison to wild-type cells, there appeared to be a decrease in the amount of $\alpha_{IIb}\beta_3$ co-immunoprecipitated with R995A/R997A/L1000A, H722A and K716A mutated integrins. Thus, we confirmed that the mutations did result in a decrease association of skelemin with $\alpha_{IIb}\beta_3$.

3.2.3 Integrin affinity for ligands

The membrane proximal regions in the integrin cytoplasmic domains are important for integrin activation modulation, and point mutations within this region

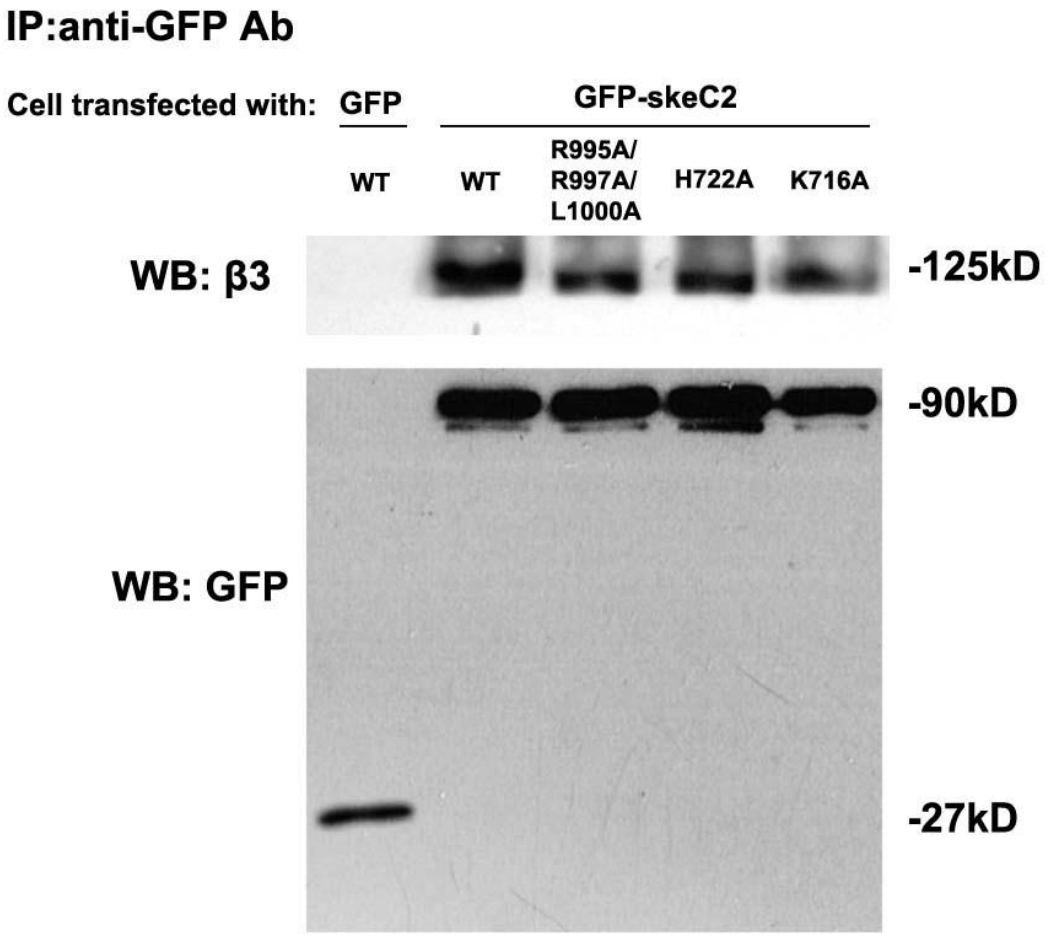

Figure 3.2 Association of GFP-skeC2 with $\alpha_{IIb}\beta_3$. Wild-type, R995A/R997A/ L1000A, H722A and K716A mutant cells were transfected with GFP-skeC2 plasmids for 48 hour, and then allowed to adhere to immobilized fibrinogen for one hour. Cell lysates were immunoprecipitated with anti-GFP. Western blot analysis using anti-β_3 antibody revealed a decreased association between GFP-skeC2 and the mutant $\alpha_{IIb}\beta_3$ receptors compared to wild-type $\alpha_{IIb}\beta_3$.

could enhance the affinity for integrin ligands and promote constitutive signalling (*39, 147*). To assess the activation state of $\alpha_{IIb}\beta_3$, flow cytometry was used to study $\alpha_{IIb}\beta_3$ binding to PAC-1, which recognizes the conformationally active form of $\alpha_{IIb}\beta_3$ (Figure 3.3). $\alpha_{IIb}\beta_3$ binding to its ligand requires divalent cations (Ca^{2+} or Mg^{2+}). Optimal $\alpha_{IIb}\beta_3$ binding to ligands occurs in the presence of Ca^{2+} at a concentration of 1-2 mM, a physiological Ca^{2+} concentration in human plasma (*148*). In the current study, 2 mM Ca^{2+} was used. EDTA chelates either Ca^{2+} or Mg^{2+} and is used as an inhibitor of integrin ligand binding. PAC-1 binding in the presence of EDTA represented non-specific ligand binding, which was subtracted from the total binding (in the presence of divalent cations) to yield specific binding. Low and negligible PAC-1 binding was observed in the presence of EDTA, suggesting that Ca^{2+}-mediated PAC-1 binding was specific (Figure 3.3C). In the presence of Ca^{2+}, wild-type $\alpha_{IIb}\beta_3$ expressed in CHO cells was in the resting state, while R995A, K716A and R995A/R997A/L1000A cells bound significant levels of PAC-1, showing that the three mutants are active (Figure 3.3A). These data are consistent with previous mutational studies (*39, 149*), suggesting that the residues K716 and R995 within β_3 tails are involved in the regulation of $\alpha_{IIb}\beta_3$ activation.

Mn^{2+} has a higher affinity for integrins than Ca^{2+} or Mg^{2+}. It strikingly increases the ligand binding affinity of almost all integrins by binding to integrins and inducing conformational changes of the integrin ectodomain from a bent to an extended and active state (*150*). Therefore, Mn^{2+} has been widely used as a positive control for integrin activation. PAC-1 binding under the condition of Mn^{2+} treatment

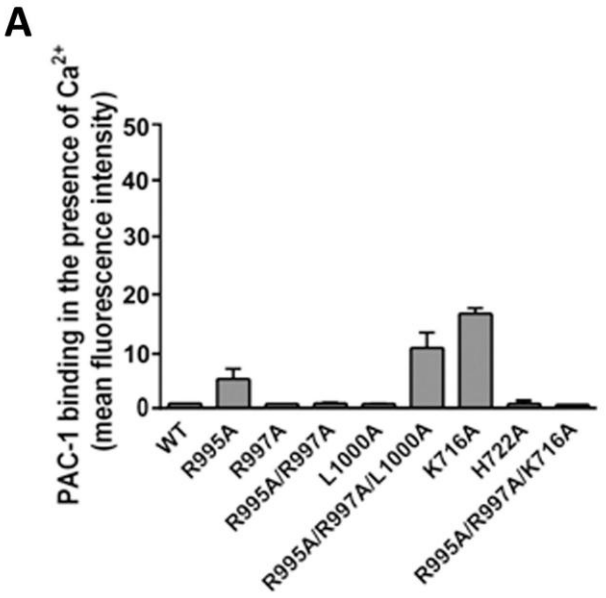
A
PAC-1 binding in the presence of Ca2+
(mean fluorescence intensity)
50
40
30
20
10
0
WT
R995A
R997A
R995A/R997A
L1000A
R995A/R997A/L1000A
K716A
H722A
R995A/R997A/K716A

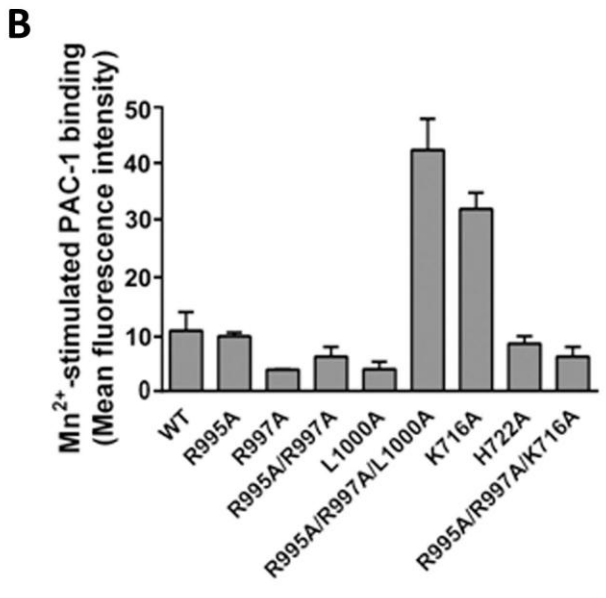
B
Mn2+-stimulated PAC-1 binding
(Mean fluorescence intensity)
50
40
30
20
10
0
WT
R995A
R997A
R995A/R997A
L1000A
R995A/R997A/L1000A
K716A
H722A
R995A/R997A/K716A

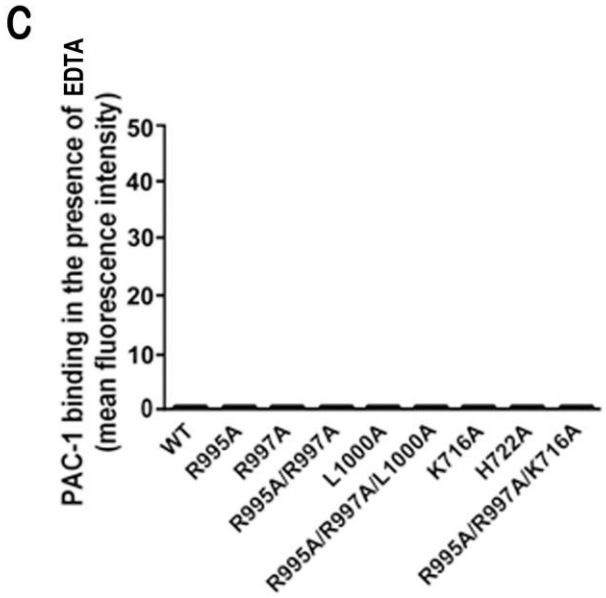
C
PAC-1 binding in the presence of EDTA
(mean fluorescence intensity)
50
40
30
20
10
0
WT
R995A
R997A
R995A/R997A
L1000A
R995A/R997A/L1000A
K716A
H722A
R995A/R997A/K716A

Figure 3.3 PAC-1 binding in the presence of metal ions. (A) PAC-1 binding in the presence of Ca^{2+}. Cells treated with 2 mM Ca^{2+} or 2 mM EDTA were incubated with PAC-1, washed, incubated with a PE-conjugated secondary antibody, and analyzed by flow cytometry. Binding was expressed as mean fluorescence intensity (MFI) of PAC-1 staining in the presence of Ca^{2+} minus that obtained in the presence of EDTA. The data represent the mean ± S.E. of three separate experiments. (B) PAC-1 binding in the presence of Mn^{2+}. (C) PAC-1 binding in the presence of EDTA. Binding was expressed as MFI of PAC-1 staining in the presence of 200 μM Mn^{2+}. The data represent the mean ± S.E. of two separate experiments.

was also tested (Figure 3.3B). Generally, Mn^{2+} was able to activate wild-type and mutant $\alpha_{IIb}\beta_3$ leading to a much higher level of PAC-1 binding. However, Mn^{2+} did not maximally activate $\alpha_{IIb}\beta_3$ integrin as Mn^{2+}-induced PAC-1 binding in wild-type cells was still significantly lower than that of K716A cells treated with Ca^{2+} alone. Even though K716A and R995A/R997A/L1000A were in a activation state, Mn^{2+} had an additional activating effect for these mutants and enhanced PAC-1 binding 3-4 fold compared to wild-type $\alpha_{IIb}\beta_3$. These results suggest that amongst all the mutants, R995A, K716A and R995A/R997A/L1000A exhibited partial activation in the presence of Ca^{2+}, but that in the presence of Mn^{2+} K716A and R995A/R997A/L1000A had higher maximal activation than that of wild-type $\alpha_{IIb}\beta_3$.

3.2.4 Transfection with skeC2 did not affect the integrin affinity states

To assess whether skelemin binding is responsible for activation of $\alpha_{IIb}\beta_3$, effects of exogenous skelemin overexpression on integrin activation were investigated by two-color flow cytometry (Figure 3.4). In this assay, wild-type and mutant cells were transiently transfected with either GFP-tagged skeC2 or GFP alone. Cells were harvested 48 hours after transfection, incubated with PAC-1 and then stained with

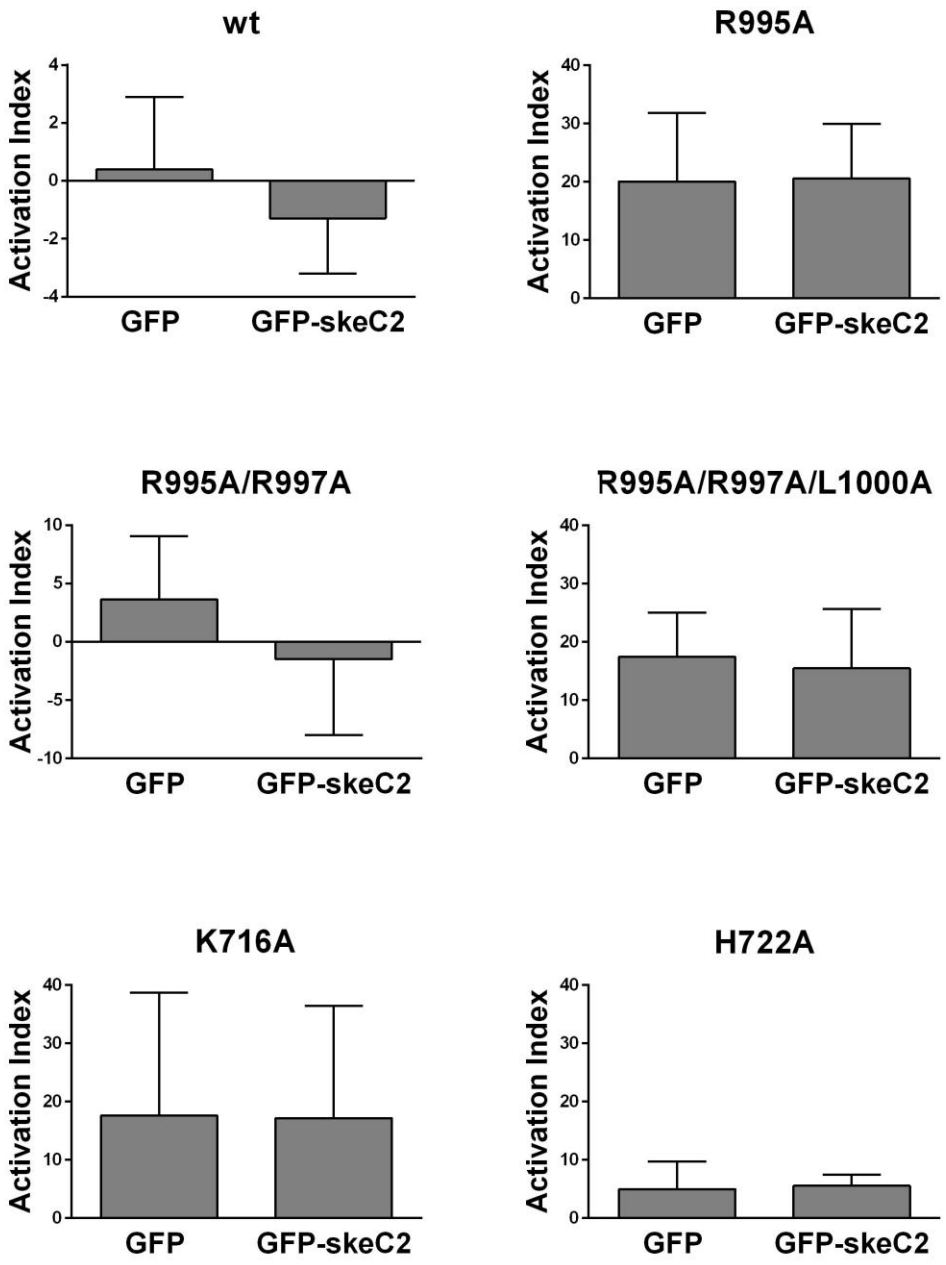

Figure 3.4 SkeC2 did not change integrin activation states in GFP-skeC2 transfected wild-type or mutant cells. Cells were transiently transfected with vectors encoding GFP or GFP-skeC2. After 48 h, cells were harvested and analyzed by two-color flow cytometry for binding of PAC-1 binding. Integrin activation index was used to compare integrin activation levels in GFP and GFP-skeC2 transfected cells for each mutant. The activation index was calculated using the formula described in Materials and Methods. The data represent the mean activation index ± S.E. of three separate experiments. The difference of activation index in GFP or GFP-skeC2 transfected cells was not statistically significant for any of the skelemin mutants using one-way ANOVA (P<0.05).

PE-labelled secondary antibody. To study successfully transfected cells, GFP-positive cells were gated for further analysis of PE staining using flow cytometry. The percentage of PE-positive cells in the population of GFP-positive cells was assigned as the PAC-1 binding level in each sample. To study the effect of skeC2 transfection on integrin activation, PAC-1 binding levels in the presence of Ca^{2+}, EDTA or Mn^{2+} were studied. Therefore, integrin activation can be quantified as an activation index, $100\times(F_{Ca} - F_{EDTA})/F_{Mn}$, where F_{Ca} is the MFI of PAC-1 binding in the presence of Ca^{2+}, F_{EDTA} is the PAC-1 binding in the presence of EDTA, and F_{Mn} is the maximal PAC-1 binding in the cells treated with Mn^{2+}. As shown in Figure 3.4, cells expressing either wild-type $\alpha_{IIb}\beta_3$ or the mutants, R995A/R997A and H722A, GFP-SkeC2 expression did not enhance PAC-1 binding. Similar results were also obtained with the three active mutants, R995A, K716A and R995A/R997A/L1000A. For each version of $\alpha_{IIb}\beta_3$ integrin, no statistically significant differences were found between cells expressing GFP-SkeC2 and GFP in their ability to bind PAC-1 ($P<0.05$). Thus, skelemin expression did not appear to alter the affinity state of $\alpha_{IIb}\beta_3$, suggesting that skelemin is not involved in $\alpha_{IIb}\beta_3$ activation.

3.2.5 Adhesion to immobilized fibrinogen

The strength of cell adhesion to ECM not only depends on integrin expression level and integrin affinity, but also relies on integrin-mediated cytoskeleton linkages. Previous studies demonstrated that skelemin and integrin association was an early response to integrin occupancy and clustering, being initiated between 30 minutes to

two hours after cell adherence. If their association is essential for linking ECM to the cell cytoskeleton, mutant cells may show decreased cell adhesion to ECM. Therefore we compared the capacity of the wild-type cells and cells expressing mutant integrins to adhere to fibrinogen over a 30 minute time period (Figure 3.5). Cells were labelled with fluorescent dye Calcein AM so that the fluorescence intensity of cells was directly proportion to the number of viable cells in each treatment. Fluorescently labelled cells were allowed to adhere to fibrinogen-coated microplates. After washing, adherent cells were counted as a percent of the number of total cells added. Non-specific cell adhesion was low, as less than 5% cells adhered to BSA-coated wells for all cell lines tested. Cell adhesion to fibrinogen was $\alpha_{IIb}\beta_3$–mediated, as adhesion of wild-type cells was 3 fold higher than that of mock-transfected cells. As shown in Figure 3.5, cell attachment of R995A, R995A/R997A, R995A/R997A/L1000A, K716A, H722A, and R995A/R997A/K716A to fibrinogen was higher than that of wild-type cells, while R997A and L1000A cell adhesion were comparable. The R995A and K716A mutations showed the strongest cell adhesion, in agreement with their active state as assessed by PAC-1 binding. In general it appears that disruption of the skelemin binding sites in $\alpha_{IIb}\beta_3$ did not impair stable cell adhesion, suggesting that skelemin-$\alpha_{IIb}\beta_3$ interaction may not be essential for the linkage of integrin to the cell cytoskeleton.

3.2.6 Cell spreading and membrane protrusions

Integrins and their associated proteins form focal adhesions in cultured cells,

which link integrin clusters to the actin cytoskeleton and initiate actin assembly into stress fibers. Here, stress fibers were stained with fluorescence-labelled phalloidin after cell adhesion to fibrinogen-coated coverslides for one hour (Figure 3.6). Normal CHO cells lacking $\alpha_{IIb}\beta_3$ expression were still round at this time point, whereas wild-type and mutant $\alpha_{IIb}\beta_3$ transfected cells were spreading and already displaying

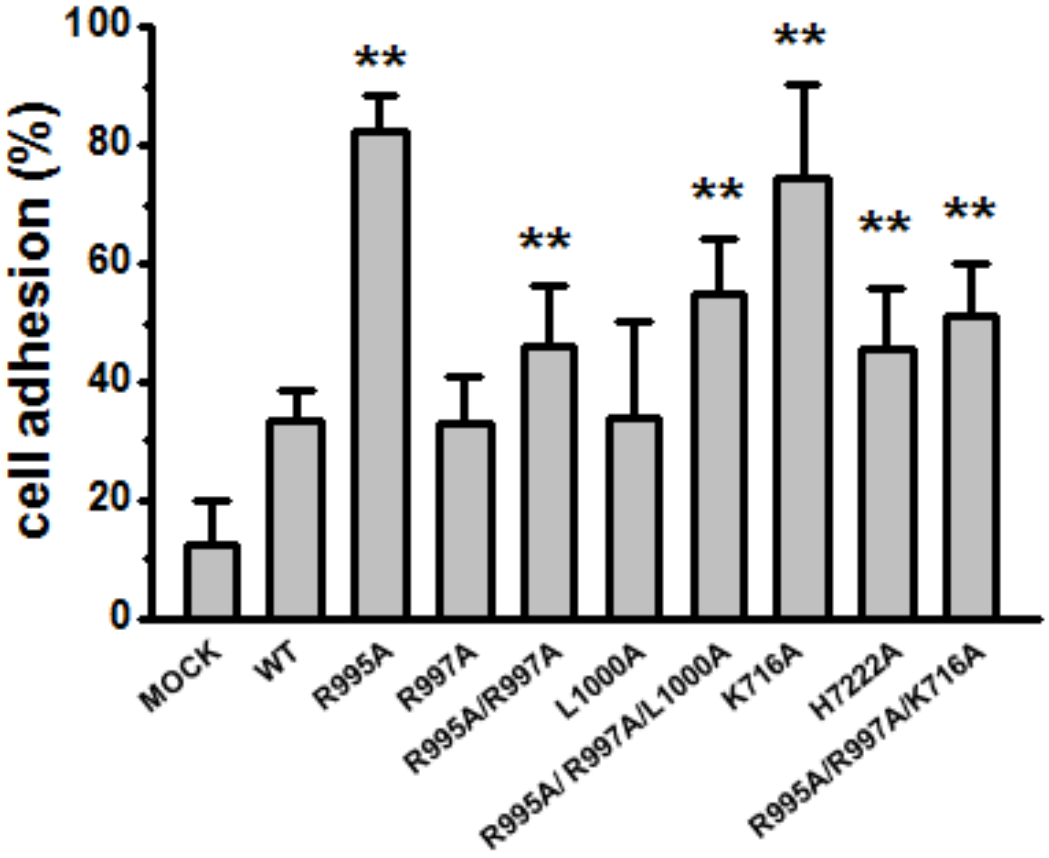

Figure 3.5 Adhesion of mutant cells to immobilized fibrinogen. Calcein-AM labelled cells were plated on 20 μg/ml fibrinogen coated wells and total cell fluorescence were measured on a fluorescence microplate reader. After 30 minutes adhesion in Tyrode's buffer, weakly and non-adherent cells were washed away and the fluorescence of remaining cells was measured. Cell adhesion, the percent of adherent cells to total cells added, was calculated using the formula described in Materials and Methods section 2.4. Cell adhesion to BSA-coated wells was subtracted as background. The data represent the mean ± S.D. of three separate experiments. **P<0.01 compared to wild-type cells using student's t-test.

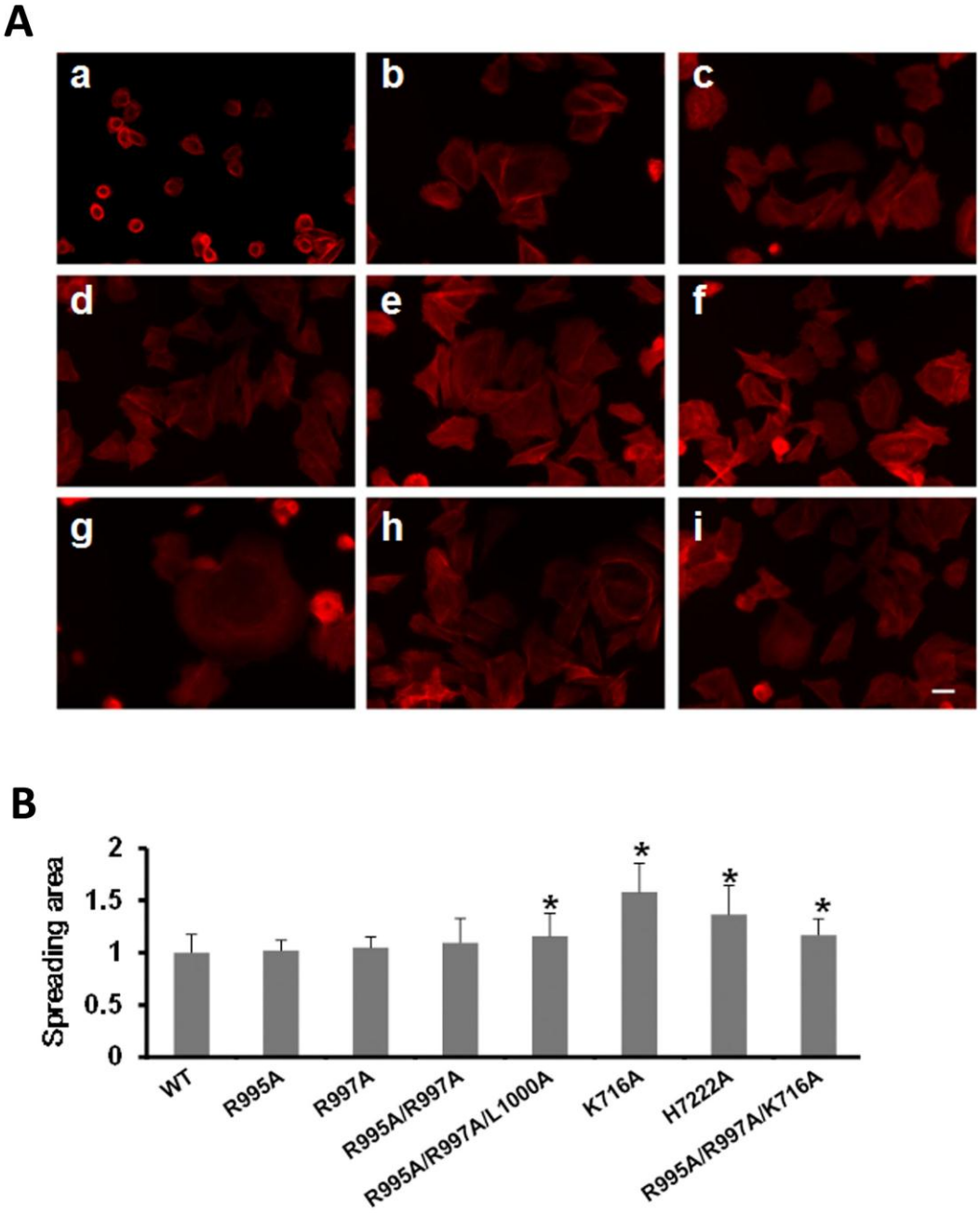

Figure 3.6 Effect of $\alpha_{IIb}\beta_3$ mutations on the actin cytoskeleton. (A) After spreading on fibrinogen-coated wells for one hour, cells were fixed, permeabilized and stained with rhodamine phalloidin to detect F- actin. a: CHO; b: wild-type; c: R995A; d: R997A; e: R995A/R997A; f: R995A/R997A/L1000A; g: K716A; h:H722A; and i: R995A/R997A/K716A. Scale bar: 10 μm. (B) Quantitative analysis of cell spreading. The area of each cell was measured using ImageJ analysis software. The mean area of wild-type cells was normalized to 1. Error bars are standard deviations. *P<0.05 compared to wild-type cells using student's t-test.

strong formation of stress fibers. There was also obvious formation of lamellipodia and filopodia within both wild-type and mutant cell lines. Quantitative measurements of cell areas clearly showed that mutant cells R995A/R997A/L1000A, K716A, H722A and R995A/R997A/K716A exhibited a greater extent of cell spreading (Figure 3.6B). We also stained cells with anti-β_3 antibody (AP3) and observed formation of many $\alpha_{IIb}\beta_3$-based focal adhesions, lamellipodia and filopodia at the leading edges of the mutant cell lines (data not shown). Taken together, these results demonstrate that defective binding of skelemin to $\alpha_{IIb}\beta_3$ does not disrupt actin cytoskeleton organization, or membrane protrusion formation and cell spreading, suggesting that other cytoskeletal proteins are capable of performing some of the functions performed by skelemin. Thus, different cytoskeletal proteins may act in unison to maintain integrin-cytoskeleton linkages.

3.2.7 Src and FAK activation downstream of integrin signalling

The increased cell adhesion ability and higher spreading level observed in some mutations suggested that there was an upregulation in integrin-downstream signalling. Therefore, activation of FAK and Src, two important tyrosine kinases in integrin signalling that are required for efficient adhesion and spreading of cells on integrin ligands were examined. After cell adherence to fibrinogen in Tyrodes buffer for one hour, activation of Src and FAK were assessed by probing the phosphorylation levels of pY416-Src, the positive regulatory autophosphorylation site of Src (*151*), and pY397-FAK, the major site of tyrosine phosphorylation on FAK (*152*). Western blot

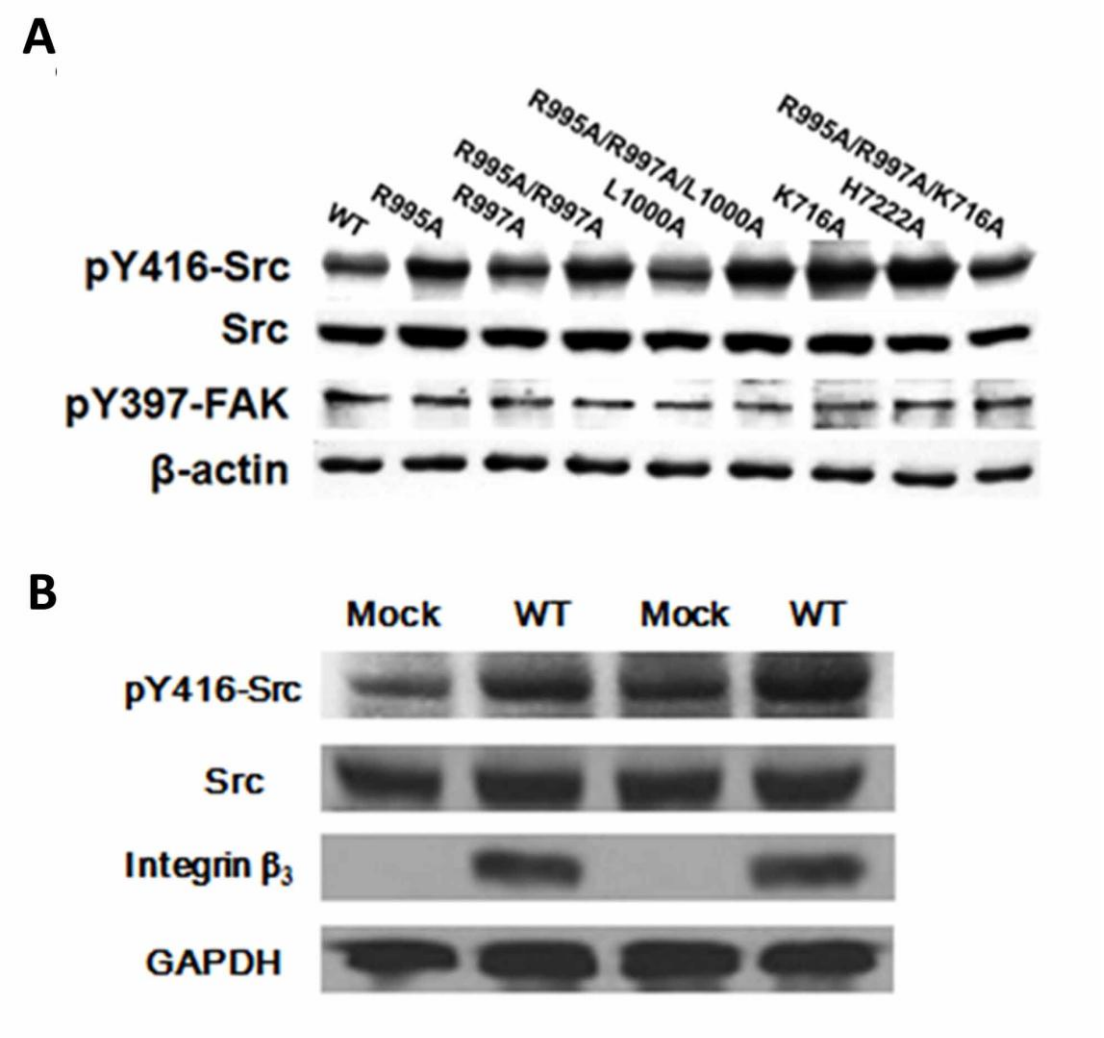

Figure 3.7 Effect of wild-type and mutant $\alpha_{IIb}\beta_3$ on Src and FAK signalling. Cells were allowed to spread on fibrinogen-coated plates for one hour, lysed and total cell extracts were subjected to SDS-PAGE. Blots were probed using antibodies against pY416-Src, Src, pY397-FAK, β_3-integrin, GAPDH and β-actin. (A) Analysis of pY416-Src and pY397-FAK in total cell lysates was done on wild-type and mutant cells. (B) Analysis of pY416-Src in total cell lysates was done on wild-type $\alpha_{IIb}\beta_3$–expressing cells and mock-transfected cells.

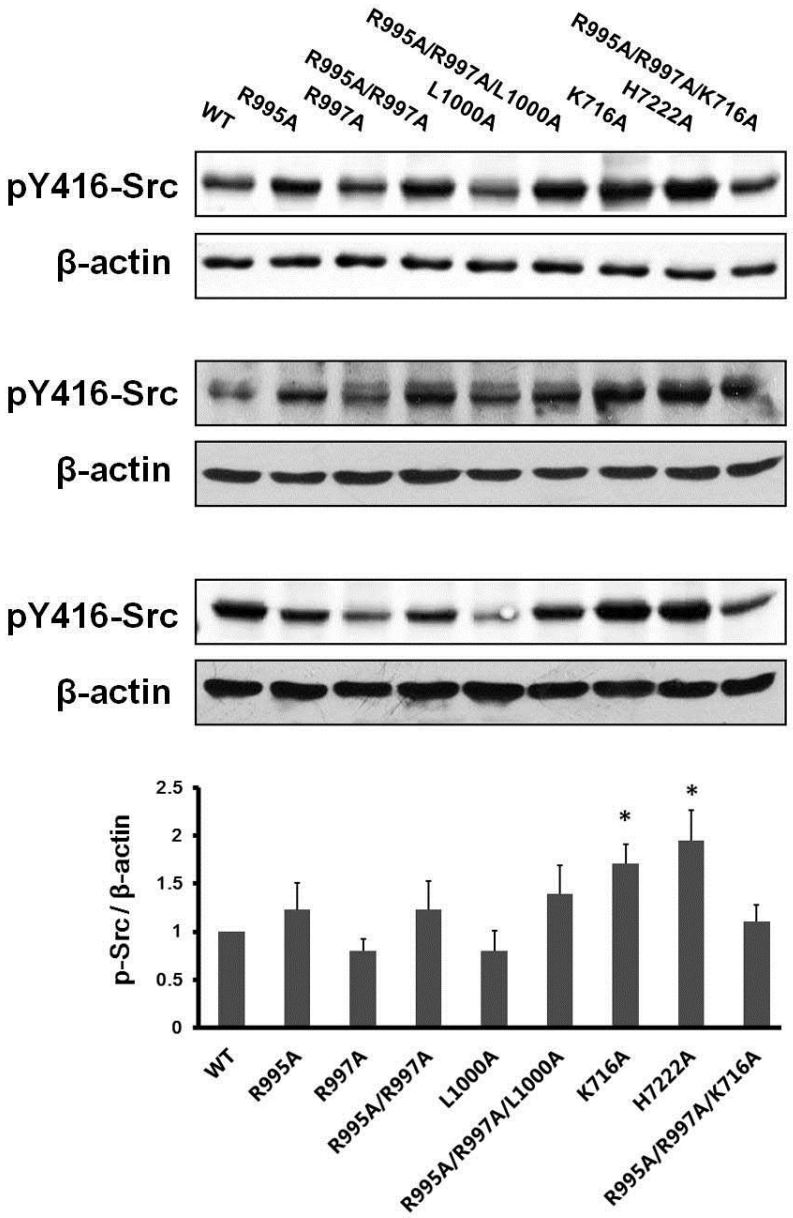

Figure 3.8 Comparable or increased pY416-Src levels in mutant $\alpha_{IIb}\beta_3$-transfected cells. Western blot analysis of pY418-Src in wild-type and mutant cells was repeated in three independent experiments. The graph shows densitometric quantification of pY416-Src/β-actin. Band density was measured by Quantity One software and normalized to the β-actin protein level. The ratio of pY416-Src/β-actin in wild-type cells was assigned as 1. K716A and H722A cells showed significantly increased pY416-Src/β-actin levels compared with wild-type cells using student's t-test, but the Kruskal–Wallis test revealed no significant difference between mutant and wild-type cells ($P<0.05$).

analysis of pY416-Src and pY397-FAK showed that comparable or potential higher levels of pY416-Src were observed in mutant cells compared to wild-type cells. However, there were no differences in cellular levels of pY397-FAK between mutant and wild-type $\alpha_{IIb}\beta_3$-expressing cells (Figure 3.7A).

To study the effects of $\alpha_{IIb}\beta_3$-expression on Src activation, pY416-Src levels in wild-type $\alpha_{IIb}\beta_3$ and mock transfected cells were examined. As shown in Figure 3.7B, wild-type $\alpha_{IIb}\beta_3$-transfected cells had increased levels of the active form of Src (pY416-Src) than mock-transfected cells when they were plated on fibrinogen. These results suggested that the transfected $\alpha_{IIb}\beta_3$ integrins and their binding to ligands attribute to elevated levels of pY416-Src.

Western blot analysis of pY416-Src in different mutant cells was repeated and the blots were quantified as shown in Figure 3.8. Bands were quantified by Quantity One software and normalized to the β-actin protein level. The levels of pY416-Src in K716A and H722A cells were slightly elevated compared with wild-type cells, which were in good agreement with their increased cell spreading.

3.2.8 Effect of overexpression of skeC2 on cell spreading

Previous studies have demonstrated that introduction of skeC2 into wild-type cells caused spread cells to round up (*108, 142*). The similar experiment was performed in Hek293 cells. Hek293 cells were transiently transfected with $\alpha_{IIb}\beta_3$, GFP-skeC2 or GFP individually and in combination, and harvested 48 hour after transfection. Transfected cells were allowed to adhere on fibrinogen-coated slides for two hours, then fixed and stained with anti-β_3 antibody. As shown in Figure 3.9, the

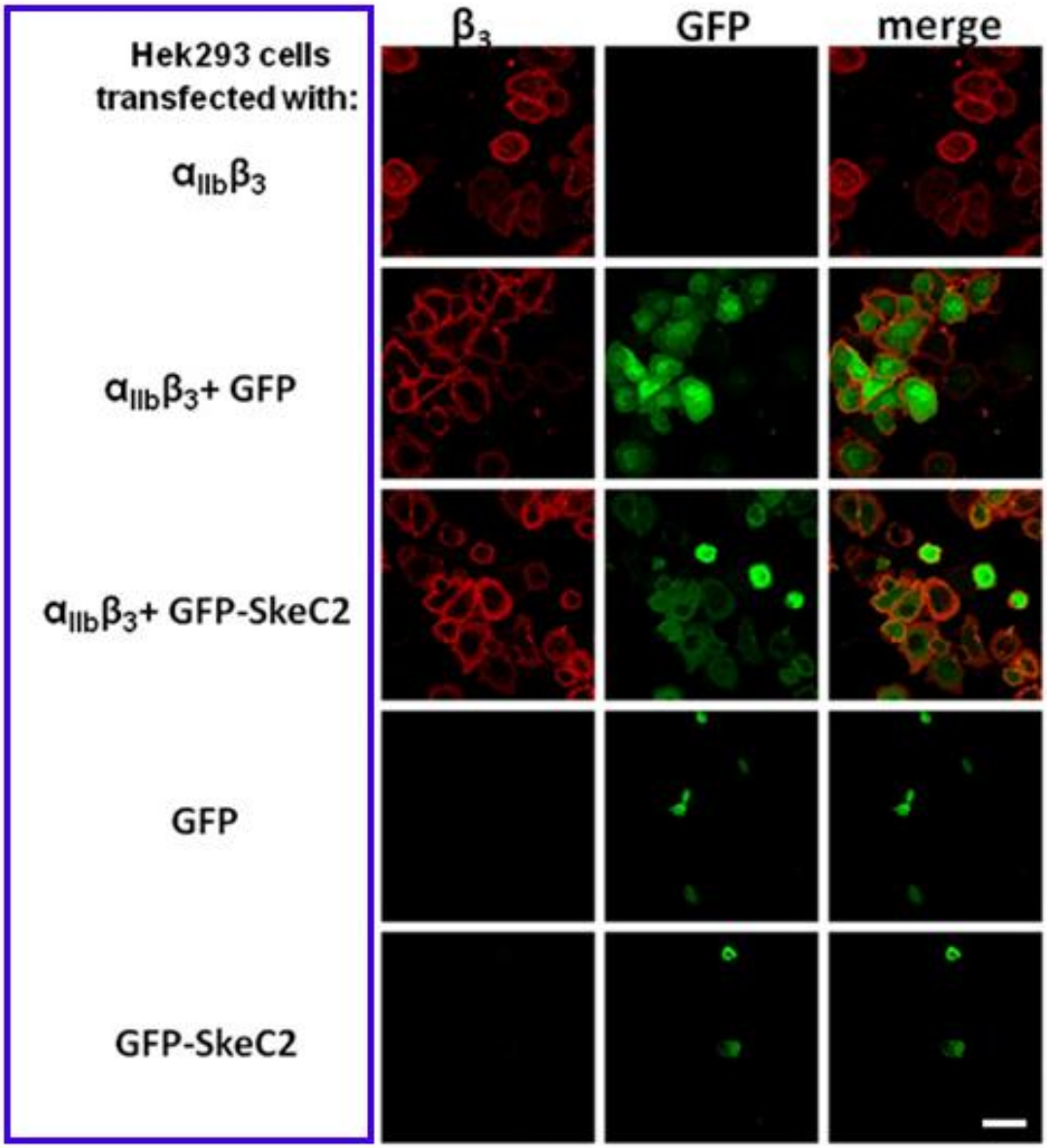

Figure 3.9 Hek293 cells co-transfected with $\alpha_{IIb}\beta_3$ and GFP-SkeC2 show inhibited cell spreading on fibrinogen. Subconfluent Hek293 cells were transfected with $\alpha_{IIb}\beta_3$, GFP-skeC2 or GFP individually and in combination, and harvested 48 hour after transfection. Cells were allowed to adhere for 2 hours on fibrinogen-coated slides, then fixed and stained with anti-β_3 antibody and PE-labelled secondary antibody. GFP and $\alpha_{IIb}\beta_3$ expression were observed with confocal microscopy. Scale bar: 50 μm.

transfection of Hek293 cells with GFP-skeC2 inhibited $\alpha_{IIb}\beta_3$-mediated cell spreading. However, the inhibitory effect only occurred when the expression amount of GFP-skeC2 was relative high.

The effect of overexpression of skeC2 on spreading in mutant $\alpha_{IIb}\beta_3$-transfected CHO cells was also investigated (Figure 3.10). Wild-type, R995A, R995A/R997A/L1000A, H722A and K716A cells transiently transfected with GFP-skeC2 or GFP were re-plated on fibrinogen, and observed by GFP immunofluorescence two hours after spreading (Figure 3.10). Wild-type cells transfected with GFP-skeC2 failed to spread on fibrinogen compared to transfection with GFP alone. A similar result was obtained in R995A cells. However, GFP-skeC2 transfection had less effect on the spreading of R995A/R997A/L1000A, H722A and K716A cells. Notably, R995A/R997A/L1000A, H722A and K716A cells with strong GFP-skeC2 expression (indicated as increased GFP fluorescence intensity) were still able to spread, suggesting that skeC2 expression had little inhibitory effect on cell spreading in these three mutant cell lines.

Figure 3.11 shows a representative confocal microscopic image of transfected wild-type and R995A/R997A/L1000A cells that were stained with anti-β_3 antibody (red) after two hours of spreading. Most wild-type cells expressing GFP-skeC2 were completely rounded up, whereas R995A/R997A/L1000A cells transfected with GFP-skeC2 were fully spread. It was noted that wild-type cells with increased expression of GFP-skeC2 were rounded up but cells that were weakly expressing GFP-skeC2 had normal spreading morphology (indicated by arrow).

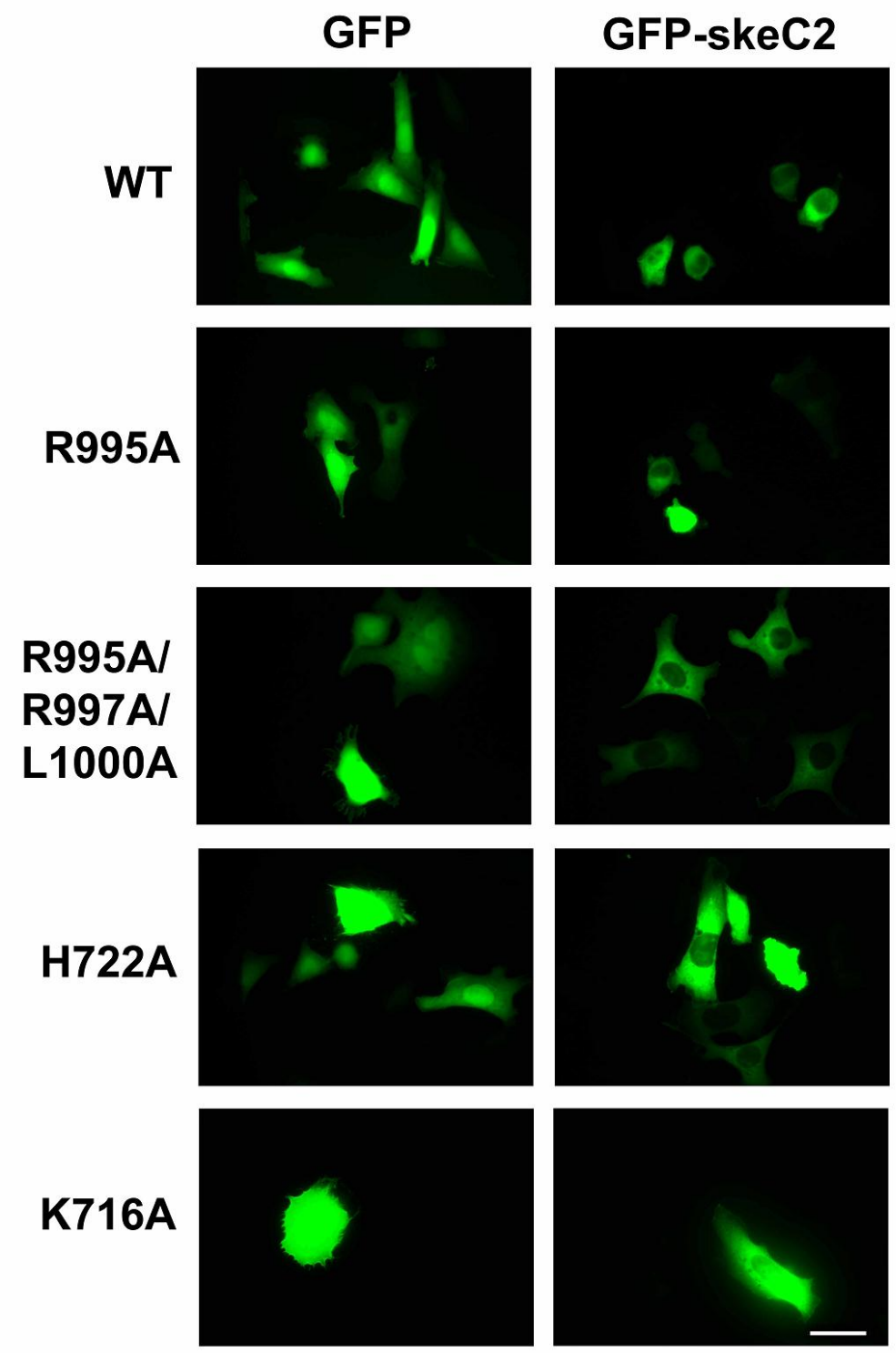

Figure 3.10 Immunofluorescence images reveal different effects of skeC2 transfection on wild-type and mutant cells. Wild-type, R995A, R995A/R997A/ L1000A, H722A and K716A mutant cells were transiently transfected with GFP-skeC2 or GFP alone, plated on fibrinogen for two hours, fixed, and GFP fluorescence was visualized. Scale bar: 50 μm.

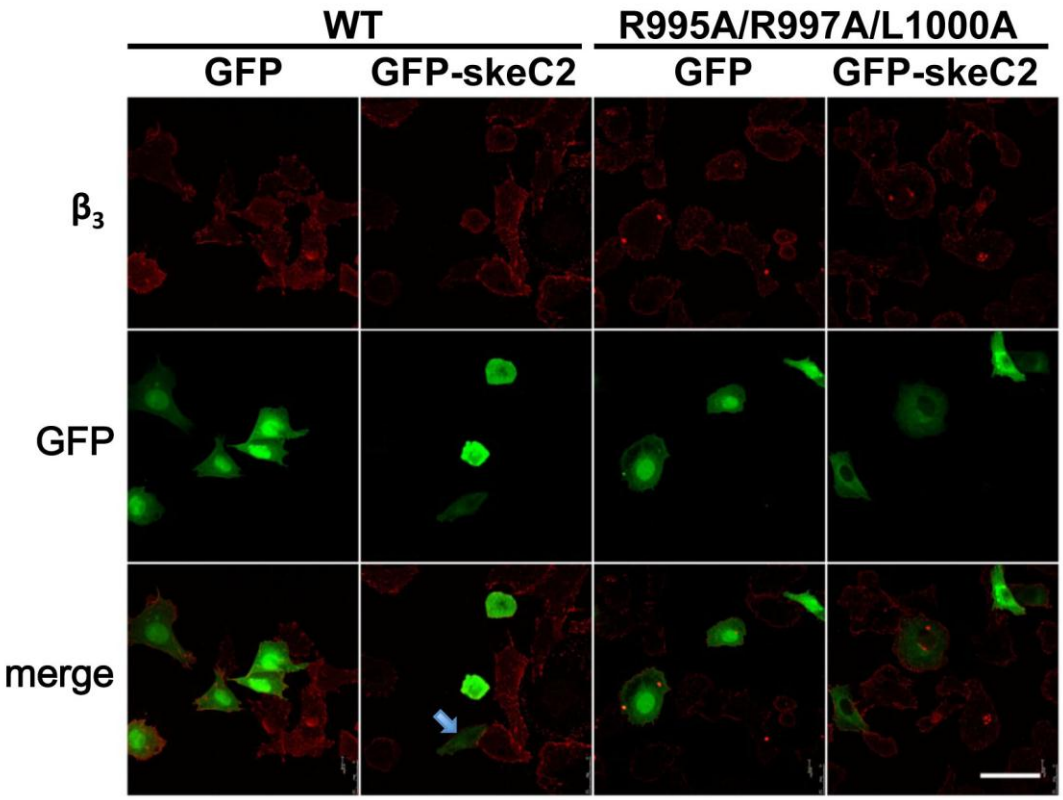

Figure 3.11 Confocal microscopy image of wild-type and R995A/R997A/L1000A cells transfected with GFP-skeC2. Wild-type and R995A/R997A/L1000A cells were transiently transfected with GFP-skeC2 or GFP alone and re-plated on fibrinogen for two hour. Cells were fixed and stained for integrins with AP3 antibody. Integrin distribution (red) and GFP fluorescence were visualized by confocal microscopy. A wild-type cell that weakly expresses GFP-skeC2 is indicated by an arrow. Scale bar: 50 μm.

The above results indicate that skeC2 expression could abolish cell spreading and was more effective in wild-type cells than in mutant cells, at least in R995A/R997A/L1000A, H722A and K716A cells. We conclude from these results that transfected GFP-skeC2 competes with endogenous skelemin for integrin binding, thus disrupting the binding of integrin tails to not only endogenous skelemin, but to other cytoskeletal proteins that physically link $\alpha_{IIb}\beta_3$ to the cell cytoskeleton.

3.2.9 Co-localization of talin and skelemin with integrin $\alpha_{IIb}\beta_3$ in wild-type and K716A mutant cells

Among the other integrin-cytoskeleton linkage candidates, talin is similar to skelemin in that it also has a membrane-proximal binding region in the β_3 tail, and it also has a distinct NPLY membrane-distal binding site (*56*). In addition, talin plays critical roles in linking integrin to the actin cytoskeleton and supporting formation of cell membrane protrusions during cell spreading (*99, 153*). Therefore, double labelling of integrin $\alpha_{IIb}\beta_3$ (red) and talin (green) or skelemin (green) was used to compare the distribution of talin and skelemin in wild-type and mutant cells at an early time point of cell spreading (40 min). Among all the mutant cell lines, K716A was chosen to be shown here (Figure 3.12), as it developed enormous integrin-based membrane protrusions of filopodia and lamellipodia during early cell spreading.

Immunocytochemistry for β_3-integrin (red) showed that cell attachment to fibrinogen promoted translocation of integrin from the cytosol to the cell periphery in wild-type cells as well as in K716A mutant cells. The K716A mutant cells had a more

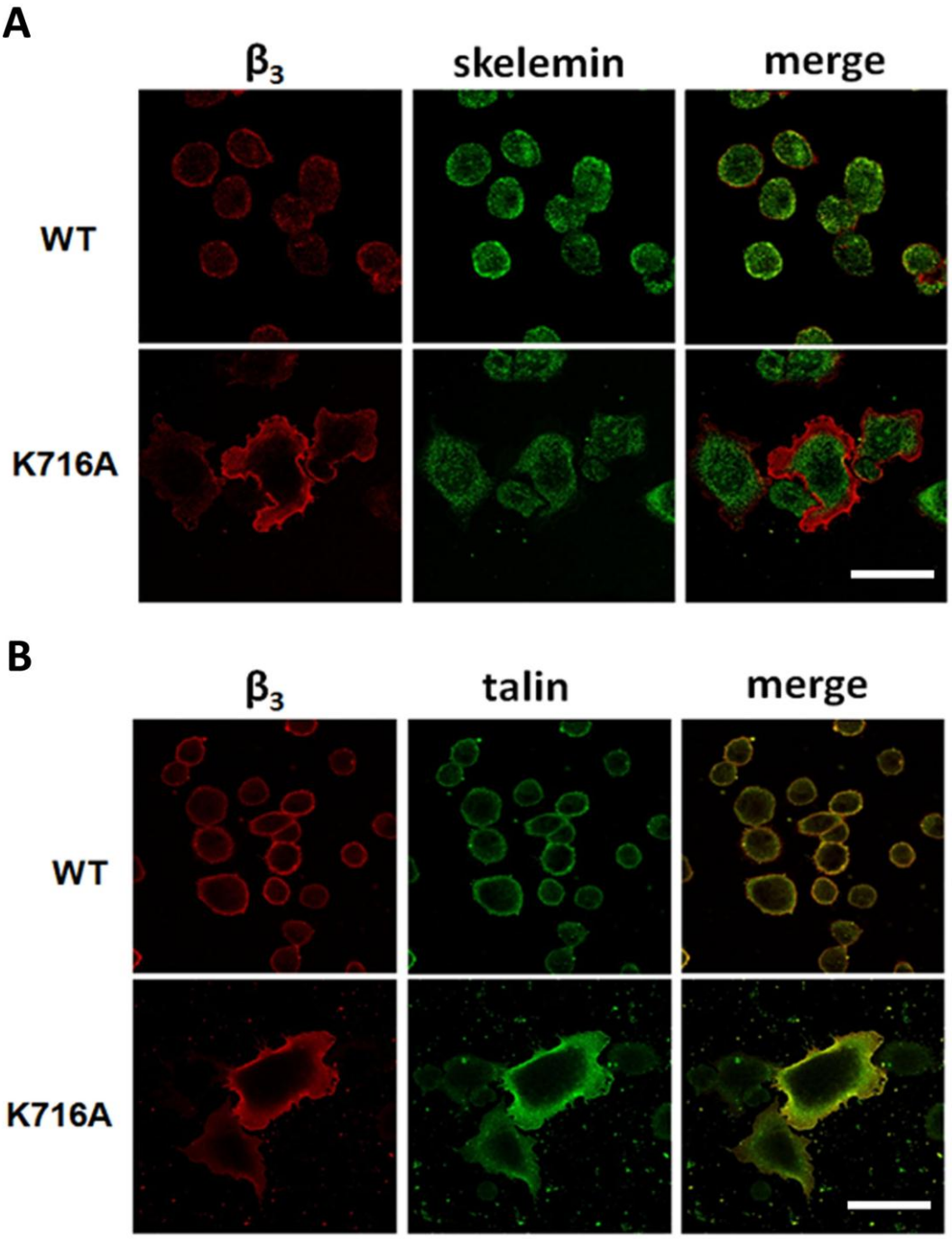

Figure 3.12 Distribution of skelemin and talin in wild-type and K716A cells. After spreading on fibrinogen-coated wells for 40 minutes, (A) wild-type or K716A cells were fixed and stained for β_3 integrin and skelemin or (B) β_3 integrin and talin. Images were captured using a confocal fluorescence microscope. Scale bar: 50 μm.

profound degree of spreading level, and filopodia and lamellipodia structures were strikingly obvious. Co-staining for skelemin showed that skelemin colocalized with $\alpha_{IIb}\beta_3$ at the cell periphery in wild-type cells, while in K716A mutant cells it was not present in sheets of membrane protrusions at the cell periphery but was found to be localized diffusely in the main cell body, thus losing its co-localization with $\alpha_{IIb}\beta_3$ (Figure 3.12A). However, both of the cell lines exhibited marked co-localization of $\alpha_{IIb}\beta_3$ and talin at the cell periphery (Figure 3.12B). Wild-type cells displayed very strong ring-shaped staining for both $\alpha_{IIb}\beta_3$ and talin at the cell periphery. This strong co-localization pattern is also clearly visible in the sheets of lamellipodia in K716A mutant cells. It seems that co-localization of talin and integrin $\alpha_{IIb}\beta_3$ in the regions of cell membrane protrusions in cells transfected with the K716A mutation could be a result of knocking down skelemin binding to $\alpha_{IIb}\beta_3$ cytoplasmic tails.

3.3 Discussion

The association of integrins with cytoskeletal proteins is crucial for the transmission of biochemical signals and mechanical force across these adhesion receptors and, thus, for integrin-mediated cell functions, such as spreading, migration and gene expression (*154*). The dynamic binding of skelemin to the cytoplasmic domains of integrin $\alpha_{IIb}\beta_3$ during the cell spreading process has been reported: skelemin did not bind to resting $\alpha_{IIb}\beta_3$ in non-adhered platelets and CHO cells; cell adhesion and spreading to immobilized fibrinogen promoted skelemin binding with $\alpha_{IIb}\beta_3$; and, the two proteins dissociate in later stages of cell spreading (*108, 142, 146*).

Since skelemin is a family member of myosin-associated myomesin, it was previously speculated to exert a contractile force by linking integrin to myosin (*142*). In the present study we tested this hypothesis and tried to elucidate the role of skelemin in integrin functions with the use of a series of stable CHO cell lines expressing mutant $\alpha_{IIb}\beta_3$ integrins in which key residues involved in the binding of skelemin to $\alpha_{IIb}\beta_3$ were mutated. We recognize that these mutations might also exhibit impaired interactions with other integrin binding proteins, and therefore we generated a number of mutants to reveal a general picture of the functional role of skelemin-integrin interactions. We found that most of the mutant cells defective in skelemin binding had unimpaired cell adhesion and spreading capacity at the early stages of cell spreading on immobilized fibrinogen. Some of the mutant cells also had increased membrane protrusion formation, a larger cell spreading area and elevated levels of activated pY416-Src. These data lead us to conclude that engagement of skelemin to the cytoplasmic tail of $\alpha_{IIb}\beta_3$ is not essential for the expansion of a cell protrusion during cell spreading. Instead, we propose that the binding of skelemin, talin and other proteins to the tail of $\alpha_{IIb}\beta_3$ are mutually exclusive events and depending on what protein is bound, a cell will either spread or contract. As discussed below, when skelemin is bound to the cytoplasmic tail of $\alpha_{IIb}\beta_3$, a contractile force is generated which supports cell contraction. To initiate cell spreading, a cell must prevent or disrupt skelemin binding to allow for the recruitment of other proteins to integrin clusters that facilitate cell spreading, such as talin and Src. Thus, modulating skelemin binding to integrin tails is one mechanism a cell can use to regulate the

highly organized process of cell spreading.

Mutations of R995A and K716A in this study are shown to activate $\alpha_{IIb}\beta_3$. To address whether the activation of the mutant is caused by disruption of skelemin binding, we characterized the binding of PAC-1, an antibody specific for activated $\alpha_{IIb}\beta_3$ integrin, to cells overexpressing GFP-skeC2. Overexpression of this fragment did not alter integrin affinity state of either wild-type or active mutant cells (Figure 3.4). Unlike talin, which is able to unclasp the membrane-proximal interface of $\alpha_{IIb}\beta_3$ cytoplasmic tails and lead to integrin activation, skelemin cannot unclasp the interface even though skelemin also binds the membrane proximal regions of $\alpha_{IIb}\beta_3$ cytoplasmic tails. It has been demonstrated that skelemin and $\alpha_{IIb}\beta_3$ association occurs after unclasping of the $\alpha_{IIb}\beta_3$ interface due to integrin-ligand ligation, which unmasked binding residues recognized by skelemin (*146*). Our data here support the view that the association of skelemin with $\alpha_{IIb}\beta_3$ is a post-ligand-binding event, but not involved in the process of integrin-ligand affinity regulation.

The binding of skelemin with integrin is dynamically regulated during cell spreading, suggesting a regulatory role for skelemin in cell spreading. Our proposed model for skelemin in cell spreading and anchorage is displayed in Figure 3.12. Focusing on cytoskeletal proteins, activation of integrins involves talin binding (Figure 3.12A) that results in integrin clustering and activation of FAK, resulting in the recruitment of skelemin and other cytoskeletal proteins to integrin clusters (Figure 3.12B). During these early phases of cell adhesion and spreading, skelemin competes with other cytoskeletal proteins for binding to the β_3 tail and prevents the activation of

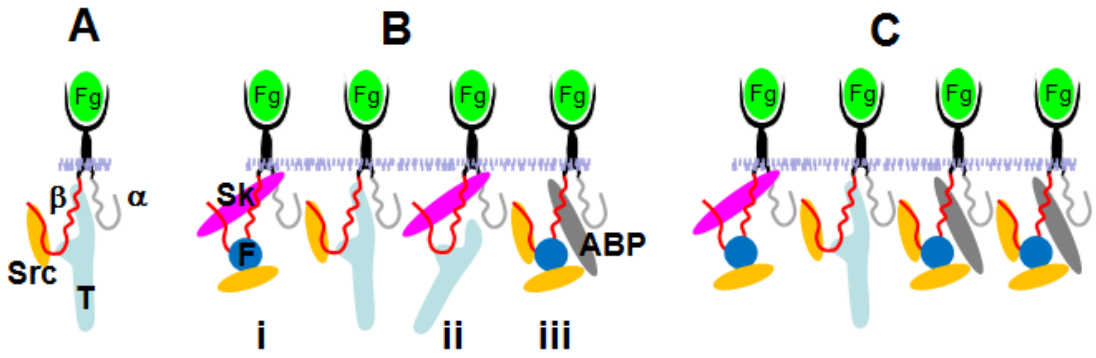

Figure 3.13 Proposed model of skelemin interaction with $\alpha_{IIb}\beta_3$ tails. (A) Activation. Integrin activation involves the binding of talin (T) to the membrane proximal and NPLY regions of β_3 that results in unclasping of the integrin tails, leading to $\alpha_{IIb}\beta_3$ binding to fibrinogen (Fg). Src is also directly bound to the C-terminus of the β_3 tail. (B) Early stages of cell anchorage and spreading. Following integrin activation, integrin clustering is initiated together with the activation of FAK (F). This results in the recruitment of additional integrins, skelemin (Sk), and other cytosolic and cytoskeletal proteins to the integrin cluster, and the formation of a focal adhesion. (i) Skelemin binds to the membrane-proximal regions of α_{IIb} and β_3 tails and to the C terminus of β_3 tails, which displaces Src from the C-terminus of β_3, but still allows Src to bind to β_3 via activated FAK bound to the NPLY region. (ii) In the presence of skelemin, talin can still bind to the β_3 NPLY region but not to its β_3 membrane-proximal binding domain. (iii) The binding of other actin-binding proteins (ABP) to integrin tails allows for maximal Src activation while providing a linkage to the actin cytoskeleton. Skelemin can also provide transient linkages to the actin cytoskeleton (i and ii). A combination of these binding scenarios would be present within a focal adhesion. (C) Late stages of cell anchorage and spreading. As cell adhesion and spreading progresses the majority of the soluble skelemin is replaced by other actin-binding proteins, allowing for increased Src activation. The remaining skelemin makes firm contacts with the actin cytoskeleton, bringing cell spreading and adhesion to completion.

Src from occurring at the C-terminus of the β_3 tail. In doing so, skelemin would counteract the activity of other proteins involved in cell adhesion, spreading and signalling, thereby providing the cell with mechanism to fine-tune its cell shape. During later stages of cell spreading, soluble skelemin either converts into insoluble skelemin, or dissociates from integrins (*146*), being replaced by talin or other actin-binding proteins, and firm adhesion occurs (Figure 3.12C).

Previous studies reported that microinjection or over-expression of skeC2 fragments into cultured cells abolished cell spreading (*108, 142*). It was assumed that skelemin was essential for cell spreading based on the interpretation that skeC2 competes with the binding of endogenous skelemin to integrins but, lacks a cytoskeletal binding site, thus resulting in breakage of the integrin-cytoskeleton linkage. However, we found that mutant cells defective in skelemin binding had unimpaired adhesion and spreading capacity on integrin ligands, suggesting that skelemin binding to integrin was not essential for cell spreading. These apparently contradictory results can be resolved if one reinterprets the earlier study with the new data generated herein. We propose that the binding of skeC2 with integrin tails results in a loss of the control mechanisms governing the dynamics of cell adhesion and spreading by blocking the binding of endogenous skelemin and other cytoplasmic proteins to integrin tails that are important in regulating the formation of cellular protrusions and cell spreading. We found that the use of cells expressing receptors containing site-specific point mutations impeded the binding of endogenous skelemin (but not other cellular proteins) with the integrin tails.

The stoichiometry of skelemin and integrin needs to be considered when using GFP-skeC2 since we found that GFP-skeC2 inhibited the $\alpha_{IIb}\beta_3$-mediated cell spreading only when the proportion of GFP-skeC2 to $\alpha_{IIb}\beta_3$ was high (Figures 3.9 and 3.11). The interaction between integrin and skelemin is robust. A previous NMR study showed that the association between skelemin C2 and integrin β_3 tail is increased by increasing the ratio of skelemin C2 to β_3 (*11*). If the ratio of skelemin C2 to integrin is much higher in plasmid-transfected CHO cells than in wild type cells, such as platelets, one may over-estimate or incorrectly define the role of skelemin in integrin biology. One problem with over-expressing skelemin C2 is that it would saturate the skelemin binding sites on integrins and not only block endogenous skelemin binding but also the association of other integrin binding partners that compete for the skelemin binding site. This is likely why we were able to obtain some novel insights into skelemin function from experiments utilizing our wild-type and mutant integrin cell lines, but not from skelemin C2 over-expression experiments.

The cytoplasmic tails of $\alpha_{IIb}\beta_3$ are key structures for outside-in signalling in that they recruit a substantial number of cell signalling and cytoskeletal proteins (*71*). Notable amongst these are Src and talin, which are obligatory for cell spreading (*153, 155*). Data in the current study show that the levels of pY416-Src in H722A and K716A cells were increased (Figure 3.7 and 3.8). Several mechanisms are brought into play following Src activation (*151*). One is the direct association of the C-terminal region of β_3 tails with Src, which destroys the autoinhibitory state of Src upon cell adhesion, and integrin clustering stabilizes the activated Src by inducing

intermolecular autophosphorylation (*115*). We suggest that a reduction in skelemin bound to integrins may allow more Src to be bound and priming it for activation. An NMR spectroscopy study revealed that immunoglobulin C2-like repeat 4 (SkIgC4), interacts weakly with the C termini of β_3 tails, which is also the binding site for Src involved in binding with integrin $\alpha_{IIb}\beta_3$ (*96, 115*). Therefore, it is possible that the binding of SkIgC4 with the C termini of β_3 tails occupies the Src binding site and thereby reduces the capacity to maximally activate Src. However, it does not completely block Src activation as Src can still bind to and become activated at the membrane distal NPLY motif of β_3 through activated FAK (*156*). Other integrin-associated proteins may play a role in upregulating pY416-Src, such as FAK, PTP SHP-2, and CSK (c-Src kinase), which has been demonstrated to participate in regulating Src activity (*113, 152, 157*). Mutants in the cytoplasmic tails may also affect the association of integrins with other modulators of Src activation.

Recent structural studies identified the critical roles of K716 of β_3 integrin in the $\alpha_{IIb}\beta_3$ interface and its interactions with α_{IIb} via hydrogen bonds and electrostatic interactions (*149, 158, 159*). Our PAC-1 binding assay confirmed that K716A is an activated integrin mutant. Highly developed filopodia and lamellipodia were visualized at the early cell spreading stage in K716A mutant cells (Figure 3.9). Furthermore, the K716 residue appeared to be the most important for skelemin binding in *in vitro* studies (*146*). Given the overlapping binding areas within the β_3 membrane proximal region, we predict that binding of skelemin and talin to the β_3 membrane proximal region are mutually exclusive events. This is supported by our

findings that talin is strongly co-localized with $\alpha_{IIb}\beta_3$ in the ruffle structure of the K716A cell protrusions, but that skelemin still remained in the main cell bodies (Figure 3.9). Disrupting skelemin binding in K716A mutant cells may facilitate talin recruitment that promotes actin polymerization and membrane protrusion formation.

Filopodia and lamellipodia are the two integrin and actin-based membrane protrusions formed at the leading edge of a moving cell or the periphery of a spreading cell that are prerequisite for cell motility and spreading (*6*). The elongation of these protrusions pushes the leading edge forward while the tail edge undergoes retraction enabling the cell to migrate (*160*). Dynamic cell spreading requires a balance of extending and contractile forces. In platelets, contractile forces also play an important role in blood clot retraction, where the fibrin meshwork is bound to $\alpha_{IIb}\beta_3$ and pulled together by the platelet cytoskeleton. Contractile forces are provided by myosin II (*79*). Similar to myomesin, skelemin was thought to regulate the organization of myosin filaments and mediate the interaction of myosin with integrins (*142*). In our study, skelemin was not present in the sheets of lamellipodia, and reducing skelemin-integrin interactions promoted cell protrusion formation in K716A cell and cell spreading in other mutant cells. These results do not support a role for skelemin in generating an extending force but are consistent with skelemin exerting a contractile force.

In summary, our results extend the current understanding of skelemin function as an integrin-cytoskeleton linker. We propose a model in which soluble and insoluble forms of skelemin might differ in their importance for particular integrin functions.

During the initial stages of cell spreading, soluble skelemin proteins bind to $\alpha_{IIb}\beta_3$ integrin clusters at the leading edges of cells. These skelemin-integrin interactions function to coordinate the binding of different cytoskeletal proteins to the membrane proximal region of integrin tails, such as talin and Src (Figure 3.12B). However, the NPLY region remains exposed during skelemin binding and thus talin and Src can still bind to β_3. During this time period, talin can therefore function as a linker of integrin and actin filaments, and maximal Src activation can be modulated by skelemin. This might afford a mechanism to dampen Src activation and consequently suppress integrin signalling. As cell adhesion and spreading progresses and large amounts of cell protrusion form, a majority of skelemin then dissociates from integrins to allow for other actin-binding proteins to bind to integrins, bringing cell spreading and adhesion to completion (Figure 3.12C). Concurrently, there is an increase in active Src levels and talin at the cell leading edges, due to skelemin dissociation. Some of the soluble skelemin can remain bound to $\alpha_{IIb}\beta_3$ and function as a linker between integrins and the myosin cytoskeleton, thereby transforming it into insoluble skelemin.

CHAPTER 4

EFFECTS OF BIOACTIVE PEPTIDES DERIVED FROM CENTRAL TURN MOTIFS WITHIN CYTOPLASMIC TAILS OF α_{IIb} AND α_v INTEGRINS

4.1 Introduction:

The binding of integrin to extracellular ligands is not usually constitutive but precisely and strictly regulated by a process known as integrin activation. The regulation of integrin activation is important for physiological and pathological processes such as homeostasis, inflammation, and tumour metastasis. It is clear that the ligand binding capacity of integrin can be switched on through an affinity change mechanism, which is triggered by intracellular signals and transmitted by the cytoplasmic tails of integrin α and β subunits (*45*). The cytoplasmic tails propagate their conformational changes induced by intracellular signals through the transmembrane region, and cause allosteric and long-range conformational rearrangement within the extracellular domain of the receptor dimer (*45, 161, 162*). Studies with $\alpha_{IIb}\beta_3$ integrin found that the membrane-proximal α and β cytoplasmic domains forms a 'clasp' that maintains integrin in a default low affinity state (*36, 39, 158*). Cytosolic proteins, such as talin and kindlin cooperatively bind to the membrane-distal region of β_3 subunits and open the activation-constraining α-β clasp，triggering integrin activation and ligand binding (*163*). Cytoplasmic tails of integrin can also regulate integrin-ligand binding by affinity-independent mechanisms,

including integrin clustering, integrin diffusion within the membrane, and linkage of integrins with the cytoskeleton (*162, 164*). Integrin lateral diffusion and clustering, commonly referred as avidity regulation, are secondary events occurring after the initial integrin affinity change and further increase cell adhesive function (*61*).

Integrin α-tails are very short and more diverse compared with β-tails. Truncating almost the entire α_{IIb}-cytoplasmic tail (G991–E1008) constitutively activates $\alpha_{IIb}\beta_3$ (*37*). Cell-permeable peptides derived from full-length α_{IIb} tail (K989–E1008) inhibited agonist-activated and $\alpha_{IIb}\beta_3$-mediated platelet binding to fibrinogen (*4*). These data indicate that the α-tail negatively regulates integrin functions. A major structural feature in α-tails is the central turn motif, which contains a conserved region in α_{IIb} (RPPLEE) and α_V (RPPQEE). NMR structures of α_{IIb} cytoplasmic tails showed that in this motif, a turn structure formed at the double proline (P998 and P999) allowing the negatively charged C-terminus of an α_{IIb} tail to fold back and interact with its N-terminal helix (*4*). Mutation of both prolines (P998A/P999A) completely abolished the inhibition of the full-length α_{IIb} tail peptide on integrin activation, suggesting that the turn motif could be a key inhibitory region. It was supported by the observations that truncated α_{IIb} tail peptides with the removal of the central and C-terminal regions activated $\alpha_{IIb}\beta_3$ (*165, 166*), while double mutation (P998A/P999A) of the α_{IIb} tail expressed in CHO cells rendered $\alpha_{IIb}\beta_3$ constitutively active to bind PAC-1(anti-$\alpha_{IIb}\beta_3$ mAb specifically recognizing active form of $\alpha_{IIb}\beta_3$) (*46, 167*).

To evaluate the contributions of different motifs to the α-tail's inhibitory effect, we used cell-permeable peptides that derive from full length or different segments of

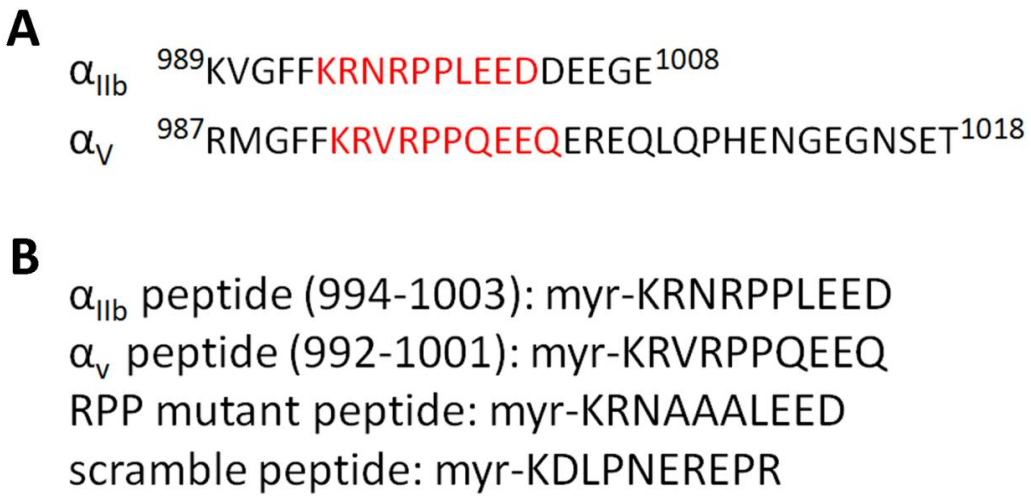

Figure 4.1: The sequences of α_{IIb} and α_v cytoplasmic tails and the peptides. (A) The sequences of α_{IIb} and α_v cytoplasmic tails. The amino acid sequences used in the experimental peptides are shown in red. (B) Sequences of the α_{IIb} and α_v peptides, RPP/AAA mutant and α_{IIb} scrambled peptides.

α-tails (*168, 169*) . The amino-termini of these peptides were coupled to myristic acid, which effectively targets peptides to the plasma membrane and also helps stabilize the secondary structure of flexible peptides (*4*, *170*). We found that myristoylated peptides derived from full-length α_V tails inhibited PMA-induced and $\alpha_v\beta_3$-mediated cell adhesion (*168, 169*). The turn motif peptide α_V (^{993}RVRPPQEEQ) was identified as the minimal inhibitory sequence in α_V tail (*169*). However, the peptide α_{IIb} (995–1003) ^{995}RNRPPLEED, which is homologous to α_V (^{993}RVRPPQEEQ), was functionally silent for inhibiting $\alpha_{IIb}\beta_3$ activation (*169*). As the removal of several amino acids from the two ends of full-length α_{IIb} tail would not destroy the inhibitory capacity (*4*), we hypothesize that the turn motif in the α_{IIb} tail is an inhibitory domain, but that extra amino acid(s) outside of α_{IIb} (995–1003) are required for its full inhibitory capacity.

In the present study, myristoylated peptide KRNRPPLEED (named as α_{IIb} peptide, Figure 4.1) was examined in assays of cell adhesion as well as soluble ligand binding in breast cancer cells lines (MDA-MB-435 and MCF-7) and $\alpha_{IIb}\beta_3$-expressing CHO cells. Including the lysine residue allows introduction of a biotin-tag to the lysine side chain. Cellular proteins that interact with α_{IIb} peptide were also investigated. The homologous peptide from α_V tails, myr-KRVRPPQEEQ (named as α_V peptide, Figure 4.1) was used in parallel to compare their potency to influent integrin-ligand binding.

4.2 Results

4.2.1 α_{IIb} and α_v peptides inhibited adhesion of $\alpha_{IIb}\beta_3$-expressing CHO cells to fibrinogen

To determine whether our α_{IIb} peptide is inhibitory for $\alpha_{IIb}\beta_3$-mediated cell adhesion, CHO cells stably expressing $\alpha_{IIb}\beta_3$ were used (Figure 4.2). Cells were labelled with fluorescent dye Calcein AM and treated with peptides as described in Materials and Methods. Significantly decreased cell adhesion was observed when cells were treated with 50, 100, or 150 μM α_{IIb} peptide compared with its scrambled form (Figure 4.2A). At a higher concentration, 200μM α_{IIb} peptide showed no difference from the scrambled peptide, possibly because the high concentration of myristoyl group was cytotoxic, leading to dramatic adverse effect on cell adhesion. Figure 4.2B showed that the α_v peptide also had inhibitory effects on CHO cell adhesion at the tested concentrations.

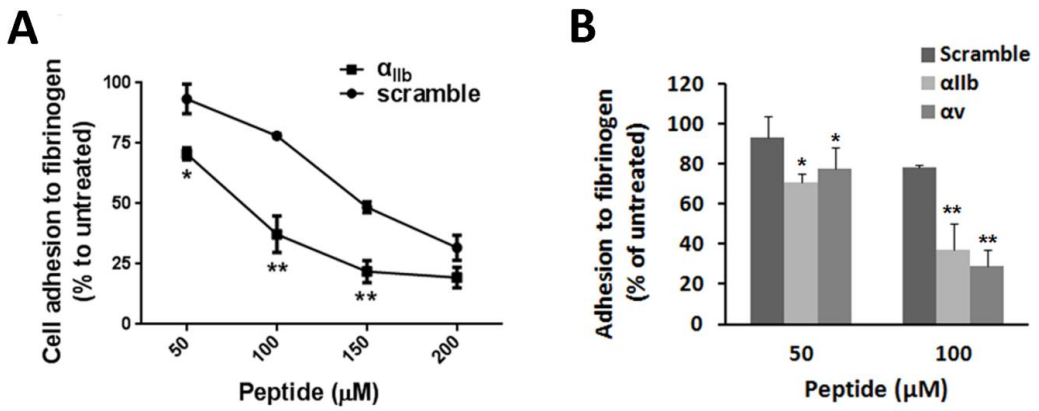

Figure 4.2: Capacity of α_v and α_{IIb} peptides to inhibit $\alpha_{IIb}\beta_3$–overexpressing CHO cell adhesion to fibrinogen. (A) Measurement of cell adhesion when calcein AM-labelled CHO cells were incubated with α_{IIb} or scrambled peptides for 20 minutes at 37℃. (B) Measurement of cell adhesion when α_{IIb}, α_v or scrambled peptide was introduced at the indicated concentrations. Treated or untreated cells were added to fibrinogen-coated wells. After adhesion, unattached cells were removed by washing. Adhesion was quantified by fluorescent intensity changes as indicated in Materials and Methods. Adhesion for untreated cells was assigned a value of 100%. The data shown are means and SEM from three different experiments. * $P<0.05$ vs. scrambled peptide treatment; ** $P<0.01$ vs. scrambled peptide treatment, by two-way ANOVA. ** $P<0.01$ compared with scrambled peptide treatment by two-way ANOVA(Bonferroni's multiple comparisons test).

4.2.2 α_{IIb} and α_v peptides inhibited MDA-MB-435 and MCF-7 cell adhesion to vitronectin

We were interested in determining whether the α_{IIb} peptide could inhibit α_v integrin-mediated cell adhesion. Two breast cancer cell lines were used, highly metastatic MDA-MB-435 cells and poorly metastatic MCF-7 cells. Peptide effects on the adhesion of both cell types to vitronectin were examined. Vitronectin is a classic α_v integrin ligand and it is abundantly expressed in cancer tissues, such as the small vessels surrounding breast cancer cells, and in high-grade glioblastomas (*171, 172*). α_v integrin binding to vitronectin promotes cancer cell survival and migration, and contributes to tumour invasion and metastasis in breast cancer, melanoma and glioma (*172-174*).

Immunofluorescence images showed that α_v integrin binding to vitronectin results in the formation of stress fibers and focal adhesions in both types of breast cancer cells (Figure 4.3). Specifically, many bundles of stress fibers span the core of the MDA-MB-435 cells and distribution of F-actin in some MCF7 cells was condensed and localized at the cell periphery. Focal adhesions visualized by vinculin staining were also highly-developed and exhibited a dot-like distribution pattern. Our observations of the presence of these structures suggest that inhibiting α_v integrin-vitronectin binding may potentially target their integrin-mediated migration in the two cancer cell lines.

MDA-MB-435 cells express three α_v integrin subfamily members including $\alpha_v\beta_3$, $\alpha_v\beta_5$ and $\alpha_v\beta_6$ (*175*), and all of them have the capacity to bind vitronectin (*176*).

Figure 4.4A revealed that both α_{IIb} and α_v peptides inhibited MDA-MB-435 adhesion to vitronectin in a dose-dependent manner. Interestingly the α_{IIb} peptide had a similar inhibitory effect on MDA-MB-435 adhesion as did α_v peptide. Both peptides could inhibit cell adhesion to vitronectin by 50% at a concentration of 8 μM, and totally inhibited cell adhesion at 100 μM. Various function-blocking antibodies were used to determine which of the three present α_v-containing integrins support MDA-MB-435 cell adhesion to vitronectin. Figure 4.4B showed that treatment with anti-$\alpha_v\beta_3$ or $\alpha_v\beta_5$ antibodies, but not anti-$\alpha_v\beta_6$ antibody, could inhibit cell adhesion. Combined treatment with anti-$\alpha_v\beta_3$ and $\alpha_v\beta_5$ antibodies completely prevented cell adhesion. Taken together, these results suggest that α_{IIb} and α_v peptides blocked $\alpha_v\beta_3$ and $\alpha_v\beta_5$-mediated MDA-MB-435 cell adhesion to vitronectin.

To further explore if the peptides are capable of inhibiting both $\alpha_v\beta_3$ and $\alpha_v\beta_5$-dependent cell adhesion, MCF7 cells that do not express $\alpha_v\beta_3$ were used in this assay (*175*). Both α_{IIb} and α_v appeared to inhibit MCF7 adhesion to vitronectin. Treatment of 25 μM peptide inhibited 50% of the cell adhesion, a lower potency of activity compared with the peptide's effect on MDA-MB-435 cells (Figure 4.4C). Among the three different function-blocking antibodies, only anti-$\alpha_v\beta_5$ antibody partially inhibited cell adhesion, indicating MCF7 adhesion to vitronectin was primarily mediated by $\alpha_v\beta_5$ integrin (Figure 4.4D). The above data suggest that α_{IIb} and α_v peptides also inhibited $\alpha_v\beta_5$-mediated cell adhesion.

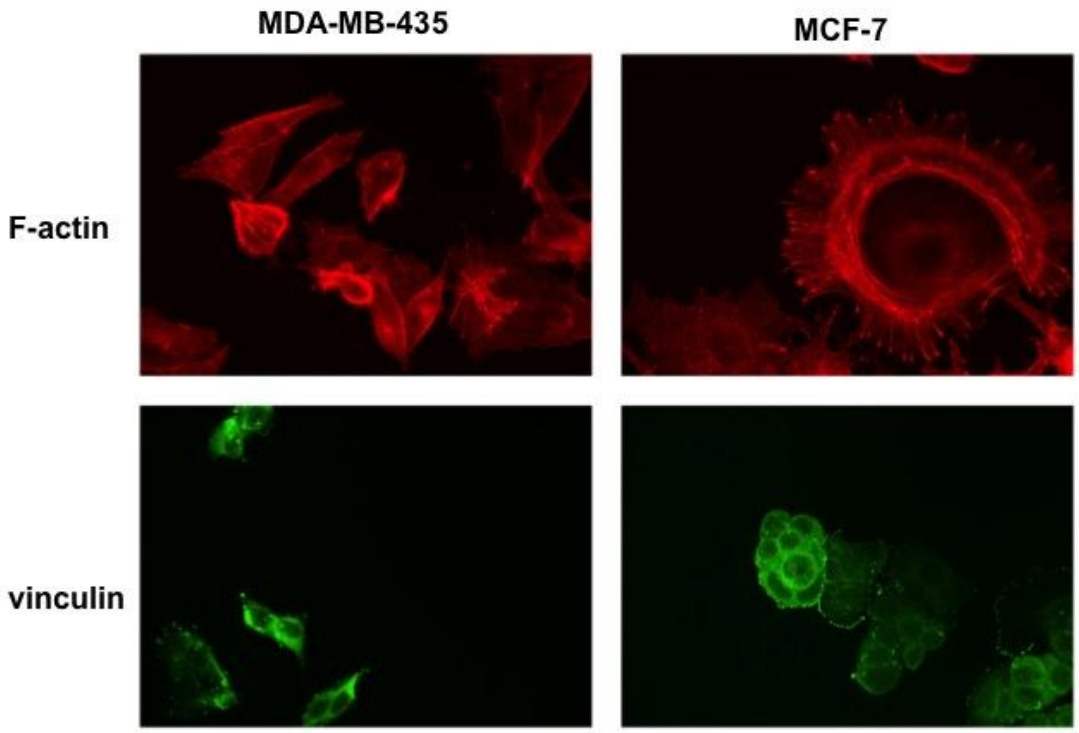

Figure 4.3: Immunofluorescence images showing stress fibers and focal adhesions in MDA-MB-435 and MCF-7 cells grown on vitronectin. Cells were grown on vitronectin-coated chamber slides for overnight, and then fixed, permeabilized and stained with rhodamine phalloidin to detect F-actin-containing stress fibers (red) and anti-vinculin antibody to detect focal adhesions (green).

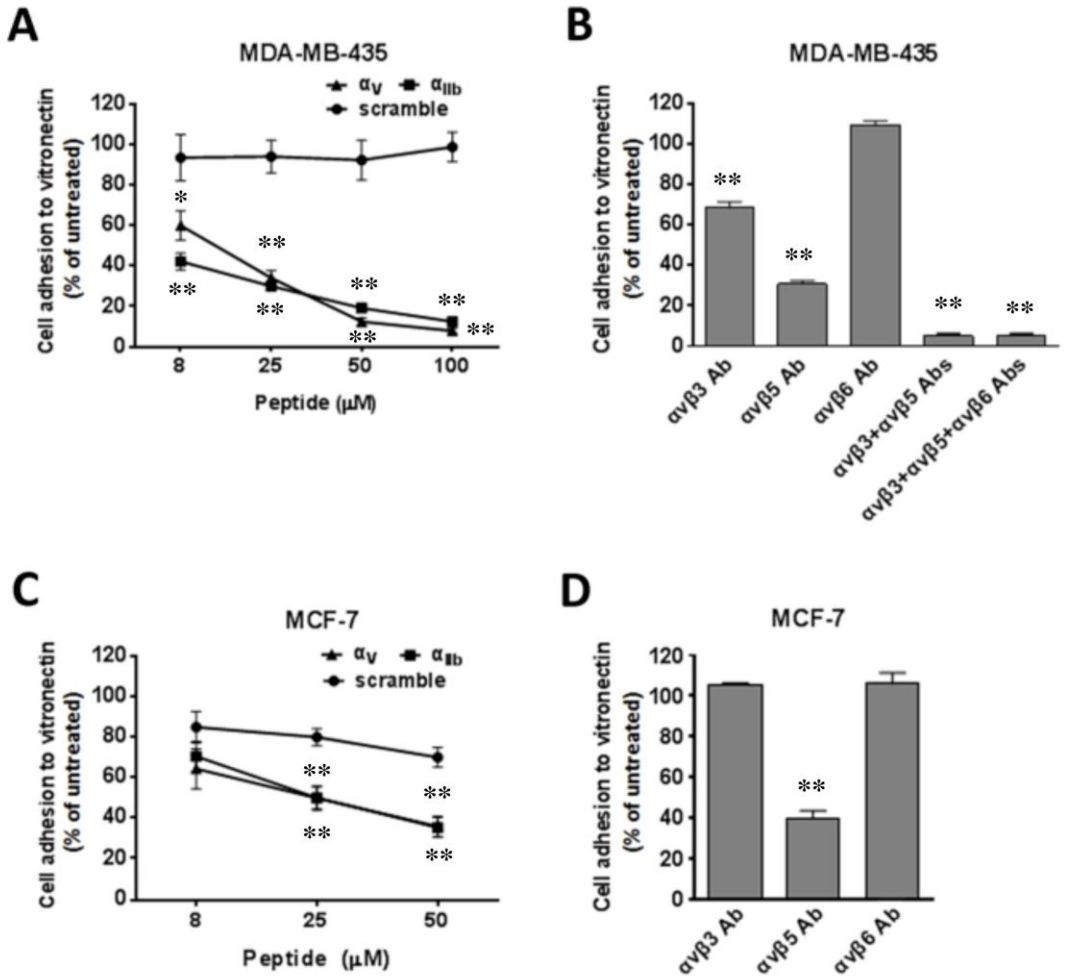

Figure 4.4: Capacity of α_v and α_{IIb} peptides to inhibit MDA-MB-435 and MCF-7 cell adhesion to vitronectin. Calcein AM-labelled cells in suspension were incubated with α_v, α_{IIb} and scramble peptides at the indicated concentrations for 20 minutes at 37℃ (A, C), or 10 μg/mL of each antibody for 20 minutes at room temperature (B, D). Treated or untreated cells were then added into vitronectin-coated wells. After adhesion, unattached cells were removed by washing. Adhesion was quantified by measuring fluorescence intensity change as indicated in Materials and Methods. Adhesion for untreated wells was assigned a value of 100%. The data shown are means and SEM from three different experiments. Statistical analysis was performed with two-way ANOVA and Bonferroni's multiple comparisons test in A and C. Statistical analysis with one-way ANOVA and Tukey's multiple comparisons test in B and D.

4.2.3 α_{IIb} and α_v peptide inhibited the ability of $\alpha_{IIb}\beta_3$-expressing CHO cells to bind soluble fibrinogen

Agonist-stimulated fibrinogen binding to $\alpha_{IIb}\beta_3$ on circulating platelets following vascular injury is critical for platelet aggregation and homeostasis. Wild-type $\alpha_{IIb}\beta_3$ expressed in CHO cells remains in an inactive state as in non-activated platelets. The artificial activator Mn^{2+} was then used to reconstitute integrin activation and peptide effects on Mn^{2+}-stimulated $\alpha_{IIb}\beta_3$ binding to soluble fibrinogen were investigated by confocal microscopy. Figure 4.5 showed that CHO cells stimulated with Mn^{2+} displayed a high amount of fibrinogen binding. Clustering of cells upon soluble fibrinogen binding to $\alpha_{IIb}\beta_3$ was visible. In contrast, the presence of α_{IIb} or α_v peptide decreased fibrinogen binding and cell aggregation.

Next, fibrinogen binding levels on CHO cells treated with different concentrations of each peptide were measured by flow cytometry (Figure 4.6). Cells without Mn^{2+} and peptide treatment showed low fluorescence intensity, indicating little background fibrinogen binding. Adding Mn^{2+} promoted substantial fibrinogen binding, reflected by the right shift of fluorescence intensity. Both α_{IIb} and α_v peptide treatment decreased the percentage of cells that bound fibrinogen in a dose-dependent manner. No detectable difference of fluorescence intensity was observed when cells were treated with different concentrations of scrambled peptide (data not shown). These findings provided evidence that α_{IIb} and α_v peptides were able to inhibit Mn^{2+} promoted soluble fibrinogen-$\alpha_{IIb}\beta_3$ binding. However, to address whether findings in CHO cells are relevant to what actually occurs in human platelets, studies

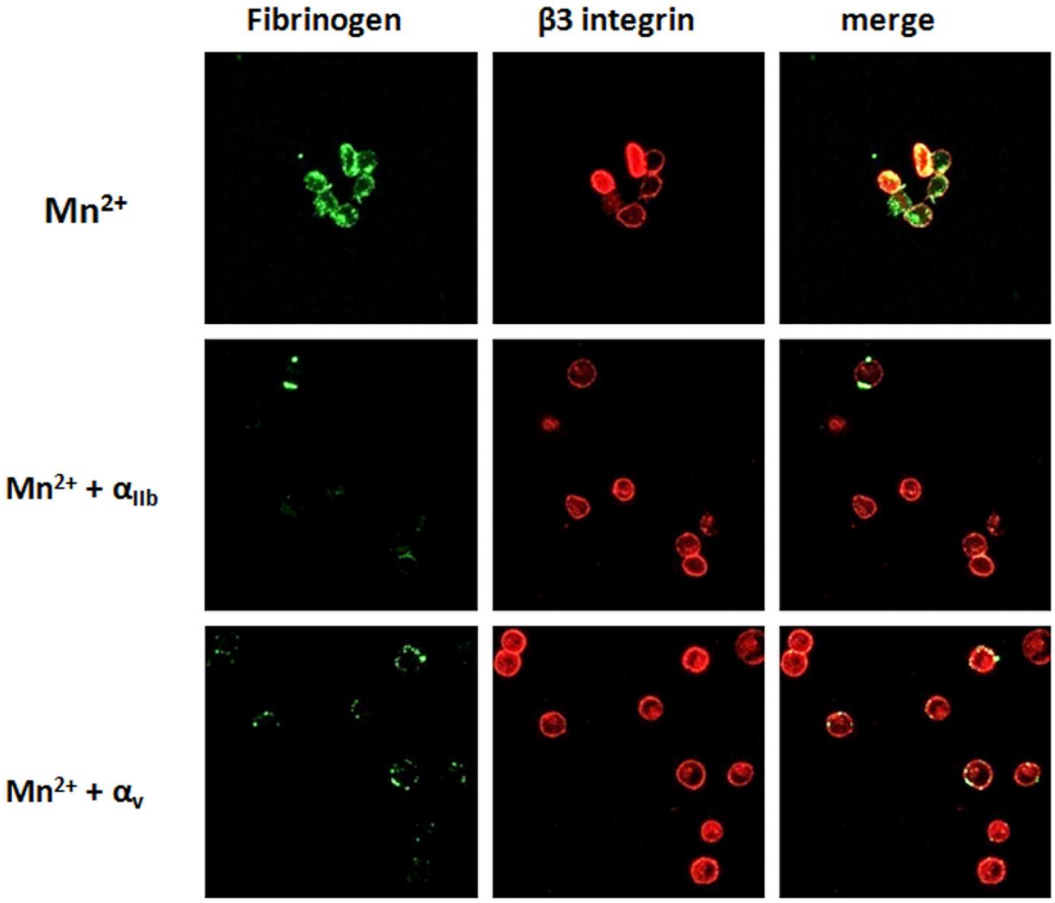

Figure 4.5: Confocal images showing α_v and α_{IIb} peptide inhibition of Mn^{2+}-stimulated soluble fibrinogen binding to $\alpha_{IIb}\beta_3$-expressing CHO cells. $\alpha_{IIb}\beta_3$-expressing CHO cells were first treated with 100 μM peptides, and then stimulated with Mn^{2+} (0.2 mM). Alexa 488-fibrinogen was then added. After washing, cells were fixed and stained for β_3 integrin. Cells in mounting media were plated on coverslips and visualized by confocal microscopy.

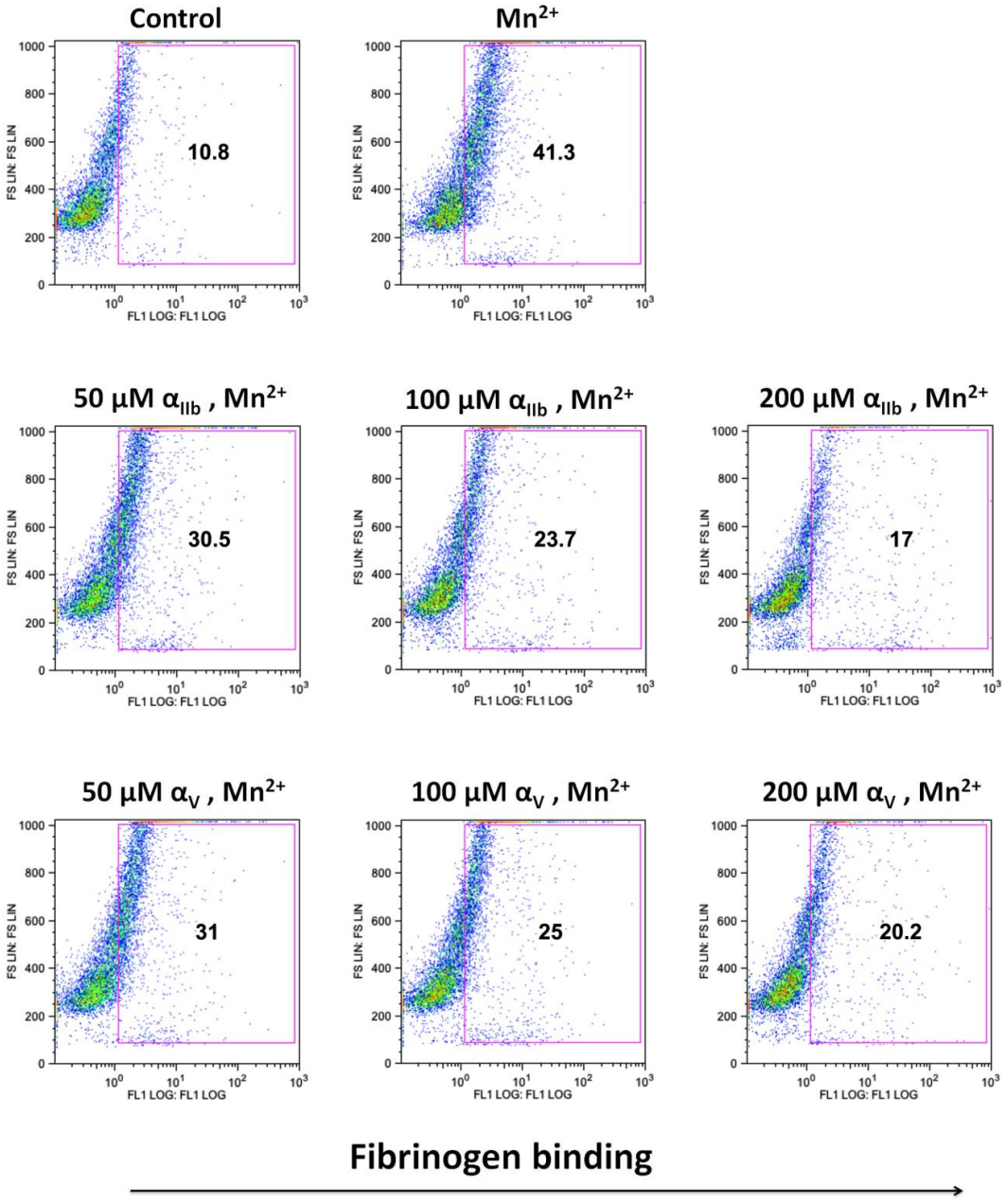

Figure 4.6: Flow cytometric analysis showing α_v and α_{IIb} peptide inhibition of Mn^{2+}-stimulated fibrinogen binding to $\alpha_{IIb}\beta_3$-expressing CHO cells. $\alpha_{IIb}\beta_3$-expressing CHO cells were first treated with peptides at the indicated concentrations, and then stimulated with Mn^{2+} (0.2 mM). Alexa 488-fibrinogen was then added. After washing, binding of Alexa 488-fibrinogen was measured by flow cytometry. In the figure, the x-axis is fluorescence intensity and the y-axis is forward scattering. A rectangular gate was drawn to indicate dots that were considered to represent positively stained cells. The percentages of positively stained cells were indicated in the rectangular gates.

using thrombin or ADP-activated human platelets need to be carried out.

4.2.4 Peptide mobility on SDS-PAGE gel

The α_{IIb}, α_v, scrambled peptide and $\alpha_v$mut (Q998A) were examined on 20% SDS-PAGE gel (Figure 4.7). Staining the polyacrylamide gel with Coomassie blue showed that α_{IIb}, α_v and $\alpha_v$mut peptides migrated with the same apparent molecular weight, whereas the scrambled peptide migrated faster than the other peptides in the gels. Compared with proteins, the intrinsic charge and conformation were found to be important for electrophoretic mobilities of oligopeptides (*177*). Because α_{IIb} and scrambled peptide had the same molecular weight and intrinsic charge based on their same amino acid composition, their different mobilities on SDS-PAGE gel suggested they may have different conformations. Myristoylated α_{IIb} cytoplasmic tail peptide was reported to form a closed structure conformation highlighted by a turn formed at the double proline in the middle and electronic interactions between the two ends. We expect that the scrambled peptide formed an unstructured conformation as two proline residues were separated and positive charged N-terminus and negative charged C-terminus were also disrupted. A possible reason for the scrambled peptide's higher electrophoretic mobility is that its disordered form may facilitate a more rapid traverse through the polyacrylamide matrix. From the gel electrophoresis result, it was hypothesized that a closed conformation, lost in the scrambled peptide, may be important for the inhibitory capacity of bioactive α_{IIb} and α_v peptides.

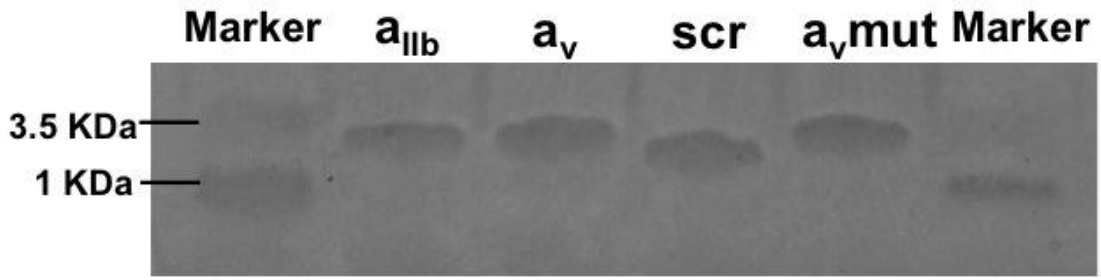

Figure 4.7 The scramble peptide migrates faster than α_v and α_{IIb} peptides in SDS gel electrophoresis. 1μg of each peptide was electrophoresed in 20% SDS gels, and the gel was stained with Coomassie blue. Molecular markers are shown left. The molecular weights of the peptides are a_{IIb} 1.46 kDa, a_v 1.47kDa, scramble 1.46 kDa.

4.2.5 The turn structure is important for the inhibitory capacity of α_{IIb} peptide

The RPP sequence, conserved in α_{IIb} and α_v tails, was predicted to form a β turn structure of the peptides. Previous studies have shown that a double proline mutant of full-length α_{IIb} cytoplasmic peptide was functionally inactive as was the shorter α_v peptide (*4, 168*). We found that mutant peptide with the RPP to AAA (RPP/AAA) substitution attenuated the inhibitory effects of α_{IIb} on cell adhesion. As shown in Figure 4.8A, at a concentration of 8 μM, α_{IIb} peptide treatment inhibited MDA-MB-435 cell adhesion to vitronectin by 58%, significantly greater than the RPP/AAA mutant which showed only 23% inhibition ($P<0.01$). Similarly, α_{IIb} peptide-induced inhibition on cell adhesion was decreased by RPP/AAA mutant in MCF-7 cells from 53% to 30 % when 25 μM peptides were used, and in $\alpha_{IIb}\beta_3$-expressing CHO cells from 49% to 4% when 100 μM peptides were used (Figures 4.8B and 4.8C). These results showed that the RPP/AAA mutant peptide still retained some inhibitory capacity, but with a less potent effect than the α_{IIb} peptide.

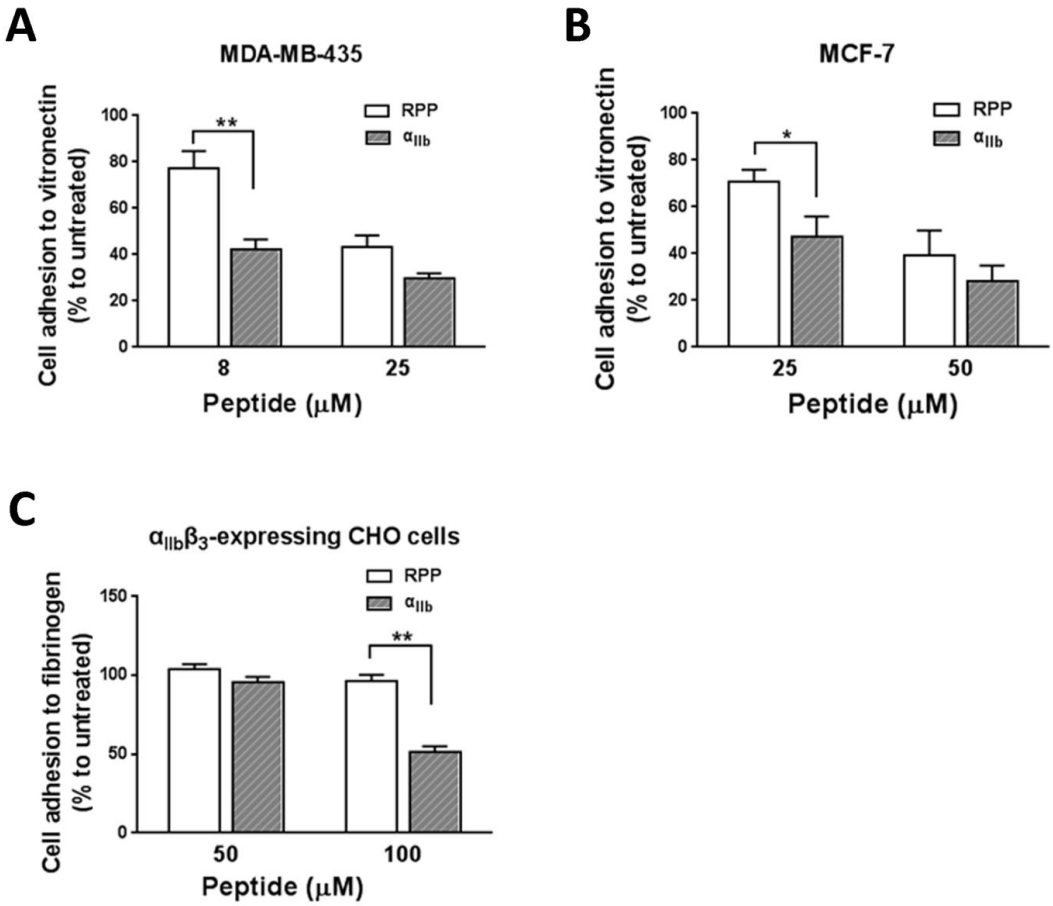

Figure 4.8: Decreased inhibitory capacity of the RPP/AAA mutant peptide. Calcein AM-labelled (A) MDA-MB-435, (B) MCF-7, (C) $\alpha_{IIb}\beta_3$-expressing CHO cells were treated with α_{IIb} and RPP/AAA mutant peptides at the indicated concentrations, and then added into ligand protein-coated wells. After adhesion, unattached cells were removed by washing. Adhesion was quantified by measuring fluorescence intensity as indicated in Materials and Methods. Adhesion for untreated wells was assigned a value of 100%. The data shown are means and SEM from three different experiments. ** $P<0.01$ compared with α_{IIb} peptide treatment (two way-ANOVA, Bonferroni's multiple comparisons test).

4.2.6 Identification of intracellular binding partner

To search for intracellular binding partners associated with the bioactive peptides, we performed immunoprecipitation of total cell lysate from $\alpha_{IIb}\beta_3$-expressing CHO cells with the use of biotin tagged α_{IIb} peptide, bio-KRNRPPLEED. Biotin-tagged scrambled peptide was used as a negative control. Biotin-tagged peptides were first immobilized onto streptavidin-dynabeads and then incubated with CHO cell lysate. Proteins pulled down via interaction with biotin-tagged peptides were separated on SDS-PAGE gels and visualized by silver staining (Figure 4.9). To search for proteins that specifically interacted with the bio-α_{IIb} peptide, protein bands that were present in higher amount in the bio-α_{IIb} immunocomplex lane than in the bio-scrambled peptide lane were of interest. The 55 kD bands on the SDS-PAGE gel appeared unique in the bio-α_{IIb} immunocomplex (Figure 4.9A). The bands were cut out and identified with mass spectrometry. The putatively identified proteins via MASCOT search are listed in Figure 4.9B. The results indicated that β-tubulin was enriched in the sample pulled down by bio-α_{IIb} peptide. Tubulin-β5 chain and tubulin-4B chain showed higher protein score (protein score is $-10 \times \text{Log}(P)$, where P is the probability that the observed match is a random event). Furthermore, the apparent molecular weight of the bands is 55 kD, which is consistent with the actual molecular weight of tubulin. The overall sequence coverage of tubulin-β5 chain and tubulin-4B chain is presented in Figure 4.9C. 8 peptides matching tubulin-β5 were identified with a protein sequence coverage of 19% (protein sequence coverage is calculated by dividing the number of amino acids observed by the protein amino acid length).

A

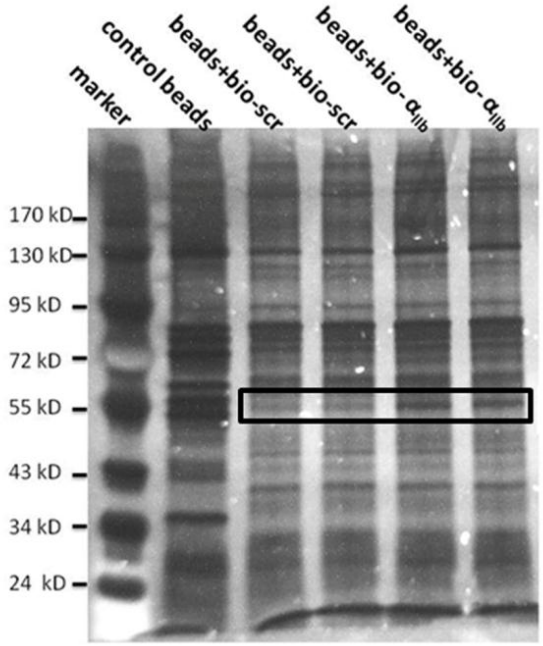

B

	Protein hits (bio- scramble pull down)	Score
1	tubulin beta-5 chain [Mus musculus]	96
2	Fatty acyl-CoA reductase 1 [Rattus norvegicus]	88
3	Snx25 protein [Mus musculus]	35

	Protein hits (bio- α_{IIb} pull down)	Score
1	tubulin beta-5 chain [Mus musculus]	340
2	tubulin beta-4B chain [Homo sapiens]	213
3	alpha-tubulin isotype M-alpha-2 [Mus musculus]	104
4	tubulin beta-1 chain - mouse	97
5	PREDICTED: beta tubulin 1, class VI-like [Rattus norvegicus]	88
6	unnamed protein product [Mus musculus]	79

C

tubulin beta-5 chain (protein sequence coverage:19%)

1	MREIVHIQAG	QCGNQIGAKF	WEVISDEHGI	DPTGTYHGDS	DLQLDR**ISVY**
51	**YNEATGGK**YV	PR**AILVDLEP**	**GTMDSVR**SGP	FGQIFRPDNF	VFGQSGAGNN
101	WAKGHYTEGA	ELVDSVLDVV	RKEAESCDCL	QGFQLTHSLG	GGTGSGMGTL
151	LISKIREEYP	DR**IMNTFSVV**	**PSPK**VSDTVV	EPYNATLSVH	QLVENTDETY
201	CIDNEALYDI	CFRTLKLTTP	TYGDLNHLVS	ATMSGVTTCL	R**FPGQLNADL**
251	**RKLAVNMVPF**	**PR**LHFFMPGF	APLTSRGSQQ	YR**ALTVPELT**	**QQVFDAK**NMM
301	AACDPRHGRY	LTVAAVFRGR	MSMK**EVDEQM**	**LNVQNK**NSSY	FVEWIPNNVK
351	TAVCDIPPRG	LKMAVTFIGN	STAIQELFKR	ISEQFTAMFR	RKAFLHWYTG
401	EGMDEMEFTE	AESNMNDLVS	EYQQYQDATA	EEEEDFGEEA	EEEA

tubulin beta-4B chain (protein sequence coverage:12%)

1	MREIVHLQAG	QCGNQIGAKF	WEVISDEHGI	DPTGTYHGDS	DLQLER**INVY**
51	**YNEATGGK**YV	PRAVLVDLEP	GTMDSVRSGP	FGQIFRPDNF	VFGQSGAGNN
101	WAKGHYTEGA	ELVDSVLDVV	RKEAESCDCL	QGFQLTHSLG	GGTGSGMGTL
151	LISKIREEYP	DR**IMNTFSVV**	**PSPK**VSDTVV	EPYNATLSVH	QLVENTDETY
201	CIDNEALYDI	CFRTLKLTTP	TYGDLNHLVS	ATMSGVTTCL	R**FPGQLNADL**
251	**RKLAVNMVPF**	**PR**LHFFMPGF	APLTSRGSQQ	YRALTVPELT	QQMFDAKNMM
301	AACDPRHGRY	LTVAAVFRGR	MSMK**EVDEQM**	**LNVQNK**NSSY	FVEWIPNNVK
351	TAVCDIPPRG	LKMSATFIGN	STAIQELFKR	ISEQFTAMFR	RKAFLHWYTG
401	EGMDEMEFTE	AESNMNDLVS	EYQQYQDATA	EEEGEFEEEA	EEEVA

Figure 4.9: Potential identification of β-tubulin as an α_{IIb} peptide-associated protein with a bio-peptide pull-down assay and mass spectrometry. (A) Peptide pull-down assays using bio-α_{IIb} or bio-scrambled peptide. Bio-α_{IIb} or bio-scrambled peptide was incubated with streptavidin-coated dynabeads. After washing away unbound peptides, the beads were then incubated with $\alpha_{IIb}\beta_3$-expressing CHO cell lysate overnight. Proteins interacting with bio-peptides were separated by SDS-PAGE and visualized by silver staining. The bands inside the black rectangle were cut out, digested with trypsin and analyzed by mass spectrometry. (B) MASCOT search results that indicated that β-tubulin was enriched in the sample pulled down by bio-α_{IIb} peptide. Proteins listed in the column have protein scores higher than the threshold, which can be considered as identified ($p<0.05$). (C) Sequence of tubulin beta-5 and beta-4B chain. Recovered peptides matching the sequences of tubulin beta-5 (top sequence) and tubulin beta-4B chain (bottom sequence) are depicted in dark, whereas regions not identified by recovered peptides are shown in gray.

4.2.7 α_v and α_{IIb} peptides did not change the levels of p-ERK and pY397-FAK in MDA-MB-435 cells

As our mutations of integrin cytoplasmic tails did not affect downstream signalling through FAK in CHO cells (Figure 3.7A), we then examined the role of the central turn motif of α-tails by studying the effects of peptides on integrin outside-in signalling through FAK and ERK in MDA-MB-435 breast cancer cells. Serum-starved cells were trypsinized and suspended in Tyrodes buffer. Cells in suspension were treated with or without peptides for 20 minutes and then plated on vitronectin. After one hour of adhesion, cells were solubilised and the levels of p-ERK and pY397-FAK were studied by Western blot. Figure 4.10 shows that cells contained constitutively activated ERK and FAK by measuring the levels of p-ERK and pY397-FAK in non-adherent suspension cells (the first lanes of the blots). Cell adhesion on vitronectin increased p-ERK levels only slightly compared with cells in suspension. Treatment with scr, α_{IIb} or α_v peptide did not cause any observable changes of p-ERK levels in the adherent cells (Figure 4.10A). Similar results were obtained for pY397-FAK. As shown in Figure 4.10B, pY397-FAK levels showed little difference when comparing adherent to non-adherent cells, and pY397-FAK remained at the same level in adherent cells treated with α_{IIb}, α_v or scrambled peptide.

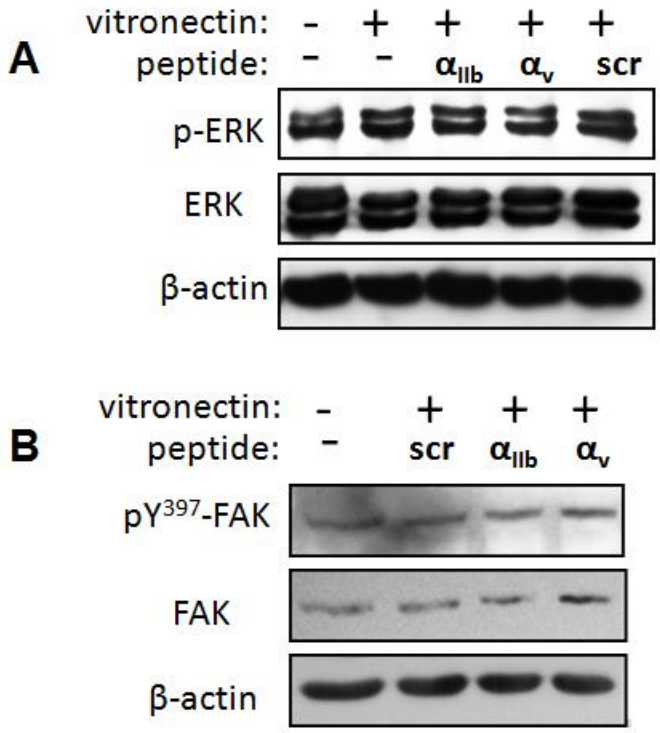

Figure 4.10 α_v and α_{IIb} peptides did not change the levels of p-ERK and pY397-FAK in MDA-MB-435 cells. Serum-starved MDA-MB-435 cells were exposed to α_{IIb}, α_v and scramble peptide (100 μM each) for 20 minutes, and allowed to adhere on vitronectin for 2 hours. Total cell extracts were subjected to SDS-PAGE. Blots were probed using antibodies against pERK (P42/P44), ERK, Y^{397}-FAK, FAK and β-actin.

4.2.8 Post-treatment with α_{IIb} peptide did not reverse ligand-integrin engagement

Our data showed that α_{IIb} and α_v peptides were potent integrin antagonists when they were pre-treated. Thus, a new question is raised whether the peptides still possess inhibitory capacity after the integrin is activated and ligand engagement has occurred. The functional consequences of peptide treatment before and after integrin activation were compared using platelet aggregation and cell adhesion experiments. Platelet aggregation assays were carried out in an aggregometer, which measures light transmission changes of sample solution caused by platelet aggregation. As shown in Figure 4.11A, adding agonists ADP/EPI induced platelet aggregation which lead to less light absorption and increased transmission as recorded in the aggregometer. Pre-incubation with 50 μM α_{IIb} full-length CT (cytoplasmic tail) peptide before the addition of agonists effectively blocked platelet aggregation, indicated as the decreased light transmission (Figure 4.11A). However, post-treatment with α_{IIb} CT peptide had no inhibitory effect on platelet aggregation (Figure 4.11B).

We also found that the central turn peptides, α_{IIb} and α_v, could not detach $\alpha_{IIb}\beta_3$-expressing CHO cells adhered on fibrinogen (Figure 4.11C). Cells were first allowed to adhere to integrin ligand for one hour, and then treated with buffer or 100 μM α_{IIb}, α_v or scramble peptide. After one more hour of adhesion, unattached cells were removed by washing. Cell adhesions in the presence of buffer were displayed as 100%. No statistically significant differences were observed between the buffer and peptide-treated groups (($p<0.05$), suggesting that neither α_{IIb} nor α_v peptide was able to detach $\alpha_{IIb}\beta_3$-expressing CHO cells from fibrinogen. Similar results were obtained

for adherent MDA-MB-435 and MCF-7 cells (Figure 11 D and E).

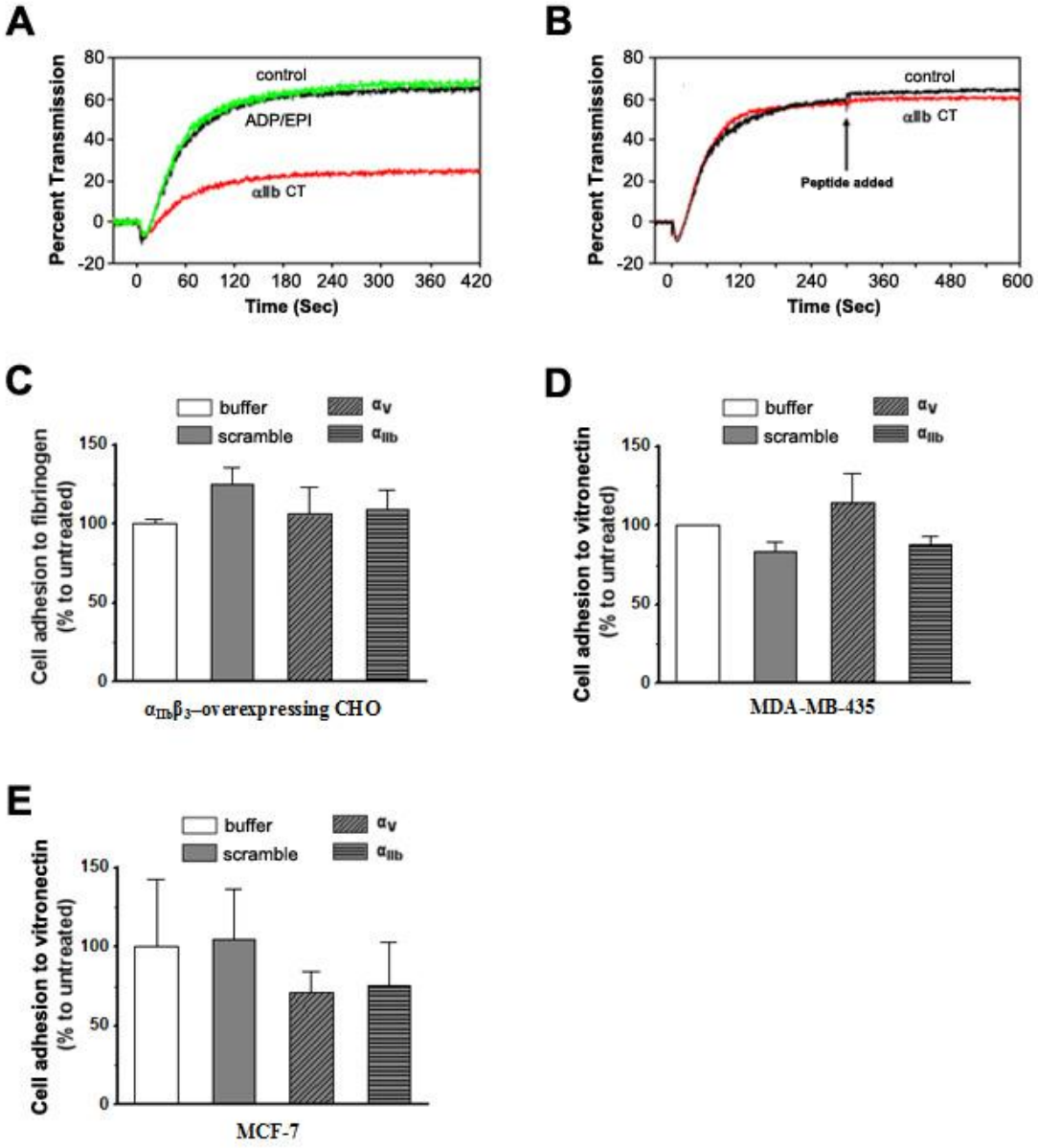

Figure 4.10 Treatment of the inhibitory α_{IIb} or α_v peptides did not reverse ligand-integrin engagement. Effect of pre-treatment (A) and post-treatment (B) of α_{IIb} CT peptide on platelet aggregation stimulated by ADP/EPI. (A) PRP was stimulated with ADP/EPI to induce platelet aggregation (indicated as ADP/EPI). 50μM α_{IIb} CT peptide-treated PRP were stimulated with ADP/EPI to generate an inhibition curve (indicated as α_{IIb} CT). PP/AA mutant peptide was used as a control. (B) PRP was treated with 50μM α_{IIb} CT peptide or control peptide five minutes after the agonists were added. No inhibition of platelet aggregation was observed. (C, D and E) Neither α_{IIb} nor α_v peptide was able to detach $\alpha_{IIb}\beta_3$-expressing CHO cell

adhesion on fibrinogen (C), and MDA-MB-435 (D) and MCF-7 (E) cell adhesion on vitronectin. Cells were harvested, labelled by Calcein AM, and allowed to adhesion on integrin ligand in Tyrodes buffer for one hour. 100μM α_{IIb}, α_v or scramble peptides were then added. After one more hour adhesion, unattached cells were removed by washing. Adhesion was quantified by measuring fluorescence intensity before and after wash as indicated in Materials and Methods. The buffer bars represent untreated groups, which were assigned a value of 100%. The data shown are means and SEM from three different experiments. Student's t-test was performed and no statistically significant difference was found between the buffer and peptide-treated groups ($p<0.05$).

4.3 Discussion

The full-length cytoplasmic tail peptides from α_{IIb} (989-1008) and α_V (987–1006) suppressed the ligand binding function of $\alpha_{IIb}\beta_3$ and $\alpha_V\beta_3$ integrins, respectively (*169*). We previously found that peptide RVRPPQEEQ (993-1001), corresponding to the central motif of α_V tail, inhibited $\alpha_V\beta_3$ and $\alpha_{IIb}\beta_3$ ligand binding, and it appeared to be the shortest sequence among truncated cytoplasmic tail peptides that still retained the inhibitory capacity. However, its homologous peptide RNRPPLEED (995-1003) derived from α_{IIb} tails was functionally silent for inhibiting $\alpha_{IIb}\beta_3$-mediated fibrinogen binding to platelets (*169*). In the present study, α_{IIb} peptide KRNRPPLEED (994-1003) that include the adjacent lysine residue was examined. We found that it blocked $\alpha_{IIb}\beta_3$-expressing CHO cells binding to immobilized or soluble fibrinogen (Figures 4.2, 4.5 and 4.6). This work suggests the α_{IIb} central turn motif is the inhibitory domain of the α_{IIb} cytoplasmic tail and that the residue lysine (K994) is required for full inhibitory capacity.

More importantly, we found that the homologous peptides α_{IIb} (994-1003) and α_V (992-1001) suppressed both $\alpha_{IIb}\beta_3$ and $\alpha_V\beta_3$ functions, which may lead to a new

therapeutic strategy for an anti-cancer and anti-platelet dual-role drug. Our work showed that peptides α_{IIb} (994-1003) and α_V (992-1001) were equally effective at inhibiting $\alpha_{IIb}\beta_3$ and $\alpha_V\beta_3$ mediated-cell adhesion to the immobilized and soluble ligands (Figures 4.2 and 4.4), although peptides derived from the full-length α_{IIb} and α_V tails can only block their parent integrin's functions. A previous study showed that α_{IIb} (989-1008) tail peptide only blocked $\alpha_{IIb}\beta_3$ activation, and α_V (987–1006) tail peptide only blocked $\alpha_V\beta_3$ activation (*169*). The functional specificity of the full-length tails may attribute to their membrane proximal regions. Cytoplasmic tails of α_{IIb} and β_3 subunits interact to form a complex through their membrane-proximal regions, which maintains integrin α_{IIb} and β_3 in an inactive state (22, 23). A possible mechanism for the inhibitory effect of the full-length tail peptides is due to their competition with the native tails of their parent integrins in binding to β tails (*4*). Our recent work using surface plasmon resonance (SPR) spectroscopy found that the α_V and β_3 tails also interacted with each other (*169*). However, the α_V turn motif peptide (993–1001) had low affinity for β_3 tails and was ineffective at perturbing of α_V-β_3 tail interaction (*169*). Moreover, the highly conserved KXGFFKR motif in the membrane proximal region acts as a recognition site for multiple intracellular proteins. Studies using protein chips have identified 68 direct binding proteins to this conserved motif derived from different α integrin isoforms (*47*). However, most of these binding proteins are specific for different integrin family members (*47*), suggesting that the protein binding sites in membrane proximal region are different among α integrin isoforms.

The conserved amino acid composition and similar activity of α_{IIb} and α_V turn peptides indicate that the same functional mechanism occurs with both peptides. The cytoplasmic tail of the integrin α_{IIb}-subunit has often served as a typical prototype for structure-function analyses (*45*). Here we used the wild-type, mutant and scrambled α_{IIb} turn motif peptides to investigate the possible mechanism shared by the α_{IIb} and α_V turn motifs.

RPP residues are important for maintaining the backbone structure of the turn. The NMR structure of the α_{IIb} tail (PDB# 1DPK) showed that the turn motif allowed the acidic C-terminus to fold back and interact with the positively charged N-terminal, resulting in a "closed" conformation. However, mutation of PP (α_{IIb} 998,999) to AA (PDB# 1DPQ) disrupted the turn and opened the closed conformation (*4*). This double proline mutant peptide was inactive in α_{IIb} inhibition (*4*). Moreover, D-isomeric replacement of the α_V (993-1001) at RPPQ abolished its capacity to block integrin activation (*169*). The L- to D-amino acid conversion in the α_V tail may reverse the direction of the turn fold and the spatial orientation of the side chains. Similarly, we found that, compared to its original α_{IIb} peptide (994-1003), the mutant peptide RPP/AAA had significantly decreased capacity for inhibiting the adhesion of MDA-MB-435, MCF-7 and $\alpha_{IIb}\beta_3$-expressing CHO cells (Figure 4.7). The α_{IIb} peptide (994-1003) KRNRPPLEED retains the elements that facilitate formation of a turn structure: positive charged lysine and arginine residues at the N-terminus, negative charged glutamic acid and aspartic acid residues at the C-terminus, and double proline residues in the middle. In addition, K994 is possibly important for the activity of the

α_{IIb} peptide because the turn structure is stabilized by K994 binding with the negatively charged C-terminus of the peptide.

The NMR structure of α_{IIb} (989–1008) and molecular models of α_V (987–1018) suggest that the central turn motif is highly exposed and accessible to intracellular binding partners (*168, 169*). Thus, it is possible that the inhibitory activity of the turn peptides is due to their competition with the native turn in binding to these partners. In the present study, we used bio-peptide pull-down assay followed by MS/MS peptide sequencing to identify β-tubulin as a potential binding partner with the bio-α_{IIb} peptide. Although a large number of proteins were pulled down, the protein band identified to be β-tubulins were enriched in bio-α_{IIb} pull-down samples, indicating its higher binding affinity for α_{IIb} peptide than scrambled peptide. β-tubulin has been previously shown to have high binding affinity for integrin KVGFFKR regulatory motif, the N-terminus of α_{IIb} cytoplasmic tails (*47*). The current study potentially identified the binding of β-tubulin to the central turn motif KRNRPPLEED, where the first two amino acids (KR) overlap with KVGFFKR. Two β-tubulin-binding motifs within α_{IIb} tails suggest a potential role of β-tubulin in integrin function through binding with α_{IIb} tails. β-tubulin is a microtubule component. Microtubules function in intracellular organelle transport, mechanical support of cells and cell mitosis. Interestingly, microtubules have also been shown to affect integrin β_2 avidity regulation (*178*), cell adhesion (*179, 180*) and cell spreading (*64*). The data presented here were consistent with the previous report that pharmacological disruption of microtubules inhibited early adhesive interactions between circulating tumour cells and host organ

microvasculature in vivo (*179*). Our findings should improve our understanding of the importance of microtubule-integrin linkage in integrin activation regulation and integrin-mediated adhesion.

Interestingly, we also found that α_{IIb} and α_V peptides inhibited Mn^{2+}-stimulated soluble fibrinogen binding to $\alpha_{IIb}\beta_3$-expressing CHO cells. First, confocal images showed that there was less labelled fibrinogen binding in cells treated with α_{IIb} or α_V peptide, and cell aggregation mediated by multivalent fibrinogen linking adjacent cells (Figure 4.5). Second, flow cytometry confirmed that α_{IIb} inhibits soluble fibrinogen binding in a dose dependent manner using scrambled peptide as a control (Figure 4.6). Mn^{2+} replaces an inhibitory Ca^{2+} at the adjacent metal ion-binding site in integrin ectodomain and induces an extended and high-affinity integrin conformation (*181, 182*). Recent studies using living cells demonstrated that the conformational changes induced in the ectodomain by Mn^{2+} can be transmitted toward the transmembrane and cytoplasmic domains where integrin oligomers or clusters are formed, even in the absence of extracellular ligands (*183-185*). Integrin clustering increases the local density of integrins and recruits adaptors or cytoskeletal proteins to form adhesions which link cytoskeleton to extracellular matrix (*3*). Given that myristoylation allows delivery of the experimental peptides into cells and that nonmyristoylated peptides causes little inhibition (*4, 169*), our work indicates that the inhibitory effect of the α_{IIb} peptide likely occurs by disturbing Mn^{2+}-induced intracellular integrin clustering. Previous work found that integrin clustering did not spontaneously occur when integrin affinity increased, but required a driving force

from integrin binding partner, such as talin (*185*). Our data suggest that α_{IIb} peptide may inhibit the interactions between α_{IIb} tail and its binding proteins. However, whether β-tubulin is actually an integrin binding protein and target of α_{IIb} turn peptide remains further investigation.

Our observations showed that treatment of the agonist-stimulated platelets and adhered cells with the α_{IIb} and α_V peptides did not reverse ligand-integrin engagement. The initiating step in integrin activation is a conformational change in the integrin cytoplasmic tails and the transmembrane domains. The conformational changes then propagate from the transmembrane domains to the ligand binding headpiece, which increases integrin affinity for ligand. The data here indicates that the CT peptides can block the initiating event. However, once it has occurred it cannot be reversed as the numerous interactions that occur following ligand binding to stabilize the ligand-bound state.

In summary, the current work suggests that the central turn motif in α_{IIb} and α_V tails is not only a structural support, but also an important protein anchoring site. Some cytosolic proteins, such as β-tubulin, may recognize and bind to the central turn, participating in control of integrin activation. These binding proteins function as activators which change α tail's conformation (for example, opening the "closed" conformation), or promote integrin clustering. α_{IIb} and α_v turn peptide may inhibit integrin activation as a result of sequestration of the cytosolic factors.

CHAPTER 5

DISCUSSION AND CONCULSIONS

Bidirectional signalling across integrin receptors includes both ‘inside-out’ and ‘outside-in’ signalling pathways. Intracellular signals trigger direct interactions of β cytoplasmic tails with talin and kindlin, leading to tail separation and conformational changes in the extracellular domain of integrin (integrin activation or inside-out signalling). Following ligand binding, integrins transduce signals into cells (outside-in signalling) by recruiting proteins to their cytoplasmic tails, which results in actin reorganization and modulation of signalling pathways. The cytoplasmic tails of integrins are short, but they serve as receivers and transmitters of the bidirectional signalling and are involved in assembly and disassembly of many binding partners. Despite years of extensive studies on specific amino acids, motifs within integrin cytoplasmic tails and their binding partners involved in integrin bidirectional signalling, a number of key questions still remain (*186*). What is the role of the distal region of α and β cytoplasmic tails in integrin activation? What are the precise molecular linkages between integrin cytoplasmic tails and the cytoskeleton? How do these interactions regulate cell adhesion, spreading and migration? Two main experimental approaches have been used to address these questions, specifically the expression of $\alpha_{IIb}\beta_3$ in heterologous cells, and the introduction of membrane permeable peptides derived from the segments of cytoplasmic tails.

We began with an investigation of the role of skelemin-integrin binding in

integrin activation and cell spreading using protein mutagenesis (Chapter 3). Wild-type or mutant $\alpha_{IIb}\beta_3$ receptors defective in skelemin binding were stably expressed in CHO cells and their inside-out and outside-in signalling were examined.

A previous NMR spectrometry study showed that skelemin can bind with both α_{IIb} and β_3 tails and had a weak capacity to separate the complex of $\alpha_{IIb}\beta_3$ cytoplasmic tails, which raises a question whether skelemin can activate integrins by unclasping the interface of α_{IIb} and β_3 tails. The current work showed that overexpression of the integrin-binding domain of skelemin (skeC2) neither activated wild-type $\alpha_{IIb}\beta_3$, nor changed the affinity state of mutant integrins in a PAC-1 binding assay. It suggests that skelemin cannot unclasp the membrane-proximal interface of $\alpha_{IIb}\beta_3$ cytoplasmic tails in CHO cells, even though skelemin binds both of the subunits, as does the head domain of talin. This result is consistent with previous immunoprecipitation results showing that associations of skelemin and integrin $\alpha_{IIb}\beta_3$ only occur following integrin ligation in platelets and CHO cells. It fortifies the conclusion that skelemin is not an upstream activator of inside-out signalling, but is more likely to be a downstream effector following integrin activation or inside-out signalling.

Integrin outside-in signalling can be evaluated by cell spreading. A previous view regarded skelemin as an essential protein linking integrins to the cytoskeleton was based on the observation that microinjection or overexpression of skeC2 fragments into cultured cells abolished cell spreading. The skeC2 fragments were thought to do so by competing with endogenous skelemin binding to integrins and breaking the integrin-cytoskeleton linkage. Similar results were obtained here with the use of CHO

cells and Hek293 cells, which showed inhibited $\alpha_{IIb}\beta_3$-mediated cell spreading on fibrinogen after co-transfection with skeC2 and $\alpha_{IIb}\beta_3$ integrin. However, that view is challenged by the observation that mutant $\alpha_{IIb}\beta_3$-transfected cells have unchanged or even increased cell adhesion and spreading capacity at the early stages of cell spreading on immobilized fibrinogen. These cells formed membrane protrusions, focal adhesions and stress fibers, suggesting unimpaired integrin outside-in signalling leading to focal adhesion assembly and actin polymerization. These data lead us to conclude that engagement of skelemin to the cytoplasmic tail of $\alpha_{IIb}\beta_3$ is not essential for cell spreading.

Some of the integrin mutant cells, namely H722A and K716A had a larger cell spreading area. This is in agreement with their elevated levels of pY416-Src which are required for integrin-mediated cell spreading. The immunofluorescence study further investigated K716A mutation-expressing cells, as the K716 residue appeared to be the most important for skelemin binding in *in vitro* studies. It showed that wild-type integrins were colocalized with both skelemin and talin in the cell periphery at the early stage of cell spreading, whereas K716A cells showed strong colocalization of talin with mutated $\alpha_{IIb}\beta_3$ in the cell protrusions even with a loss in skelemin binding. These results suggest that binding of skelemin and talin to the membrane proximal region of β3 tails may be mutually exclusive, and that disrupting skelemin binding could facilitate talin recruitment that promotes actin polymerization and formation of membrane protrusions.

We hypothesize that the skelemin-integrin interactions function to coordinate the

binding of different cytoskeletal proteins to the membrane proximal region of integrin tails, such as talin. As a member of the family of myosin-associated proteins, skelemin was thought to exert a contractile force by linking integrin to myosin. The enhanced cell spreading in some mutant cells support this view. Thus, modulating skelemin binding to integrin tails is one mechanism a cell can use to fine tune the highly organized process of cell spreading.

Meanwhile, this work also shows that the stoichiometry of skelemin and integrin is important for integrin-mediated function. We found that GFP-skeC2 inhibited the $\alpha_{IIb}\beta_3$-mediated cell spreading only when the ratio of GFP-skeC2 to $\alpha_{IIb}\beta_3$ was high. However, if the ratio of skeC2 to integrin is much higher in plasmid-transfected CHO cells than it is in wild type cells, such as platelets, this conclusion about skelemin's function could be over-evaluated or even wrong, as the over-expressed skeC2 may saturate the skelemin binding sites of integrin and affect the association of integrin with other integrin binding partners that compete with skelemin. Therefore, we think that studies utilizing the transfection of wild-type and mutant integrin may offer an alternative, and perhaps better, way to evaluate the function of skelemin than simple overexpression of skelemin.

Platelets are anucleate and therefore not amenable to direct genetic manipulations. CHO cell lines expressing wild-type and mutant $\alpha_{IIb}\beta_3$ have been successfully used to study the role of individual amino acids and specific interactions in integrin bidirectional signalling. Since the experiments reported here are done with CHO cells, the question arises whether the conclusions reached will apply to other cell types and

platelets. Transfection of primary megakaryocytes, the precursor of platelets, and generation of mice bearing mutant $\alpha_{IIb}\beta_3$ integrin may be considered in the future for a better understanding of the significance of skelemin in $\alpha_{IIb}\beta_3$ biology.

Chapter 4 examines how the central motif of the α_{IIb} tail regulates integrin activation and integrin-mediated cell adhesion. Previously, we located the minimal α_V cytoplasmic tail sequence that suppressed integrin activation at the central turn region. The central motifs of the integrin α_{IIb} and α_V cytoplasmic tails are highly conserved. The present study showed that a cell-permeable peptide corresponding to the central motif of the α_{IIb} tail, myr-KRNRPPLEED (α_{IIb} peptide) inhibited $\alpha_{IIb}\beta_3$-mediated cell adhesion to fibrinogen. It also inhibited $\alpha_V\beta_3$ and $\alpha_V\beta_5$-mediated breast cancer cell (MDA-MB-435 and MCF7) adhesion to vitronectin. The homologous peptide derived from α_V tails, myr-KRVRPPQEEQ (α_V peptide) inhibited these cell adhesive functions with a similar capacity, suggesting that the two inhibitory peptides share a common functional mode. Structural studies show that the RPP residues are important for maintaining the turn structure of the α_{IIb} tail peptide (*4*). In this project, replacement of RPP with AAA significantly attenuated the inhibitory activity of the α_{IIb} peptide, suggesting that the turn structure formed by PP is important for its inhibitory capacity. The turn structure could be an anchoring point for some cytosolic factors to regulate integrin activation.

In addition, α_{IIb} peptide blocks soluble fibrinogen binding of $\alpha_{IIb}\beta_3$ integrins if they are activated from outside the cell by Mn^{2+}. This result suggests that the peptide can interfere with the allosteric conformational changes in integrin cytoplasmic

domain induced by Mn^{2+}. One possible mechanism is that the α_{IIb} peptide may disturb Mn^{2+}-induced integrin clustering in the presence of fibrinogen.

The peptide pull-down assay identified β-tubulin as a potential novel binding partner with the central turn motif KRNRPPLEED within α_{IIb} tails. However, this experiment was done only once and needs to be reproduced. In addition, the interaction between β-tubulin and α_{IIb} peptide needs to be confirmed with other biochemical studies, such as SPR or co-immunoprecipitation. Moreover, whether any potential peptide binding with β-tubulin contributes to its inhibitory capacity was not addressed. The role of β-tubulin in integrin activation and/or integrin clustering requires extensive further studies.

Integrin $\alpha_{IIb}\beta_3$ has a critical role in thrombosis and haemostasis. Active $\alpha_{IIb}\beta_3$ expressed on platelets binding to fibrinogen in plasma leads to platelet aggregation, an important process to stop bleeding at the site of vascular injury. In contrast, abnormal integrin activation may result in life-threatening platelet aggregation and thromobosis formation. $\alpha_{IIb}\beta_3$ antagonists are widely used for the treatment of acute coronary syndromes. However, they have only shown significant promise with percutaneous coronary interventions. The reason for their limited use in the clinic may be due to their activating effects on platelet aggregation and thromobosis at low concentrations (*135*). Future antagonists will likely be designed for use as anti-platelet agents with the rational of maintaining $\alpha_{IIb}\beta_3$ in its quiescent, noncompetent state. One possible approach is targeting to the intracellular domain of integrin $\alpha_{IIb}\beta_3$ (*7*). Our peptides corresponding to the central turn motifs of cytoplasmic tails of α_{IIb} and α_V are shown

to inhibit $\alpha_{IIb}\beta_3$-mediated fibrinogen binding, and these inhibitory peptides may be a starting point for development of anti-thrombotic drugs.

Thrombosis is also a common complication of patients with cancer (*187*). Cancer patients have an increase in the risk for developing thrombosis events, both in arteries and in veins (*188, 189*). Multiple and complex mechanisms contribute to cancer-related thrombosis, including tissue factor released by tumour cells, production of MP and inflammatory cytokines by tumour and/or host cells, and direct adhesion of tumour cells to platelets, leukocytes, and endothelial cells (*187*). These clot-promoting factors in turn contribute to tumour progression and metastasis. Platelets appear to be important for tumour progression as platelet-tumour cell interaction can protecting tumour cells from clearance by immune cells and facilitate their arrest in the vasculature, inducing subsequent tissue invasion (*16, 190-192*). Fibrinogen functions as a bridge between integrins $\alpha_{IIb}\beta_3$ on platelets and $\alpha_V\beta_3$ on tumour cells (*191*). In a mouse model, $\alpha_{IIb}\beta_3$ antagonists showed potential for blocking tumour metastasis (*193*). These results indicate that the combined blockade of $\alpha_V\beta_3$ and $\alpha_{IIb}\beta_3$ may be effective in inhibiting tumour progression. Administration of abciximab, which binds both $\alpha_V\beta_3$ and $\alpha_{IIb}\beta_3$ with equivalent affinity, showed increased anti-angiogenic and anti-tumour effects compared with blocking tumour integrin $\alpha_V\beta_3$ alone (*194*). A recent study showed that anti-angiogenic drugs could increase invasive and metastatic properties of breast cancer cells via hypoxia-response program (*195, 196*). Therefore, combination of anti-angiogenic drugs with others targeting tumour metastasis may improve clinical outcome. α_V integrins promote

tumour initiation, progression and metastasis by regulating tumour cell proliferation, migration and invasion, angiogenesis and ECM remodelling (*129*). These studies suggest that the homologous peptides α_{IIb} (994-1003) and α_V (992-1001) with similar inhibitory activity for $\alpha_{IIb}\beta_3$ and α_V functions may lead to a new therapeutic strategy for an anti-cancer and anti-platelet dual-role drug. This holds clinical promise for cancer patients at high risk of developing thrombosis.

REFERENCES:

1. Hynes, R. O. (2002) Integrins: bidirectional, allosteric signaling machines, *Cell 110*, 673-687.
2. Plow, E. F., Haas, T. A., Zhang, L., Loftus, J., and Smith, J. W. (2000) Ligand binding to integrins, *J Biol Chem 275*, 21785-21788.
3. Legate, K. R., Wickstrom, S. A., and Fassler, R. (2009) Genetic and cell biological analysis of integrin outside-in signaling, *Genes & development 23*, 397-418.
4. Vinogradova, O., Haas, T., Plow, E. F., and Qin, J. (2000) A structural basis for integrin activation by the cytoplasmic tail of the alpha IIb-subunit, *Proc Natl Acad Sci U S A 97*, 1450-1455.
5. Tan, S. M. (2012) The leucocyte beta2 (CD18) integrins: the structure, functional regulation and signalling properties, *Bioscience reports 32*, 241-269.
6. Geiger, B., Spatz, J. P., and Bershadsky, A. D. (2009) Environmental sensing through focal adhesions, *Nature reviews. Molecular cell biology 10*, 21-33.
7. Bledzka, K., Smyth, S. S., and Plow, E. F. (2013) Integrin alphaIIbbeta3: from discovery to efficacious therapeutic target, *Circulation research 112*, 1189-1200.
8. Nurden, A. T., and Caen, J. P. (1975) Specific roles for platelet surface glycoproteins in platelet function, *Nature 255*, 720-722.

9. Gong, H., Shen, B., Flevaris, P., Chow, C., Lam, S. C., Voyno-Yasenetskaya, T. A., Kozasa, T., and Du, X. (2010) G protein subunit Galpha13 binds to integrin alphaIIbbeta3 and mediates integrin "outside-in" signaling, *Science 327*, 340-343.

10. Brooks, P. C., Clark, R. A., and Cheresh, D. A. (1994) Requirement of vascular integrin alpha v beta 3 for angiogenesis, *Science 264*, 569-571.

11. Byzova, T. V., and Plow, E. F. (1998) Activation of alphaVbeta3 on vascular cells controls recognition of prothrombin, *The Journal of cell biology 143*, 2081-2092.

12. Danilov, Y. N., and Juliano, R. L. (1989) Phorbol ester modulation of integrin-mediated cell adhesion: a postreceptor event, *The Journal of cell biology 108*, 1925-1933.

13. Suzuki, K., Saido, T. C., and Hirai, S. (1992) Modulation of cellular signals by calpain, *Annals of the New York Academy of Sciences 674*, 218-227.

14. Albelda, S. M., Mette, S. A., Elder, D. E., Stewart, R., Damjanovich, L., Herlyn, M., and Buck, C. A. (1990) Integrin distribution in malignant melanoma: association of the beta 3 subunit with tumor progression, *Cancer research 50*, 6757-6764.

15. Gingras, M. C., Roussel, E., Bruner, J. M., Branch, C. D., and Moser, R. P. (1995) Comparison of cell adhesion molecule expression between glioblastoma multiforme and autologous normal brain tissue, *Journal of neuroimmunology 57*, 143-153.

16. Felding-Habermann, B., O'Toole, T. E., Smith, J. W., Fransvea, E., Ruggeri, Z. M., Ginsberg, M. H., Hughes, P. E., Pampori, N., Shattil, S. J., Saven, A., and Mueller, B. M. (2001) Integrin activation controls metastasis in human breast cancer, *Proc Natl Acad Sci U S A 98*, 1853-1858.

17. Pilch, J., Habermann, R., and Felding-Habermann, B. (2002) Unique ability of integrin alpha(v)beta 3 to support tumor cell arrest under dynamic flow conditions, *J Biol Chem 277*, 21930-21938.

18. Rolli, M., Fransvea, E., Pilch, J., Saven, A., and Felding-Habermann, B. (2003) Activated integrin alphavbeta3 cooperates with metalloproteinase MMP-9 in regulating migration of metastatic breast cancer cells, *Proc Natl Acad Sci U S A 100*, 9482-9487.

19. Lorger, M., Krueger, J. S., O'Neal, M., Staflin, K., and Felding-Habermann, B. (2009) Activation of tumor cell integrin alphavbeta3 controls angiogenesis and metastatic growth in the brain, *Proc Natl Acad Sci U S A 106*, 10666-10671.

20. Xiong, J. P., Stehle, T., Zhang, R., Joachimiak, A., Frech, M., Goodman, S. L., and Arnaout, M. A. (2002) Crystal structure of the extracellular segment of integrin alpha Vbeta3 in complex with an Arg-Gly-Asp ligand, *Science 296*, 151-155.

21. Xiong, J. P., Stehle, T., Diefenbach, B., Zhang, R., Dunker, R., Scott, D. L., Joachimiak, A., Goodman, S. L., and Arnaout, M. A. (2001) Crystal structure of the extracellular segment of integrin alpha Vbeta3, *Science 294*, 339-345.

22. Erb, E. M., Tangemann, K., Bohrmann, B., Muller, B., and Engel, J. (1997) Integrin alphaIIb beta3 reconstituted into lipid bilayers is nonclustered in its activated state but clusters after fibrinogen binding, *Biochemistry 36*, 7395-7402.

23. Takagi, J., and Springer, T. A. (2002) Integrin activation and structural rearrangement, *Immunological reviews 186*, 141-163.

24. Zhu, J., Luo, B. H., Xiao, T., Zhang, C., Nishida, N., and Springer, T. A. (2008) Structure of a complete integrin ectodomain in a physiologic resting state and activation and deactivation by applied forces, *Molecular cell 32*, 849-861.

25. Xiao, T., Takagi, J., Coller, B. S., Wang, J. H., and Springer, T. A. (2004) Structural basis for allostery in integrins and binding to fibrinogen-mimetic therapeutics, *Nature 432*, 59-67.

26. Adair, B. D., and Yeager, M. (2002) Three-dimensional model of the human platelet integrin alpha IIbbeta 3 based on electron cryomicroscopy and x-ray crystallography, *Proc Natl Acad Sci U S A 99*, 14059-14064.

27. Ye, F., Liu, J., Winkler, H., and Taylor, K. A. (2008) Integrin alpha IIb beta 3 in a membrane environment remains the same height after Mn2+ activation when observed by cryoelectron tomography, *Journal of molecular biology 378*, 976-986.

28. Ye, F., Hu, G., Taylor, D., Ratnikov, B., Bobkov, A. A., McLean, M. A., Sligar, S. G., Taylor, K. A., and Ginsberg, M. H. (2010) Recreation of the

terminal events in physiological integrin activation, *The Journal of cell biology 188*, 157-173.

29. Humphries, M. J., Symonds, E. J., and Mould, A. P. (2003) Mapping functional residues onto integrin crystal structures, *Current opinion in structural biology 13*, 236-243.

30. Schneider, D., and Engelman, D. M. (2004) Involvement of transmembrane domain interactions in signal transduction by alpha/beta integrins, *J Biol Chem 279*, 9840-9846.

31. Lau, T. L., Kim, C., Ginsberg, M. H., and Ulmer, T. S. (2009) The structure of the integrin alphaIIbbeta3 transmembrane complex explains integrin transmembrane signalling, *The EMBO journal 28*, 1351-1361.

32. Luo, B. H., Springer, T. A., and Takagi, J. (2004) A specific interface between integrin transmembrane helices and affinity for ligand, *PLoS biology 2*, e153.

33. Luo, B. H., Carman, C. V., Takagi, J., and Springer, T. A. (2005) Disrupting integrin transmembrane domain heterodimerization increases ligand binding affinity, not valency or clustering, *Proc Natl Acad Sci U S A 102*, 3679-3684.

34. Partridge, A. W., Liu, S., Kim, S., Bowie, J. U., and Ginsberg, M. H. (2005) Transmembrane domain helix packing stabilizes integrin alphaIIbbeta3 in the low affinity state, *J Biol Chem 280*, 7294-7300.

35. Kim, C., Lau, T. L., Ulmer, T. S., and Ginsberg, M. H. (2009) Interactions of platelet integrin alphaIIb and beta3 transmembrane domains in mammalian cell membranes and their role in integrin activation, *Blood 113*, 4747-4753.

36. Yang, J., Ma, Y. Q., Page, R. C., Misra, S., Plow, E. F., and Qin, J. (2009) Structure of an integrin alphaIIb beta3 transmembrane-cytoplasmic heterocomplex provides insight into integrin activation, *Proc Natl Acad Sci U S A 106*, 17729-17734.

37. O'Toole, T. E., Mandelman, D., Forsyth, J., Shattil, S. J., Plow, E. F., and Ginsberg, M. H. (1991) Modulation of the affinity of integrin alpha IIb beta 3 (GPIIb-IIIa) by the cytoplasmic domain of alpha IIb, *Science 254*, 845-847.

38. Hughes, P. E., O'Toole, T. E., Ylanne, J., Shattil, S. J., and Ginsberg, M. H. (1995) The conserved membrane-proximal region of an integrin cytoplasmic domain specifies ligand binding affinity, *J Biol Chem 270*, 12411-12417.

39. Hughes, P. E., Diaz-Gonzalez, F., Leong, L., Wu, C., McDonald, J. A., Shattil, S. J., and Ginsberg, M. H. (1996) Breaking the integrin hinge. A defined structural constraint regulates integrin signaling, *J Biol Chem 271*, 6571-6574.

40. Vallar, L., Melchior, C., Plancon, S., Drobecq, H., Lippens, G., Regnault, V., and Kieffer, N. (1999) Divalent cations differentially regulate integrin alphaIIb cytoplasmic tail binding to beta3 and to calcium- and integrin-binding protein, *J Biol Chem 274*, 17257-17266.

41. Ulmer, T. S., Yaspan, B., Ginsberg, M. H., and Campbell, I. D. (2001) NMR analysis of structure and dynamics of the cytosolic tails of integrin alpha IIb beta 3 in aqueous solution, *Biochemistry 40*, 7498-7508.

42. Weljie, A. M., Hwang, P. M., and Vogel, H. J. (2002) Solution structures of the cytoplasmic tail complex from platelet integrin alpha IIb- and beta 3-subunits, *Proc Natl Acad Sci U S A 99*, 5878-5883.

43. Vinogradova, O., Velyvis, A., Velyviene, A., Hu, B., Haas, T., Plow, E., and Qin, J. (2002) A structural mechanism of integrin alpha(IIb)beta(3) "inside-out" activation as regulated by its cytoplasmic face, *Cell 110*, 587-597.

44. Vinogradova, O., Vaynberg, J., Kong, X., Haas, T. A., Plow, E. F., and Qin, J. (2004) Membrane-mediated structural transitions at the cytoplasmic face during integrin activation, *Proc Natl Acad Sci U S A 101*, 4094-4099.

45. Kim, C., Ye, F., and Ginsberg, M. H. (2011) Regulation of integrin activation, *Annual review of cell and developmental biology 27*, 321-345.

46. Leisner, T. M., Wencel-Drake, J. D., Wang, W., and Lam, S. C. (1999) Bidirectional transmembrane modulation of integrin alphaIIbbeta3 conformations, *J Biol Chem 274*, 12945-12949.

47. Raab, M., Daxecker, H., Edwards, R. J., Treumann, A., Murphy, D., and Moran, N. (2010) Protein interactions with the platelet integrin alpha(IIb) regulatory motif, *Proteomics 10*, 2790-2800.

48. Larkin, D., Murphy, D., Reilly, D. F., Cahill, M., Sattler, E., Harriott, P., Cahill, D. J., and Moran, N. (2004) ICln, a novel integrin alphaIIbbeta3-associated protein, functionally regulates platelet activation, *J Biol Chem 279*, 27286-27293.

49. Naik, U. P., Patel, P. M., and Parise, L. V. (1997) Identification of a novel calcium-binding protein that interacts with the integrin alphaIIb cytoplasmic domain, *J Biol Chem 272*, 4651-4654.

50. Vijayan, K. V., Liu, Y., Li, T. T., and Bray, P. F. (2004) Protein phosphatase 1 associates with the integrin alphaIIb subunit and regulates signaling, *J Biol Chem 279*, 33039-33042.

51. Calderwood, D. A., Fujioka, Y., de Pereda, J. M., Garcia-Alvarez, B., Nakamoto, T., Margolis, B., McGlade, C. J., Liddington, R. C., and Ginsberg, M. H. (2003) Integrin beta cytoplasmic domain interactions with phosphotyrosine-binding domains: a structural prototype for diversity in integrin signaling, *Proc Natl Acad Sci U S A 100*, 2272-2277.

52. Tadokoro, S., Shattil, S. J., Eto, K., Tai, V., Liddington, R. C., de Pereda, J. M., Ginsberg, M. H., and Calderwood, D. A. (2003) Talin binding to integrin beta tails: a final common step in integrin activation, *Science 302*, 103-106.

53. Tanentzapf, G., and Brown, N. H. (2006) An interaction between integrin and the talin FERM domain mediates integrin activation but not linkage to the cytoskeleton, *Nat Cell Biol 8*, 601-606.

54. Calderwood, D. A., Zent, R., Grant, R., Rees, D. J., Hynes, R. O., and Ginsberg, M. H. (1999) The Talin head domain binds to integrin beta subunit cytoplasmic tails and regulates integrin activation, *J Biol Chem 274*, 28071-28074.

55. Calderwood, D. A., Yan, B., de Pereda, J. M., Alvarez, B. G., Fujioka, Y., Liddington, R. C., and Ginsberg, M. H. (2002) The phosphotyrosine binding-like domain of talin activates integrins, *J Biol Chem 277*, 21749-21758.

56. Wegener, K. L., Partridge, A. W., Han, J., Pickford, A. R., Liddington, R. C., Ginsberg, M. H., and Campbell, I. D. (2007) Structural basis of integrin activation by talin, *Cell 128*, 171-182.

57. Kiema, T., Lad, Y., Jiang, P., Oxley, C. L., Baldassarre, M., Wegener, K. L., Campbell, I. D., Ylanne, J., and Calderwood, D. A. (2006) The molecular basis of filamin binding to integrins and competition with talin, *Molecular cell 21*, 337-347.

58. Moser, M., Nieswandt, B., Ussar, S., Pozgajova, M., and Fassler, R. (2008) Kindlin-3 is essential for integrin activation and platelet aggregation, *Nat Med 14*, 325-330.

59. Ma, Y. Q., Qin, J., Wu, C., and Plow, E. F. (2008) Kindlin-2 (Mig-2): a co-activator of beta3 integrins, *J Cell Biol 181*, 439-446.

60. Ussar, S., Moser, M., Widmaier, M., Rognoni, E., Harrer, C., Genzel-Boroviczeny, O., and Fassler, R. (2008) Loss of Kindlin-1 causes skin atrophy and lethal neonatal intestinal epithelial dysfunction, *PLoS Genet 4*, e1000289.

61. Hato, T., Pampori, N., and Shattil, S. J. (1998) Complementary roles for receptor clustering and conformational change in the adhesive and signaling

functions of integrin alphaIIb beta3, *The Journal of cell biology 141*, 1685-1695.

62. Li, R., Mitra, N., Gratkowski, H., Vilaire, G., Litvinov, R., Nagasami, C., Weisel, J. W., Lear, J. D., DeGrado, W. F., and Bennett, J. S. (2003) Activation of integrin alphaIIbbeta3 by modulation of transmembrane helix associations, *Science 300*, 795-798.

63. Simmons, S. R., and Albrecht, R. M. (1996) Self-association of bound fibrinogen on platelet surfaces, *The Journal of laboratory and clinical medicine 128*, 39-50.

64. Buensuceso, C., de Virgilio, M., and Shattil, S. J. (2003) Detection of integrin alpha IIbbeta 3 clustering in living cells, *J Biol Chem 278*, 15217-15224.

65. Bennett, J. S., Zigmond, S., Vilaire, G., Cunningham, M. E., and Bednar, B. (1999) The platelet cytoskeleton regulates the affinity of the integrin alpha(IIb)beta(3) for fibrinogen, *J Biol Chem 274*, 25301-25307.

66. Hantgan, R. R., Gibbs, W., Stahle, M. C., Aster, R. H., and Peterson, J. A. (2004) Integrin clustering mechanisms explored with a soluble alphaIIbbeta3 ectodomain construct, *Biochimica et biophysica acta 1700*, 19-25.

67. Li, R., Babu, C. R., Lear, J. D., Wand, A. J., Bennett, J. S., and DeGrado, W. F. (2001) Oligomerization of the integrin alphaIIbbeta3: roles of the transmembrane and cytoplasmic domains, *Proc Natl Acad Sci U S A 98*, 12462-12467.

68. Li, R., Gorelik, R., Nanda, V., Law, P. B., Lear, J. D., DeGrado, W. F., and Bennett, J. S. (2004) Dimerization of the transmembrane domain of Integrin alphaIIb subunit in cell membranes, *J Biol Chem 279*, 26666-26673.

69. Wang, W., Zhu, J., Springer, T. A., and Luo, B. H. (2011) Tests of integrin transmembrane domain homo-oligomerization during integrin ligand binding and signaling, *J Biol Chem 286*, 1860-1867.

70. Legate, K. R., and Fassler, R. (2009) Mechanisms that regulate adaptor binding to beta-integrin cytoplasmic tails, *Journal of cell science 122*, 187-198.

71. Liu, S., Calderwood, D. A., and Ginsberg, M. H. (2000) Integrin cytoplasmic domain-binding proteins, *Journal of cell science 113 (Pt 20)*, 3563-3571.

72. Parsons, J. T., Horwitz, A. R., and Schwartz, M. A. (2010) Cell adhesion: integrating cytoskeletal dynamics and cellular tension, *Nature reviews. Molecular cell biology 11*, 633-643.

73. Lawson, C., Lim, S. T., Uryu, S., Chen, X. L., Calderwood, D. A., and Schlaepfer, D. D. (2012) FAK promotes recruitment of talin to nascent adhesions to control cell motility, *The Journal of cell biology 196*, 223-232.

74. Clark, E. A., King, W. G., Brugge, J. S., Symons, M., and Hynes, R. O. (1998) Integrin-mediated signals regulated by members of the rho family of GTPases, *The Journal of cell biology 142*, 573-586.

75. Zaidel-Bar, R., and Geiger, B. (2010) The switchable integrin adhesome, *Journal of cell science 123*, 1385-1388.

76. Zaidel-Bar, R., Itzkovitz, S., Ma'ayan, A., Iyengar, R., and Geiger, B. (2007) Functional atlas of the integrin adhesome, *Nature cell biology 9*, 858-867.

77. Burridge, K., and Chrzanowska-Wodnicka, M. (1996) Focal adhesions, contractility, and signaling, *Annual review of cell and developmental biology 12*, 463-518.

78. Harburger, D. S., and Calderwood, D. A. (2009) Integrin signalling at a glance, *Journal of cell science 122*, 159-163.

79. Wakatsuki, T., Wysolmerski, R. B., and Elson, E. L. (2003) Mechanics of cell spreading: role of myosin II, *Journal of cell science 116*, 1617-1625.

80. Huveneers, S., and Danen, E. H. (2009) Adhesion signaling - crosstalk between integrins, Src and Rho, *Journal of cell science 122*, 1059-1069.

81. Ponti, A., Machacek, M., Gupton, S. L., Waterman-Storer, C. M., and Danuser, G. (2004) Two distinct actin networks drive the protrusion of migrating cells, *Science 305*, 1782-1786.

82. Borisy, G. G., and Svitkina, T. M. (2000) Actin machinery: pushing the envelope, *Current opinion in cell biology 12*, 104-112.

83. Craig, R., and Woodhead, J. L. (2006) Structure and function of myosin filaments, *Current opinion in structural biology 16*, 204-212.

84. Jaffe, A. B., and Hall, A. (2005) Rho GTPases: biochemistry and biology, *Annual review of cell and developmental biology 21*, 247-269.

85. Pollard, T. D., and Borisy, G. G. (2003) Cellular motility driven by assembly and disassembly of actin filaments, *Cell 112*, 453-465.

86. Somlyo, A. P., and Somlyo, A. V. (2003) Ca2+ sensitivity of smooth muscle and nonmuscle myosin II: modulated by G proteins, kinases, and myosin phosphatase, *Physiological reviews 83*, 1325-1358.

87. Fukata, M., Nakagawa, M., and Kaibuchi, K. (2003) Roles of Rho-family GTPases in cell polarisation and directional migration, *Current opinion in cell biology 15*, 590-597.

88. Fritz, M., Radmacher, M., and Gaub, H. E. (1993) In vitro activation of human platelets triggered and probed by atomic force microscopy, *Experimental cell research 205*, 187-190.

89. Kiyokawa, E., Hashimoto, Y., Kobayashi, S., Sugimura, H., Kurata, T., and Matsuda, M. (1998) Activation of Rac1 by a Crk SH3-binding protein, DOCK180, *Genes & development 12*, 3331-3336.

90. del Pozo, M. A., Alderson, N. B., Kiosses, W. B., Chiang, H. H., Anderson, R. G., and Schwartz, M. A. (2004) Integrins regulate Rac targeting by internalization of membrane domains, *Science 303*, 839-842.

91. Playford, M. P., and Schaller, M. D. (2004) The interplay between Src and integrins in normal and tumor biology, *Oncogene 23*, 7928-7946.

92. Shattil, S. J., and Newman, P. J. (2004) Integrins: dynamic scaffolds for adhesion and signaling in platelets, *Blood 104*, 1606-1615.

93. Shattil, S. J. (2009) The beta3 integrin cytoplasmic tail: protein scaffold and control freak, *Journal of thrombosis and haemostasis : JTH 7 Suppl 1*, 210-213.

94. Reddy, K. B., Smith, D. M., and Plow, E. F. (2008) Analysis of Fyn function in hemostasis and alphaIIbbeta3-integrin signaling, *Journal of cell science 121*, 1641-1648.

95. Schaller, M. D., Otey, C. A., Hildebrand, J. D., and Parsons, J. T. (1995) Focal adhesion kinase and paxillin bind to peptides mimicking beta integrin cytoplasmic domains, *The Journal of cell biology 130*, 1181-1187.

96. Deshmukh, L., Tyukhtenko, S., Liu, J., Fox, J. E., Qin, J., and Vinogradova, O. (2007) Structural insight into the interaction between platelet integrin alphaIIbbeta3 and cytoskeletal protein skelemin, *J Biol Chem 282*, 32349-32356.

97. Critchley, D. R., and Gingras, A. R. (2008) Talin at a glance, *Journal of cell science 121*, 1345-1347.

98. Baumann, K. (2012) Cell adhesion: FAK or talin: who goes first?, *Nature reviews. Molecular cell biology 13*, 138.

99. Calderwood, D. A., Shattil, S. J., and Ginsberg, M. H. (2000) Integrins and actin filaments: reciprocal regulation of cell adhesion and signaling, *J Biol Chem 275*, 22607-22610.

100. Jiang, G., Giannone, G., Critchley, D. R., Fukumoto, E., and Sheetz, M. P. (2003) Two-piconewton slip bond between fibronectin and the cytoskeleton depends on talin, *Nature 424*, 334-337.

101. Zhao, R., Pathak, A. S., and Stouffer, G. A. (2004) beta(3)-Integrin cytoplasmic binding proteins, *Archivum immunologiae et therapiae experimentalis 52*, 348-355.

102. van der Flier, A., and Sonnenberg, A. (2001) Structural and functional aspects of filamins, *Biochimica et biophysica acta 1538*, 99-117.

103. Pelletier, O., Pokidysheva, E., Hirst, L. S., Bouxsein, N., Li, Y., and Safinya, C. R. (2003) Structure of actin cross-linked with alpha-actinin: a network of bundles, *Physical review letters 91*, 148102.

104. Courson, D. S., and Rock, R. S. (2010) Actin cross-link assembly and disassembly mechanics for alpha-Actinin and fascin, *J Biol Chem 285*, 26350-26357.

105. Choi, C. K., Vicente-Manzanares, M., Zareno, J., Whitmore, L. A., Mogilner, A., and Horwitz, A. R. (2008) Actin and alpha-actinin orchestrate the assembly and maturation of nascent adhesions in a myosin II motor-independent manner, *Nature cell biology 10*, 1039-1050.

106. Auerbach, D., Bantle, S., Keller, S., Hinderling, V., Leu, M., Ehler, E., and Perriard, J. C. (1999) Different domains of the M-band protein myomesin are involved in myosin binding and M-band targeting, *Molecular biology of the cell 10*, 1297-1308.

107. Price, M. G., and Gomer, R. H. (1993) Skelemin, a cytoskeletal M-disc periphery protein, contains motifs of adhesion/recognition and intermediate filament proteins, *J Biol Chem 268*, 21800-21810.

108. Reddy, K. B., Bialkowska, K., and Fox, J. E. (2001) Dynamic modulation of cytoskeletal proteins linking integrins to signaling complexes in spreading cells. Role of skelemin in initial integrin-induced spreading, *J Biol Chem 276*, 28300-28308.

109. Calalb, M. B., Polte, T. R., and Hanks, S. K. (1995) Tyrosine phosphorylation of focal adhesion kinase at sites in the catalytic domain regulates kinase activity: a role for Src family kinases, *Molecular and cellular biology 15*, 954-963.

110. Mitra, S. K., and Schlaepfer, D. D. (2006) Integrin-regulated FAK-Src signaling in normal and cancer cells, *Current opinion in cell biology 18*, 516-523.

111. Mitra, S. K., Hanson, D. A., and Schlaepfer, D. D. (2005) Focal adhesion kinase: in command and control of cell motility, *Nature reviews. Molecular cell biology 6*, 56-68.

112. Schlaepfer, D. D., Mitra, S. K., and Ilic, D. (2004) Control of motile and invasive cell phenotypes by focal adhesion kinase, *Biochimica et biophysica acta 1692*, 77-102.

113. Obergfell, A., Eto, K., Mocsai, A., Buensuceso, C., Moores, S. L., Brugge, J. S., Lowell, C. A., and Shattil, S. J. (2002) Coordinate interactions of Csk, Src, and Syk kinases with [alpha]IIb[beta]3 initiate integrin signaling to the cytoskeleton, *The Journal of cell biology 157*, 265-275.

114. Arias-Salgado, E. G., Haj, F., Dubois, C., Moran, B., Kasirer-Friede, A., Furie, B. C., Furie, B., Neel, B. G., and Shattil, S. J. (2005) PTP-1B is an essential positive regulator of platelet integrin signaling, *The Journal of cell biology 170*, 837-845.

115. Arias-Salgado, E. G., Lizano, S., Sarkar, S., Brugge, J. S., Ginsberg, M. H., and Shattil, S. J. (2003) Src kinase activation by direct interaction with the integrin beta cytoplasmic domain, *Proc Natl Acad Sci U S A 100*, 13298-13302.

116. Zou, Z., Chen, H., Schmaier, A. A., Hynes, R. O., and Kahn, M. L. (2007) Structure-function analysis reveals discrete beta3 integrin inside-out and outside-in signaling pathways in platelets, *Blood 109*, 3284-3290.

117. Su, X., Mi, J., Yan, J., Flevaris, P., Lu, Y., Liu, H., Ruan, Z., Wang, X., Kieffer, N., Chen, S., Du, X., and Xi, X. (2008) RGT, a synthetic peptide corresponding to the integrin beta 3 cytoplasmic C-terminal sequence, selectively inhibits outside-in signaling in human platelets by disrupting the interaction of integrin alpha IIb beta 3 with Src kinase, *Blood 112*, 592-602.

118. Ablooglu, A. J., Kang, J., Petrich, B. G., Ginsberg, M. H., and Shattil, S. J. (2009) Antithrombotic effects of targeting alphaIIbbeta3 signaling in platelets, *Blood 113*, 3585-3592.

119. Thomas, J. W., Ellis, B., Boerner, R. J., Knight, W. B., White, G. C., 2nd, and Schaller, M. D. (1998) SH2- and SH3-mediated interactions between focal adhesion kinase and Src, *J Biol Chem 273*, 577-583.

120. Kaplan, K. B., Swedlow, J. R., Morgan, D. O., and Varmus, H. E. (1995) c-Src enhances the spreading of src-/- fibroblasts on fibronectin by a kinase-independent mechanism, *Genes & development 9*, 1505-1517.

121. Felsenfeld, D. P., Schwartzberg, P. L., Venegas, A., Tse, R., and Sheetz, M. P. (1999) Selective regulation of integrin--cytoskeleton interactions by the tyrosine kinase Src, *Nature cell biology 1*, 200-206.

122. Jones, R. J., Avizienyte, E., Wyke, A. W., Owens, D. W., Brunton, V. G., and Frame, M. C. (2002) Elevated c-Src is linked to altered cell-matrix adhesion rather than proliferation in KM12C human colorectal cancer cells, *British journal of cancer 87*, 1128-1135.

123. Glenney, J. R., Jr., and Zokas, L. (1989) Novel tyrosine kinase substrates from Rous sarcoma virus-transformed cells are present in the membrane skeleton, *The Journal of cell biology 108*, 2401-2408.

124. Kanner, S. B., Reynolds, A. B., Vines, R. R., and Parsons, J. T. (1990) Monoclonal antibodies to individual tyrosine-phosphorylated protein substrates of oncogene-encoded tyrosine kinases, *Proc Natl Acad Sci U S A 87*, 3328-3332.

125. Bodin, S., Soulet, C., Tronchere, H., Sie, P., Gachet, C., Plantavid, M., and Payrastre, B. (2005) Integrin-dependent interaction of lipid rafts with the actin cytoskeleton in activated human platelets, *Journal of cell science 118*, 759-769.

126. Chen, Y. P., O'Toole, T. E., Ylanne, J., Rosa, J. P., and Ginsberg, M. H. (1994) A point mutation in the integrin beta 3 cytoplasmic domain (S752-->P) impairs bidirectional signaling through alpha IIb beta 3 (platelet glycoprotein IIb-IIIa), *Blood 84*, 1857-1865.

127. Fidler, I. J. (2003) The pathogenesis of cancer metastasis: the 'seed and soil' hypothesis revisited, *Nature reviews. Cancer 3*, 453-458.

128. van der, P., Vloedgraven, H., Papapoulos, S., Lowick, C., Grzesik, W., Kerr, J., and Robey, P. G. (1997) Attachment characteristics and involvement of integrins in adhesion of breast cancer cell lines to extracellular bone matrix components, *Laboratory investigation; a journal of technical methods and pathology 77*, 665-675.

129. Desgrosellier, J. S., and Cheresh, D. A. (2010) Integrins in cancer: biological implications and therapeutic opportunities, *Nature reviews. Cancer 10*, 9-22.

130. Zhao, Y., Bachelier, R., Treilleux, I., Pujuguet, P., Peyruchaud, O., Baron, R., Clement-Lacroix, P., and Clezardin, P. (2007) Tumor alphavbeta3 integrin is a therapeutic target for breast cancer bone metastases, *Cancer research 67*, 5821-5830.

131. Harms, J. F., Welch, D. R., Samant, R. S., Shevde, L. A., Miele, M. E., Babu, G. R., Goldberg, S. F., Gilman, V. R., Sosnowski, D. M., Campo, D. A., Gay, C. V., Budgeon, L. R., Mercer, R., Jewell, J., Mastro, A. M., Donahue, H. J., Erin, N., Debies, M. T., Meehan, W. J., Jones, A. L., Mbalaviele, G., Nickols, A., Christensen, N. D., Melly, R., Beck, L. N., Kent, J., Rader, R. K., Kotyk, J.

J., Pagel, M. D., Westlin, W. F., and Griggs, D. W. (2004) A small molecule antagonist of the alpha(v)beta3 integrin suppresses MDA-MB-435 skeletal metastasis, *Clinical & experimental metastasis 21*, 119-128.

132. Quinn, M. J., Byzova, T. V., Qin, J., Topol, E. J., and Plow, E. F. (2003) Integrin alphaIIbbeta3 and its antagonism, *Arteriosclerosis, thrombosis, and vascular biology 23*, 945-952.

133. Chew, D. P., Bhatt, D. L., Sapp, S., and Topol, E. J. (2001) Increased mortality with oral platelet glycoprotein IIb/IIIa antagonists: a meta-analysis of phase III multicenter randomized trials, *Circulation 103*, 201-206.

134. Du, X. P., Plow, E. F., Frelinger, A. L., 3rd, O'Toole, T. E., Loftus, J. C., and Ginsberg, M. H. (1991) Ligands "activate" integrin alpha IIb beta 3 (platelet GPIIb-IIIa), *Cell 65*, 409-416.

135. Peter, K., Schwarz, M., Ylanne, J., Kohler, B., Moser, M., Nordt, T., Salbach, P., Kubler, W., and Bode, C. (1998) Induction of fibrinogen binding and platelet aggregation as a potential intrinsic property of various glycoprotein IIb/IIIa (alphaIIbbeta3) inhibitors, *Blood 92*, 3240-3249.

136. Schneider, D. J., Taatjes, D. J., and Sobel, B. E. (2000) Paradoxical inhibition of fibrinogen binding and potentiation of alpha-granule release by specific types of inhibitors of glycoprotein IIb-IIIa, *Cardiovascular research 45*, 437-446.

137. Cox, D., Smith, R., Quinn, M., Theroux, P., Crean, P., and Fitzgerald, D. J. (2000) Evidence of platelet activation during treatment with a GPIIb/IIIa

antagonist in patients presenting with acute coronary syndromes, *Journal of the American College of Cardiology 36*, 1514-1519.

138. Petrich, B. G., Fogelstrand, P., Partridge, A. W., Yousefi, N., Ablooglu, A. J., Shattil, S. J., and Ginsberg, M. H. (2007) The antithrombotic potential of selective blockade of talin-dependent integrin alpha IIb beta 3 (platelet GPIIb-IIIa) activation, *The Journal of clinical investigation 117*, 2250-2259.

139. Koloka, V., Christofidou, E. D., Vaxevanelis, S., Dimitriou, A. A., Tsikaris, V., Tselepis, A. D., Panou-Pomonis, E., Sakarellos-Daitsiotis, M., and Tsoukatos, D. C. (2008) A palmitoylated peptide, derived from the acidic carboxyl-terminal segment of the integrin alphaIIb cytoplasmic domain, inhibits platelet activation, *Platelets 19*, 502-511.

140. Dimitriou, A. A., Stathopoulos, P., Mitsios, J. V., Sakarellos-Daitsiotis, M., Goudevenos, J., Tsikaris, V., and Tselepis, A. D. (2009) Inhibition of platelet activation by peptide analogs of the beta(3)-intracellular domain of platelet integrin alpha(IIb)beta(3) conjugated to the cell-penetrating peptide Tat(48-60), *Platelets 20*, 539-547.

141. Liu, X. Y., Timmons, S., Lin, Y. Z., and Hawiger, J. (1996) Identification of a functionally important sequence in the cytoplasmic tail of integrin beta 3 by using cell-permeable peptide analogs, *Proc Natl Acad Sci U S A 93*, 11819-11824.

142. Reddy, K. B., Gascard, P., Price, M. G., Negrescu, E. V., and Fox, J. E. (1998) Identification of an interaction between the m-band protein skelemin and

beta-integrin subunits. Colocalization of a skelemin-like protein with beta1- and beta3-integrins in non-muscle cells, *J Biol Chem 273*, 35039-35047.

143. Price, M. G. (1987) Skelemins: cytoskeletal proteins located at the periphery of M-discs in mammalian striated muscle, *J Cell Biol 104*, 1325-1336.

144. Agarkova, I., and Perriard, J. C. (2005) The M-band: an elastic web that crosslinks thick filaments in the center of the sarcomere, *Trends Cell Biol 15*, 477-485.

145. Steiner, F., Weber, K., and Furst, D. O. (1999) M band proteins myomesin and skelemin are encoded by the same gene: analysis of its organization and expression, *Genomics 56*, 78-89.

146. Podolnikova, N. P., O'Toole, T. E., Haas, T. A., Lam, S. C., Fox, J. E., and Ugarova, T. P. (2009) Adhesion-induced unclasping of cytoplasmic tails of integrin alpha(IIb)beta3, *Biochemistry 48*, 617-629.

147. O'Toole, T. E., Katagiri, Y., Faull, R. J., Peter, K., Tamura, R., Quaranta, V., Loftus, J. C., Shattil, S. J., and Ginsberg, M. H. (1994) Integrin cytoplasmic domains mediate inside-out signal transduction, *J Cell Biol 124*, 1047-1059.

148. Phillips, D. R., and Baughan, A. K. (1983) Fibrinogen binding to human platelet plasma membranes. Identification of two steps requiring divalent cations, *J Biol Chem 258*, 10240-10246.

149. Zhu, J., Luo, B. H., Barth, P., Schonbrun, J., Baker, D., and Springer, T. A. (2009) The structure of a receptor with two associating transmembrane domains on the cell surface: integrin alphaIIbbeta3, *Mol Cell 34*, 234-249.

150. Vorup-Jensen, T., Waldron, T. T., Astrof, N., Shimaoka, M., and Springer, T. A. (2007) The connection between metal ion affinity and ligand affinity in integrin I domains, *Biochimica et biophysica acta 1774*, 1148-1155.

151. Bjorge, J. D., Jakymiw, A., and Fujita, D. J. (2000) Selected glimpses into the activation and function of Src kinase, *Oncogene 19*, 5620-5635.

152. Schaller, M. D., Hildebrand, J. D., Shannon, J. D., Fox, J. W., Vines, R. R., and Parsons, J. T. (1994) Autophosphorylation of the focal adhesion kinase, pp125FAK, directs SH2-dependent binding of pp60src, *Molecular and cellular biology 14*, 1680-1688.

153. Zhang, X., Jiang, G., Cai, Y., Monkley, S. J., Critchley, D. R., and Sheetz, M. P. (2008) Talin depletion reveals independence of initial cell spreading from integrin activation and traction, *Nature cell biology 10*, 1062-1068.

154. Choquet, D., Felsenfeld, D. P., and Sheetz, M. P. (1997) Extracellular matrix rigidity causes strengthening of integrin-cytoskeleton linkages, *Cell 88*, 39-48.

155. Arias-Salgado, E. G., Lizano, S., Shattil, S. J., and Ginsberg, M. H. (2005) Specification of the direction of adhesive signaling by the integrin beta cytoplasmic domain, *J Biol Chem 280*, 29699-29707.

156. Tahiliani, P. D., Singh, L., Auer, K. L., and LaFlamme, S. E. (1997) The role of conserved amino acid motifs within the integrin beta3 cytoplasmic domain in triggering focal adhesion kinase phosphorylation, *J Biol Chem 272*, 7892-7898.

157. Oh, E. S., Gu, H., Saxton, T. M., Timms, J. F., Hausdorff, S., Frevert, E. U., Kahn, B. B., Pawson, T., Neel, B. G., and Thomas, S. M. (1999) Regulation of early events in integrin signaling by protein tyrosine phosphatase SHP-2, *Molecular and cellular biology 19*, 3205-3215.

158. Metcalf, D. G., Moore, D. T., Wu, Y., Kielec, J. M., Molnar, K., Valentine, K. G., Wand, A. J., Bennett, J. S., and DeGrado, W. F. (2010) NMR analysis of the alphaIIb beta3 cytoplasmic interaction suggests a mechanism for integrin regulation, *Proc Natl Acad Sci U S A 107*, 22481-22486.

159. Wang, W., and Luo, B. H. (2010) Structural basis of integrin transmembrane activation, *J Cell Biochem 109*, 447-452.

160. Mattila, P. K., and Lappalainen, P. (2008) Filopodia: molecular architecture and cellular functions, *Nat Rev Mol Cell Biol 9*, 446-454.

161. Williams, M. J., Hughes, P. E., O'Toole, T. E., and Ginsberg, M. H. (1994) The inner world of cell adhesion: integrin cytoplasmic domains, *Trends in cell biology 4*, 109-112.

162. Liddington, R. C., and Ginsberg, M. H. (2002) Integrin activation takes shape, *The Journal of cell biology 158*, 833-839.

163. Moser, M., Legate, K. R., Zent, R., and Fassler, R. (2009) The tail of integrins, talin, and kindlins, *Science 324*, 895-899.

164. Calderwood, D. A. (2004) Integrin activation, *Journal of cell science 117*, 657-666.

165. Stephens, G., O'Luanaigh, N., Reilly, D., Harriott, P., Walker, B., Fitzgerald, D., and Moran, N. (1998) A sequence within the cytoplasmic tail of GpIIb independently activates platelet aggregation and thromboxane synthesis, *J Biol Chem 273*, 20317-20322.

166. Aylward, K., Meade, G., Ahrens, I., Devocelle, M., and Moran, N. (2006) A novel functional role for the highly conserved alpha-subunit KVGFFKR motif distinct from integrin alphaIIbbeta3 activation processes, *Journal of thrombosis and haemostasis : JTH 4*, 1804-1812.

167. Yamanouchi, J., Hato, T., Tamura, T., and Fujita, S. (2004) Suppression of integrin activation by the membrane-distal sequence of the integrin alphaIIb cytoplasmic tail, *The Biochemical journal 379*, 317-323.

168. Haas, T. A., Taherian, A., Berry, T., and Ma, X. (2008) Identification of residues of functional importance within the central turn motifs present in the cytoplasmic tails of integrin alphaIIb and alphaV subunits, *Thromb Res 122*, 507-516.

169. Haas, T. A. (2008) Discrete functional motifs reside within the cytoplasmic tail of alphaV integrin subunit, *Thromb Haemost 99*, 96-107.

170. Nelson, A. R., Borland, L., Allbritton, N. L., and Sims, C. E. (2007) Myristoyl-based transport of peptides into living cells, *Biochemistry 46*, 14771-14781.

171. Kadowaki, M., Sangai, T., Nagashima, T., Sakakibara, M., Yoshitomi, H., Takano, S., Sogawa, K., Umemura, H., Fushimi, K., Nakatani, Y., Nomura, F.,

and Miyazaki, M. (2011) Identification of vitronectin as a novel serum marker for early breast cancer detection using a new proteomic approach, *Journal of cancer research and clinical oncology 137*, 1105-1115.

172. Gladson, C. L., and Cheresh, D. A. (1991) Glioblastoma expression of vitronectin and the alpha v beta 3 integrin. Adhesion mechanism for transformed glial cells, *The Journal of clinical investigation 88*, 1924-1932.

173. Wong, N. C., Mueller, B. M., Barbas, C. F., Ruminski, P., Quaranta, V., Lin, E. C., and Smith, J. W. (1998) Alphav integrins mediate adhesion and migration of breast carcinoma cell lines, *Clinical & experimental metastasis 16*, 50-61.

174. Nip, J., Shibata, H., Loskutoff, D. J., Cheresh, D. A., and Brodt, P. (1992) Human melanoma cells derived from lymphatic metastases use integrin alpha v beta 3 to adhere to lymph node vitronectin, *The Journal of clinical investigation 90*, 1406-1413.

175. Taherian, A., Li, X., Liu, Y., and Haas, T. A. (2011) Differences in integrin expression and signaling within human breast cancer cells, *BMC cancer 11*, 293.

176. Schvartz, I., Seger, D., and Shaltiel, S. (1999) Vitronectin, *The international journal of biochemistry & cell biology 31*, 539-544.

177. Swank, R. T., and Munkres, K. D. (1971) Molecular weight analysis of oligopeptides by electrophoresis in polyacrylamide gel with sodium dodecyl sulfate, *Analytical biochemistry 39*, 462-477.

178. Zhou, X., Li, J., and Kucik, D. F. (2001) The microtubule cytoskeleton participates in control of beta2 integrin avidity, *J Biol Chem 276*, 44762-44769.

179. Korb, T., Schluter, K., Enns, A., Spiegel, H. U., Senninger, N., Nicolson, G. L., and Haier, J. (2004) Integrity of actin fibers and microtubules influences metastatic tumor cell adhesion, *Experimental cell research 299*, 236-247.

180. Stefansson, S., Su, E. J., Ishigami, S., Cale, J. M., Gao, Y., Gorlatova, N., and Lawrence, D. A. (2007) The contributions of integrin affinity and integrin-cytoskeletal engagement in endothelial and smooth muscle cell adhesion to vitronectin, *J Biol Chem 282*, 15679-15689.

181. Campbell, I. D., and Humphries, M. J. (2011) Integrin structure, activation, and interactions, *Cold Spring Harbor perspectives in biology 3*.

182. Takagi, J., Petre, B. M., Walz, T., and Springer, T. A. (2002) Global conformational rearrangements in integrin extracellular domains in outside-in and inside-out signaling, *Cell 110*, 599-511.

183. Bunch, T. A. (2010) Integrin alphaIIbbeta3 activation in Chinese hamster ovary cells and platelets increases clustering rather than affinity, *J Biol Chem 285*, 1841-1849.

184. Litvinov, R. I., Nagaswami, C., Vilaire, G., Shuman, H., Bennett, J. S., and Weisel, J. W. (2004) Functional and structural correlations of individual alphaIIbbeta3 molecules, *Blood 104*, 3979-3985.

185. Cluzel, C., Saltel, F., Lussi, J., Paulhe, F., Imhof, B. A., and Wehrle-Haller, B. (2005) The mechanisms and dynamics of (alpha)v(beta)3 integrin clustering in living cells, *The Journal of cell biology 171*, 383-392.

186. Qin, J., Vinogradova, O., and Plow, E. F. (2004) Integrin bidirectional signaling: a molecular view, *PLoS biology 2*, e169.

187. Karimi, M., and Cohan, N. (2010) Cancer-associated thrombosis, *The open cardiovascular medicine journal 4*, 78-82.

188. Fennerty, A. (2006) Venous thromboembolic disease and cancer, *Postgraduate medical journal 82*, 642-648.

189. Amer, M. H. (2013) Cancer-associated thrombosis: clinical presentation and survival, *Cancer management and research 5*, 165-178.

190. Bakewell, S. J., Nestor, P., Prasad, S., Tomasson, M. H., Dowland, N., Mehrotra, M., Scarborough, R., Kanter, J., Abe, K., Phillips, D., and Weilbaecher, K. N. (2003) Platelet and osteoclast beta3 integrins are critical for bone metastasis, *Proc Natl Acad Sci U S A 100*, 14205-14210.

191. Felding-Habermann, B., Habermann, R., Saldivar, E., and Ruggeri, Z. M. (1996) Role of beta3 integrins in melanoma cell adhesion to activated platelets under flow, *J Biol Chem 271*, 5892-5900.

192. Bambace, N. M., and Holmes, C. E. (2011) The platelet contribution to cancer progression, *Journal of thrombosis and haemostasis : JTH 9*, 237-249.

193. Amirkhosravi, A., Mousa, S. A., Amaya, M., Blaydes, S., Desai, H., Meyer, T., and Francis, J. L. (2003) Inhibition of tumor cell-induced platelet aggregation

and lung metastasis by the oral GpIIb/IIIa antagonist XV454, *Thromb Haemost 90*, 549-554.

194. Trikha, M., Zhou, Z., Timar, J., Raso, E., Kennel, M., Emmell, E., and Nakada, M. T. (2002) Multiple roles for platelet GPIIb/IIIa and alphavbeta3 integrins in tumor growth, angiogenesis, and metastasis, *Cancer research 62*, 2824-2833.

195. Conley, S. J., Gheordunescu, E., Kakarala, P., Newman, B., Korkaya, H., Heath, A. N., Clouthier, S. G., and Wicha, M. S. (2012) Antiangiogenic agents increase breast cancer stem cells via the generation of tumor hypoxia, *Proc Natl Acad Sci U S A 109*, 2784-2789.

196. Casanovas, O. (2012) Cancer: Limitations of therapies exposed, *Nature 484*, 44-46.